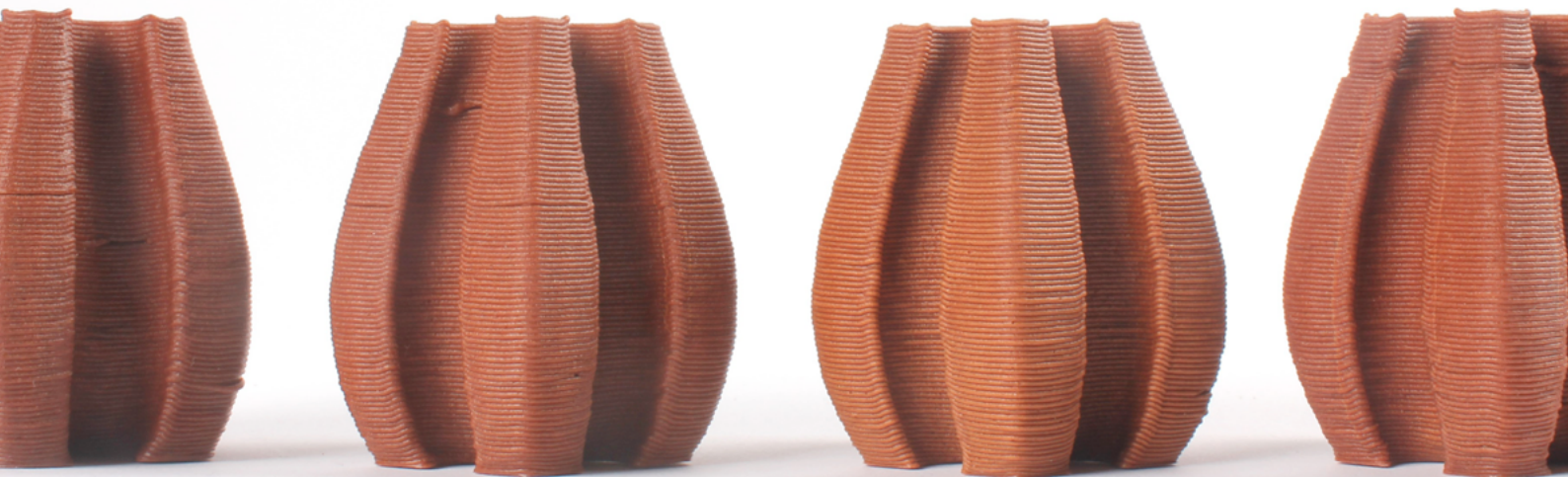


PRINT QUALITY OPTIMISATION OF UPCYCLED BIOMATERIALS FOR AMBIENT 3D-PRINTING

GRADUATION THESIS INTEGRATED PRODUCTS DESIGN | ANNE HENSSEN | NOVEMBER 2023

CHAIR: DR. JEREMY FALUDI
MENTOR: DR. SEPIDEH GHODRAT



ACKNOWLEDGEMENTS

I would like to express my deepest gratitude to my chair, Jeremy Faludi, and my mentor Sepideh Ghodrat, for their invaluable support, input and expertise throughout this research. I want to thank Jeremy for the opportunity to work on this specific subject, which allowed me to combine my passion for sustainability and additive manufacturing. Sepideh I want additionally thank you for her willingness to devote extra time, even amidst her demanding schedule to support me whenever I felt overwhelmed. This did not go unnoticed.

Additionally, I want to give special thanks to Christophe Raynaud for assisting me in the second phase of my research. Without him, I would have not been able to do as much as I did.

I also want to thank Mascha Slingland and Joren Wierenga for offering their expertise in the chemical and material lab at the IDE faculty.

Lastly, I want to thank my family and friends for their support the many times it felt like I was in over my head. Without them, I would not have been able to keep going in times of stress. I especially want to thank my partner, Lara, for being there when I got home overwhelmed.

*I would like to dedicate this thesis to my grandfather, who always showed great interest in my pursuits and supported me in all of them.
I would have loved to have him here to see me graduate.*

ABSTRACT

With growing concern over our reliance on non-renewable resources and the environmental impact of conventional manufacturing, the quest for sustainable materials and production processes has intensified. This pursuit has extended to the field of additive manufacturing, where bio-materials have emerged as promising alternatives, aiming to reduce energy consumption and utilise material waste streams. While biopolymers like PLA are a good step forward, they still pose sustainability challenges, primarily related to energy-intensive melting processes, competition with food sources for production, slow biodegradability, and inadequate waste disposal systems. Consequently, researchers have turned to utilizing biomass waste streams to create 3D printable materials that solidify at ambient temperatures. However, the currently existing bio-based materials for ambient printing exhibit inconsistencies in quality. To allow for commercial adoption of these materials, enhancements in print quality are necessary.

This thesis addresses the core issue of lower print quality in room-temperature printing of biomaterials. Its primary aim is to develop and optimize the print quality of these materials, fostering a deeper understanding of the key factors that influence their printing performance.

Within the context of print quality, the study examines parameters such as dimensional accuracy, bridging, overhang performance, warpage, corner sharpness, surface finish, and precision. Furthermore, the research investigated the feasibility of reprinting these materials and its impact on their print quality. Extra attention was dedicated to investigating the influence of the rheology characteristics of the materials on the resulting print quality.

The research led to the creation of two materials, AB1 and CLAB4 and the optimization of print parameters to enhance their print quality. In doing so it elaborates on the influences of material composition, preparation and printing parameters on the print quality of biomaterials printed at room temperatures.

Of the materials developed, AB1 demonstrated exceptional bridging capabilities, achieving distances of up to 15 mm, minimal shrinkage (averaging 6% in the xy-directions and 4% in the z-direction), and good result precision. In contrast, CLAB4 excelled in surface finish, printing overhangs up to 40 degrees, and showcased higher efficiency in material preparation. Most noteworthy of both materials is their reprintability without evident degradation in print quality, a crucial feature for sustainable printing methodologies.

In this Research, rheology characteristics have proven to be pivotal due to their direct influence on material flow and behaviour. Unlike conventional melting-based printing, where materials flow upon heating and solidify once they are extruded, ambient printing requires inks to have specific rheology behaviours caused by changes in shear. Rheology governs how easily the ink flows when extruded and its ability to retain shape once extruded. Optimizing the shear-thinning behaviour and elastic recovery behaviour is crucial. This study elaborates on the specific aspect of rheology to improve enhancements in print quality, including Yield stress, flow stress, storage modulus, loss tangent and thixotropic response and recovery.

Additionally, it presents interesting insights into how to optimise them based on material composition and preparation. Mixing the material before extrusion, for example, was shown to significantly increase the thixotropic response time, leading to more precise extrusion.

CONTENTS

1. INTRODUCTION	6
1.1 PROBLEM DEFINITION	6
1.2 RESEARCH OBJECTIVES	7
2. LITERATURE REVIEW	8
2.2 BIO-BASED INKS	11
2.3. PRINT QUALITY ASSESSMENT IN DIW	14
2.4. PRINT OPTIMIZATION	17
2.5 CHALLENGES AND LIMITATIONS	24
2.6 KNOWLEDGE GAPS	25
3. EXPERIMENTAL EXPLORATION	27
3.1 INGREDIENT SELECTION	28
3.2 INITIAL TINKERING	36
3.3 INITIAL EVALUATION OF PRINT QUALITY	44
4. PARAMETER OPTIMISATION	49
4.1 RECIPE & PRINT PARAMETER OPTIMISATIONV	50
5. EVALUATION & VALIDATION	62
5.1 PRINT QUALITY & PRECISION EVALUATION	63
5.2 RHEOLOGY CHARACTERISATION	74
5.3 REPRINTABILITY: DEGRADATION OF PRINT QUALITY	93
5.4 REPRINTABILITY: DEGRADATION OF MECHANICAL PROPERTIES	102
5.5 PRINTING LARGER STRUCTURES	106
6. THESIS CONCLUSION & DISCUSSION	109
7. RECOMMENDATIONS	116
8. PERSONAL REFLECTION	119
REFERENCES	120
APPENDIX	125



1. INTRODUCTION

1.1 PROBLEM DEFINITION

The need to reduce our reliance on fossil fuel energy and non-renewable resources, along with a growing awareness of our environmental impact, has increased interest in materials that utilise biomass and production processes that are less energy-intensive.

In the world of additive manufacturing, bio-materials have gained popularity as a sustainable approach for reducing both print energy and material footprint. Traditional materials used in additive manufacturing, such as ABS and PET, require significant amounts of energy to melt, are derived from non-renewable sources (petroleum), and are not biodegradable, creating a need for more sustainable alternatives. The commonly used biopolymer PLA already is an improvement, as it is made from renewable resources. However, it still has some sustainability challenges:

1. PLA is still a thermoplastic and thus requires significant energy to melt. This is the majority of the energy use of FDM printers.
2. PLA is produced using valuable food sources (e.g. corn), causing competition with food production and land use.

3. Although PLA is technically biodegradable, the process is very slow (> 100 years) under normal conditions (e.g. when landfilled). Only in a controlled (industrial) composting environment can PLA degrade within 3 months. Thus when not disposed of correctly, PLA can still contribute to plastic pollution.
4. Due to the specific recycling and composting demands, there are not yet reliable sorting and composting systems in place. Therefore, PLA often still ends up in a landfill or the ocean (Ghomi et al., 2021).

One way researchers are finding better alternatives is by using biomass waste streams in materials that solidify at ambient temperature; creating 3D printable materials made from e.g. oyster & mussel shells, eggshells, olive pomace and mica. Their development can reduce waste and carbon footprint; material cost compared to virgin materials; offer unique properties and textures; and contribute to a more circular economy.

However, the current limitations of these materials are that they show inconsistency in quality and processing, making it difficult to control properties and achieve consistent print quality. In addition, most of these materials are water-soluble. Though this allows for easy reprintability, it does decrease their durability.

1.2 RESEARCH OBJECTIVES

This thesis addresses a critical issue concerning the lower print quality of Bio-based materials for room-temperature printing when compared to established materials like PLA. The primary research objectives are as follows:

1. **Develop a biobased material for room-temperature printing with optimised print quality.**
2. **Identify the key factors influencing the print quality of room-temperature printed biobased materials.**

In this research, the concept of print quality is defined according to Bom et al.'s (2022) explanation of printability:

*“The ability of a certain ink to achieve extrusion and **maintain shape fidelity with high printing accuracy and precision**, which is influenced by material formulation parameters, printing parameters and post-printing parameters”*

When evaluating the print quality of the developed materials, this study examined the following factors to establish their shape fidelity and printing accuracy: dimensional accuracy, bridging and overhang performance, warpage, corner sharpness and surface finish. The precision addressed, refers to the repeatability of the print quality.

Furthermore, as a side quest, this research investigated potential enhancements in material durability and end-of-life scenarios, specifically focusing on water insolubility and reprintability.

While of secondary importance, the following objectives were also pursued throughout this research:

1. Improve the durability by developing a water-resistant material.
2. Improve the end-of-life scenario by developing a reprintable material.

Ideally, the aim was to achieve a synergy between reprintability and water resistance within a single material.

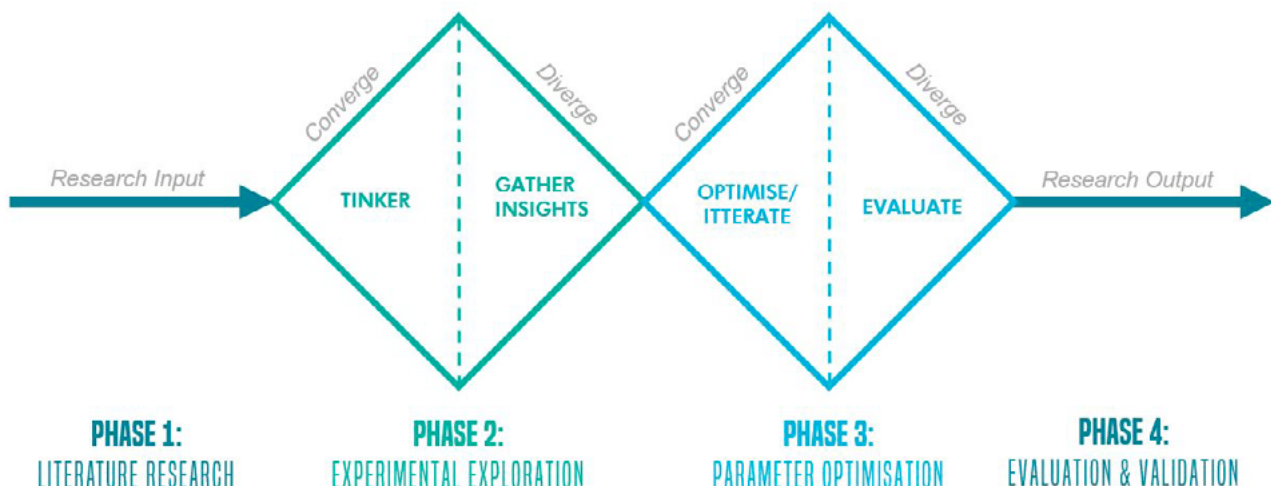
1.3 THESIS STRUCTURE

This thesis is structured based on the different phases that were gone through during this research:

- Literature Review (Chapter 2).
- Experimental Exploration (Chapter 3).
- Parameter Optimisation (Chapter 4).
- Validation and Evaluation (Chapter 5).

Figure 2 gives a summary of the phases of the research process gone through.

Figure 2: Phases of the Research Process



2. LITERATURE REVIEW

Additive manufacturing (AM), has gained popularity as a production method due to its ability to create complex geometries, accommodate small batch sizes, and produce personalized products. The industry has witnessed remarkable growth since 2003, with double-digit revenue growth observed in 25 out of the past 34 years (Scott, 2023).

While AM offers several sustainable advantages, such as possibilities for closed-loop systems and made-to-order production (Peng et al., 2018; Despeisse & Ford, 2015), concerns regarding its sustainability have garnered increasing attention from researchers. In recent years, a growing amount of research has focused on the environmental impact of additive manufacturing technologies, specifically examining factors such as energy consumption, material toxicity, durability, recyclability, and printed product performance (Suárez & Domínguez, 2020).

When considering the production of AM products, energy consumption has emerged as a key contributor to the environmental impact (Faludi et al., 2015). The choice of materials plays a significant role in determining the energy demand of the printing process, as different materials require specific energy inputs. For instance, thermoplastics require heating, while photopolymers rely on exposure to light, and so forth.

To enhance the sustainability of AM, one effective measure is to select materials that reduce the energy demand during the printing. Novel bio-based materials that

can be printed at room temperature offer promising opportunities for achieving this objective as they have low environmental impacts themselves while enabling low-energy printing. Faludi et al. (2019) demonstrated a substantial reduction in print energy (75%) and material impact (82%) when printing with a bio-based composite made from mica, water, and sodium silicate compared to ABS. This reduction resulted in a significant decrease (78%) in ReCiPe eco-impact points per part.

However, despite these evident improvements, the mechanical properties and print quality of parts made from bio-based materials have not yet reached the level of conventional AM materials such as ABS (Faludi et al., 2019). Addressing these challenges is crucial for the adoption of bio-based materials as viable alternatives to thermoplastics and ensuring their durability, which is also an important environmental consideration. Further research is required to enhance the print quality and mechanical properties of these materials, aligning them with the standards set by conventional thermoplastics.

Therefore, the main objective of this thesis is to improve the print quality of these bio-based novel materials with the aim of eventually making them competitive with thermoplastics. To achieve this, it is essential to understand the suitable additive manufacturing method and its requirements for the material being printed. Hence, the scope of this literature review is to comprehend the current state of knowledge, advancements, and challenges in this area, with a specific focus on the rheological requirements of room-temperature printing.

2.1 SUSTAINABLE AM: DIRECT INK WRITING

To fully leverage the sustainability benefits of bio-based materials which can be printed at room temperature, it is crucial to identify suitable additive manufacturing methods. Among these methods, direct ink writing (DIW) emerges as one good solution. DIW's ability to print materials with a wide range of viscosities, including bio-based, often water-based, pastes and composite inks, makes it an ideal choice for fabricating structures with varying mechanical, electrical, or biological properties. Viscosities of pastes and inks printed using DIW can range from 10^2 to 10^6 MPa.s at a shear rate of approximately 0.1s^{-1} (Saadi et al, 2022; Maguire et al, 2020; Bean et al.,2023).

Compared to other AM methods, DIW is a lot less selective regarding the type of material printed, making it a valuable method for many applications. Currently, DIW finds applications in tissue engineering, microelectronics, soft robotics, and advanced manufacturing (Saadi et al., 2022; Li et al, 2019; Corker et al, 2019)

Capitalizing on DIW's inherent flexibility and energy efficiency, it becomes possible to combine the environmental advantages of bio-based materials with a printing method that minimizes energy consumption, paving the way for sustainable and environmentally conscious additive manufacturing.

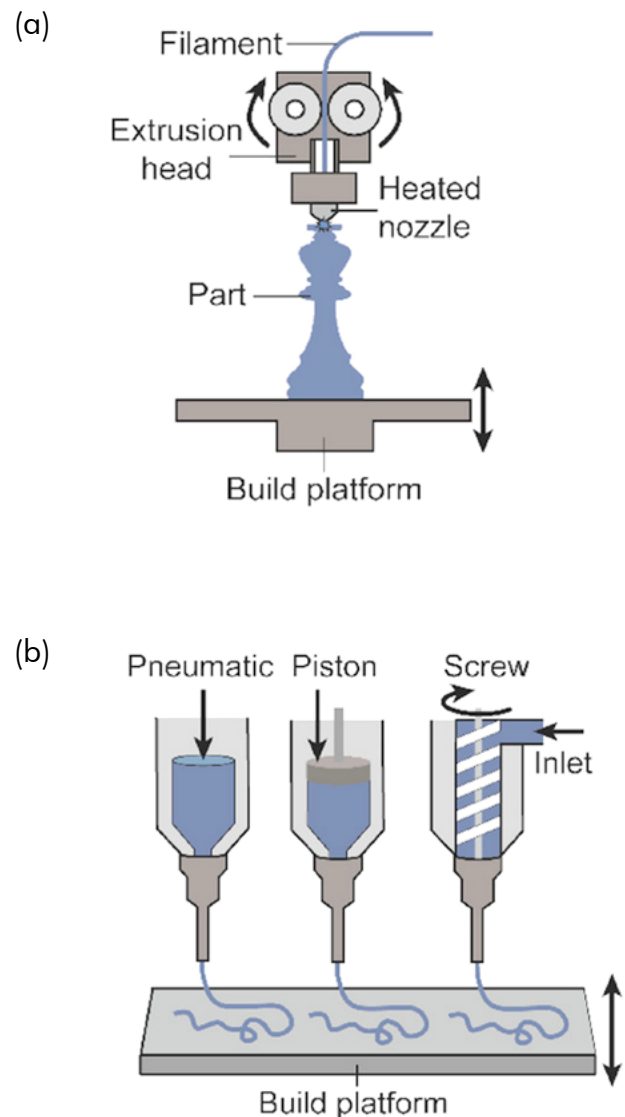
2.1.1 THE DIW PROCESS

DIW can be seen as an alternative to Fused Deposition Modelling (FDM) for printing at room temperature (Li et al., 2019). In DIW, a material's printability is primarily determined by how it responds to shear, whereas in FDM, it hinges on the material's thermal reaction (Saadi et al, 2022).

As a result, DIW is able to extrude continuous filaments without the need for high temperatures to create three-dimensional structures (Saadi et al, 2022).

Figure 3 illustrates the operational principles of FDM printing (a) and DIW (b). In DIW, the input material takes the form of a viscous paste, which is forced through a nozzle either pneumatically, via a piston, or by a screw. In contrast, FDM uses a solid filament that undergoes liquefaction through a heating element before being extruded.

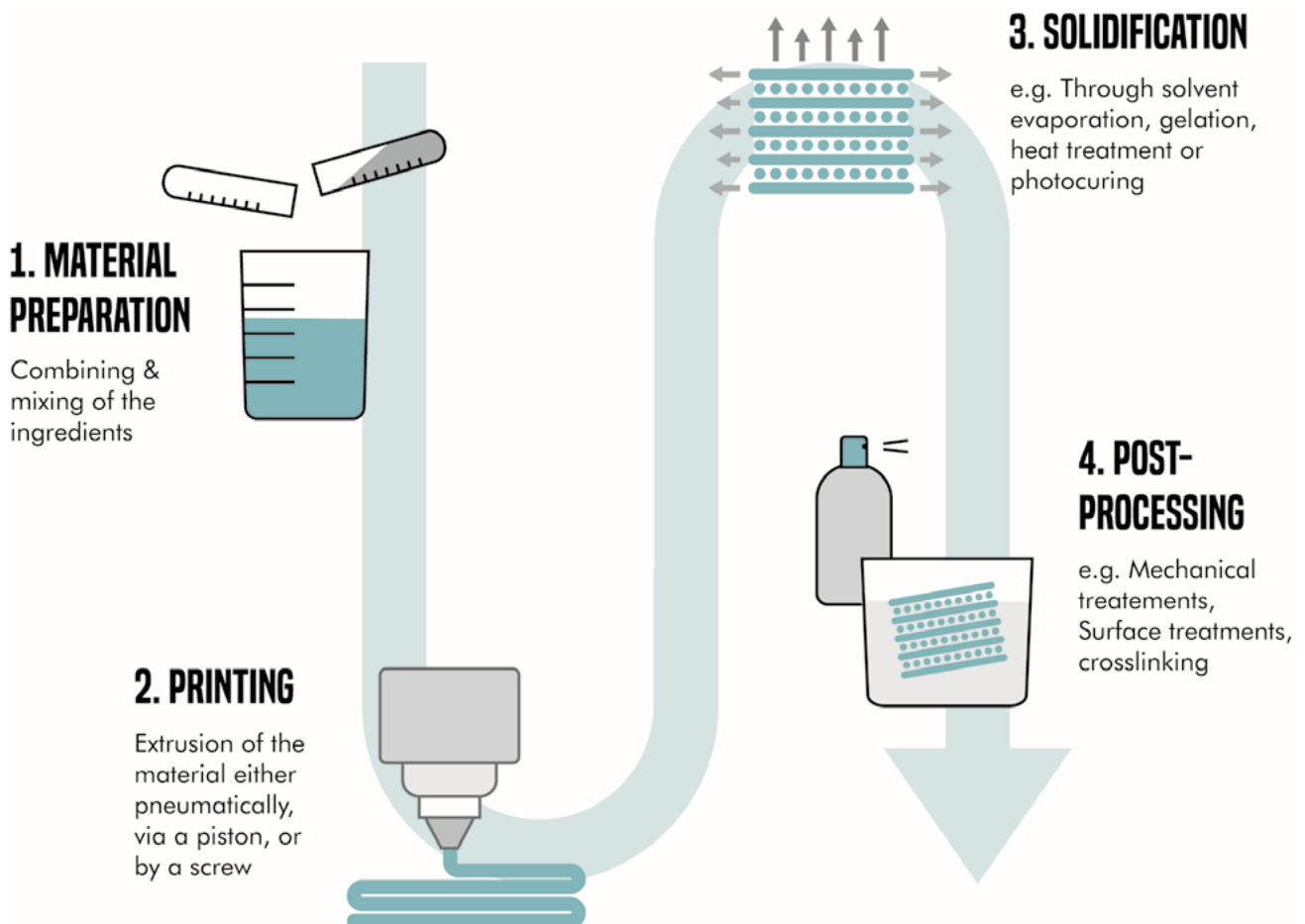
Figure 3: FDM (a) vs. DIW (b) method. Copyright 2018, John Wiley and Sons (Zhan et al., 2022)



The DIW process can be divided into 4 stages (Figure 4):

- 1. Material preparation:** in this stage, the paste is prepared to achieve the desired rheological properties, such as shear-thinning behaviour, viscoelasticity and thixotropy (Lewis et al, 2006).
- 2. Printing:** During this stage, the material is extruded through the nozzle and carefully deposited onto the print bed or previously printed layers. The precise path of deposition is determined by computer-aided design (CAD) models, which are translated into G-code instructions by slicing software (Li et al, 2018; Lewis et al, 2006).
- 3. Solidification:** Following ink deposition, solidification happens either spontaneously or with external assistance, such as solvent evaporation, gelation, heat treatment, or photo-curing. (Saadi et al, 2022; Wilt et al., 2021; Bean et al.,2023). Figure 4 shows solidification through evaporation.
- 4. Post-processing:** Additional treatments are sometimes carried out, to enhance the mechanical strength or other properties of the printed structure (Saadi et al, 2022; Bean et al.,2023). An example of a post-treatment is the post-cross-linking of alginate hydrogels with Ca-ions to achieve improved mechanical properties and water insolubility (Sauerwein et al, 2020).

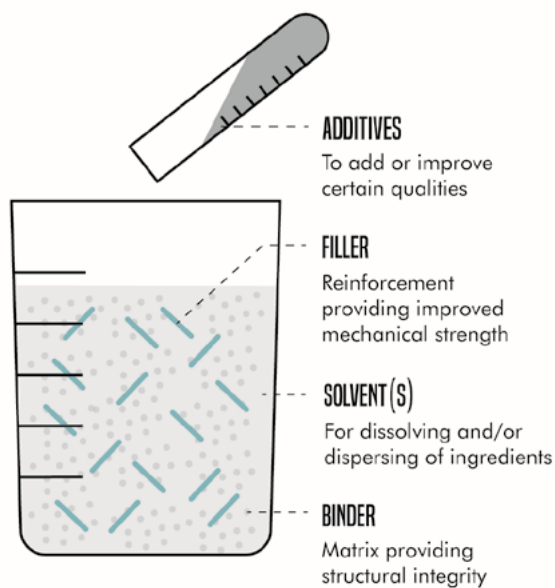
Figure 4: A step-by-step of the DIW printing process



2.2 BIO-BASED INKS

As discussed, using bio-based material can help further reduce the environmental impact of additive manufacturing. The utilization of natural materials in DIW ink formulation offers several advantages from a sustainability perspective. They allow for biodegradability, have a lower environmental impact and have the potential for biocompatibility. In addition, they allow for easy processing and modification and have an abundant raw material source (Su et al., 2022). The formulation of biobased materials for DIW can be divided into four main components: Binders, fillers, additives and solvents (Figure 5). Each will be discussed.

Figure 5: DIW ink composition



2.2.1 BINDERS

The binder in the ink formulation serves as a matrix that keeps all material components together and thus provides structural integrity. Two categories of naturally derived biodegradable matrix materials that are valuable for structural 3D printing are polysaccharides and proteins (Su et al., 2022; Andrew & Dhakal, 2022; Shahbazy & Jäger, 2021; Li et al, 2021).

2.2.1.1 POLYSACCHARIDES

Polysaccharides are in biomass occurring polymers that consist of a combination of monosaccharides, also known as sugars. Research has shown that the resolution and printing precision of polysaccharide-based materials largely depend on the degree of chain entanglement. Factors such as the concentration, chemical structure, and flow behaviour of polysaccharides influence the printing conditions. In addition, the covalent or ionic linkages of carbohydrate-based materials determine the cross-linking degree and directly impact the structural strength of the printed constructs (Shahbazy & Jäger, 2021). Commonly used polysaccharides in DIW are sodium alginate, chitin, agarose, carrageenan, Xanthan gum, Guar gum, starch and pectin (Romani et al., 2023; Su et al., 2022; Shahbazy & Jäger, 2021; Li et al, 2021).

Sauerwein et al. (2020), for example, experimented with the use of sodium alginate in combination with mussel shell waste (Figure 6). Whereas, Sanandiya et al (2020), made use of Chitin as a matrix material to print large-scale architectural structures (Figure 7).

Figure 6: Mussel shell-alginate hair pin by Sauerwein et al. (2020).



Figure 7: Chitin based bio prints of Sanandiya et al (2020)

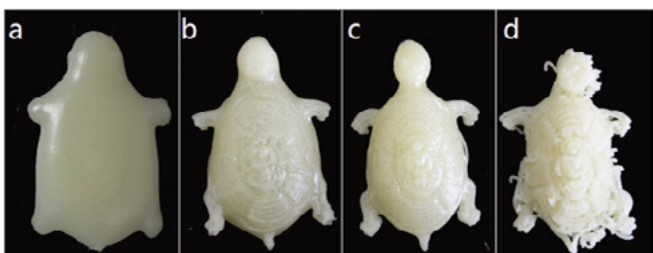


2.2.1.2 PROTEINS

Proteins consist of large molecules composed of amino acids that undergo condensation reactions to form polypeptide chains. Polypeptide chains entangle to form intricate three-dimensional structures that can serve as a matrix (Su et al., 2022). Proteins, due to their organizational states, high-molecular-weight nature, and supramolecular functionality, are widely employed in 3D printing applications. Their flexibility in molecular geometry, ease of mixing, gelation, aggregation, and deposition make them highly efficient in creating complex 3D-printed structures. Proteins exhibit unique hierarchical architectures resulting from self-assembly, which are influenced by the 3D printing process (Shahbazy & Jäger, 2021). Commonly used proteins in DIW are collagen, gelatine, albumin, fibrin, elastin, casein, soy and keratin (Shahbazy & Jäger, 2021; Andrew & Dhakal, 2022; Su et al., 2022; Li et al., 2021).

In research, protein matrixes are mostly used in the field of tissue engineering and food printing. Govindharaj et al. (2019), for example, extracted collagen from eel skin for use as a matrix in a biobased material for tissue engineering. Liu et al (2019) used casein to print 3D food structures (Figure 8).

Figure 8: Casein foodprints by Liu et al (2019)



2.2.2 FILLERS

Fillers serve as reinforcements for the ink and thus enhance the mechanical performance allowing for improved mechanical strength and dimensional stability. Additionally, fillers help reduce drying-induced shrinkage, as a high solid volume fraction improves the material's resistance towards compressive

stresses caused by capillary tension (Balani et al, 2021).

This thesis focuses on the use of cellulose biomass as a filler. Introducing cellulose waste as fillers in DIW ink formulations brings forth significant advantages compared to solely relying on biomass resources.

A concern when using biomass is the potential competition between the production of biomaterials and food resources, as many biomaterials are derived from plant-based food sources. This reliance on plant-based derivatives as raw materials may lead to food scarcity and increased demand for these resources. Using agricultural waste is an alternative approach that has several advantages. It lowers production costs, does not take away from a valuable food source, and effectively tackles the pollution issues associated with agricultural waste (Shaik et al.,2022).

Biomass waste-derived fillers can be divided into two categories: Cellulose-based, which includes woods and timber, fruits and seeds and herbaceous plants, and animal-derived. The amount of filler commonly added to the matrix material ranges from 1-29 weight % (Romani et al.,2023; Gauss et al.,2021).

Previous graduation student Ennio Donders (2022) used eggshells as a filler material (Figure 9). Whereas students from the Advanced Prototyping Minor used tangerine peel as a filler (Figure 10).

Figure 9: Eggshell filler print by Donders (2022)



Figure 10: Tangerine peel filler print by Leeuw et al. (2022, [unpublished]).



2.2.3 ADDITIVES

Additives can play a vital role in the quality improvement of DIW inks. They can help to adjust the rheology behaviour, improving printability, shape fidelity and adhesion of layers. Additionally, additives can be used to add additional functionalities.

2.2.3.1 RHEOLOGY MODIFIERS

Rheology modifiers are used to control the viscosity and flow behaviour of the ink. They help in achieving the desired printing characteristics and ensure proper deposition of the ink during the DIW process. Achayuthakan & Suphantharika (2015), experimented with both Xanthan Gum and Guar Gum as a rheology modifier. Yadav et al. (2021) review the use of Nano-cellulose as a valuable rheology modifier.

2.2.3.2 DISPERSANTS AND SURFACTANTS

Dispersants and surfactants are used to enhance the stability of the ink, prevent sedimentation, and improve the dispersion of fillers or other components in the ink. Additionally, they can help in controlling surface tension and wetting properties. An example of a dispersant agent is Calcium Lignosulfonate (Ruwoldt, 2020).

2.2.3.3 CROSSLINKING-AGENTS

Cross-linking agents are used to promote the formation of chemical bonds between the ink components, leading to improved mechanical properties and stability (Wilt et al., 2021).

Sauerwein et al. (2020), Post-crosslinked alginate-based mussel shell ink with Calcium Chloride to improve its strength and to make it water insoluble. Whereas Badr et al. (2022), use a Calcium chloride mist for in-situ cross-linking of alginate during the printing process.

2.2.3.4 ADDITIONAL FUNCTIONALITIES

Depending on the desired properties and applications, additional additives can be incorporated to provide specific functionalities to the ink, such as UV stabilisation, flame retardancy, antimicrobial properties and colour.

2.2.4 SOLVENTS

Solvents are used to dissolve and/or disperse the components of the ink formulation and are thus necessary for achieving a uniform ink. Additionally, they provide the fluidity necessary for extrusion by helping achieve the required ink viscosity.

The evaporation rate of solvents strongly influences the time it takes for printed inks to solidify. High evaporation rates will decrease the time it takes for printed layers to solidify, allowing for improved capability of supporting multiple layers. However, high evaporation rates can also cause uncontrolled and non-uniform drying which often leads to ambient drying cracks and non-uniform shrinkage (Xu et al, 2022).

Chapter 2.4.2.2. will talk more in detail about the effect of solvents and their influence on the solidification of prints.

2.3. PRINT QUALITY ASSESSMENT IN DIW

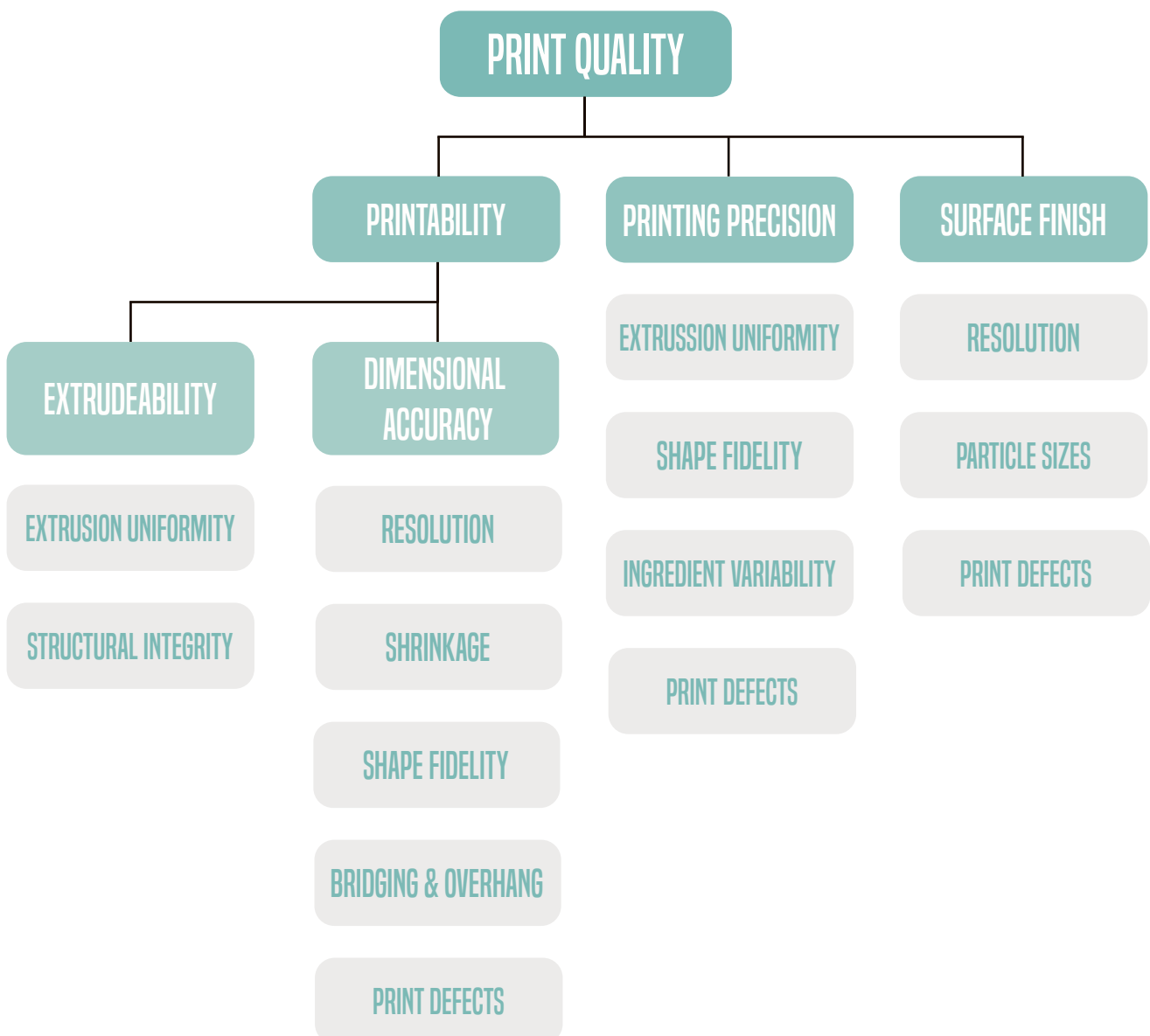
Since the main objective of this thesis is to improve the print quality of biobased materials printed with DIW, it is important to establish a consensus on the definition of print quality. In literature, the definition of print quality lacks standardisation. Different authors proposed different terms and criteria for evaluating print quality. The main concepts of print quality that are used in literature are; printability, printing precision, dimensional accuracy, extrudability (Bom et al., 2022) and surface finish (Buj-Corral et al., 2020).

Figure 11 presents a taxonomy of the concepts related to print quality and their main parameters found in literature.

2.3.1. PRINTABILITY

In 3D printing, printability relates to a material's capability to be extruded in a layer-by-layer manner to fabricate a computer-defined 3D object. Different researchers have expanded on the definition of printability, considering factors such as rheological properties, gelification mechanisms, thermal properties, surface tension, and cross-linking ability. Some also include the influence of printing parameters/settings, such as feed rate, pressure, construct design, nozzle

Figure 11: Taxonomy of print quality parameters based on literature



geometry, and printing temperature (Bom et al., 2022). Gao et al, (2018) name extrudability, extrusion uniformity and structural integrity as important parameters of printability.

When referring to printability in this thesis, the definition by Bom et al (2022, p5) is used:

“The ability of a certain ink to achieve extrusion and maintain shape fidelity with high printing accuracy, which is influenced by pre-printing (rheological and nozzle features), printing [design, slicing, g-code (e.g., pressure, temperature and feed rate) and non-g-code parameters (e.g., environmental conditions)] and post-printing parameters (e.g., cross-linking, coating or drying techniques)”

2.3.2. DIMENSIONAL ACCURACY, PRINTING PRECISION & SHAPE FIDELITY

Printing accuracy, in this thesis, referred to as dimensional accuracy, refers to the resemblance of a printed object to the intended geometry and resolution in the CAD model. Gillispie et al. (2020), define printing accuracy as the degree to which printed constructs align with their intended size, shape, and location, considering specific printing parameters. The ability of a material in combination with printing parameters to allow for overhang and bridging features can thus be seen as part of printing accuracy. The print's ability to show shape retention and minimum shrinkage is important to gain high accuracy.

Printing precision is defined as *“the repeatability or reproducibility of a print in terms of size, geometry, and spatial location”* by Bom et al. (2022, p5).

Gao et al. (2018) correlate extrusion uniformity to printing precision, with uniform extrusion leading to better precision. Factors that can negatively affect the uniformity of extrusion are the occurrence of nozzle clogging and uniform dispersion of filler material in the ink formulation. Additionally, natural materials exhibit greater inter-batch

variability compared to synthetic materials. This is caused by inherent biological diversity and environmental influences (De Prá Andrade et al., 2021).

Bom et al (2022,p5) define printing fidelity (a.k.a. shape fidelity), as an ink's ability to retain its shape after extrusion. Printing fidelity is thus closely related to accuracy and precision. Without an ink's ability to retain its shape, high printing accuracy and precision can not be reached. Gillispie et al. (2020) suggest that printing fidelity can be assessed by examining a single layer of printed material. This can be achieved by measuring the dimensions of printed filaments and evaluating factors such as spreading ratio, height maintenance, and filament collapse, which provide insights into the accuracy and integrity of the printed layer. However, this does not take into account the effect that the weight of multiple layers can have on the shape fidelity of the entire print.

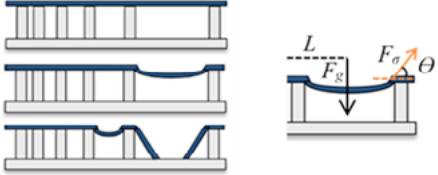
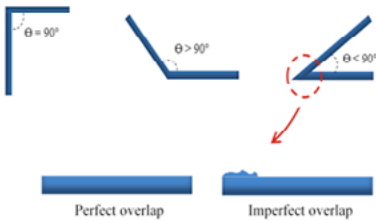
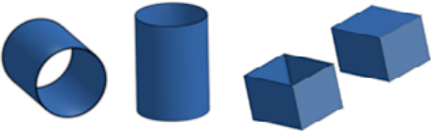
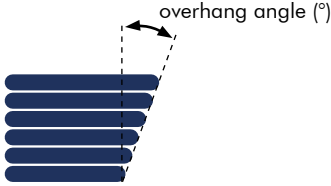
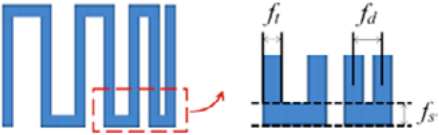
2.3.3. SURFACE FINISH

The surface finish of a print can be defined as its roughness. Which strongly correlates with the printing resolution (nozzle size) and the material mixture. When a smaller nozzle is used, the printed surfaces will be smoother compared to when a bigger nozzle is used. In the material formulation, different particles with different sizes and morphology can result in differences in surface finishes (Buj-Corral et al., 2020).

2.3.4. PRINT QUALITY ASSESSMENT TECHNIQUES

Several methods in research are used to evaluate the concepts discussed and adjust parameters such as ink formulation and printer settings accordingly. Table 1 shows an overview of the methods which were used in this research and their purpose. Print precision can be measured by repeating these tests over multiple cycles.

Table 1: Overview of print quality assesment tests found in literature

Print Quality Assesment Test	Quality Parameters Evaluated	Purpose
<p>Figure 12: Filament collapse test (Bom et al.,2020 ,p.10, Fig. 4).</p> 	<p>Printing accuracy: Bridging, Printing Fidelity</p>	<p>Evaluates the material’s ability to resist gravity-induced deformation and support overhangs or unsupported filaments in multi-layered con-structs. It involves placing the material on a structure with pillars at increasing distances and measuring the angle of deflection (Schwab et al, 2020;Bom et al, 2022) (Figure 12).</p>
<p>Figure 13: Angle test (Bom et al.,2020,p.10, Fig. 4).</p> 	<p>Printing accuracy: Printing Fidelity, Print Defects.</p> <p>Surface finish: Print defects.</p>	<p>Printing sharp angles often results in overlap, which can lead to printing failures and an uneven height of the printed construct. To address this issue, the angle test helps assess the extent of the overlap problem before printing more complex structures (Bom et al, 2022) (Figure 13).</p>
<p>Figure 14: Planar Multi-layered Structures (Bom et al.,2020,p.11, Fig. 5).</p> 	<p>Extrudability: Extrusion uniformity</p> <p>Printing accuracy: Shrinkage, Printing Fidelity, Resolution, Print defects</p>	<p>Multi-layer structures can help to evaluate the overall printability of an ink with set parameters. Squares are useful for measuring dimensional accuracy in the x y and z direct. Whereas, Cylinders are good for checking arc motion capabilities (Bom et al, 2022) (Figure 14).</p>
<p>Figure 15: Overhang test.</p> 	<p>Printing accuracy: Overhang, Printing Fidelity</p>	<p>Overhang tests can evaluate the ability of the ink composition and print parameters to print overhanging structures. It can help to define the maximum overhang that can be reached while still showing dimensional accuracy (Figure 15). Models for testing overhang thresholds differ a lot within literature and no general method can be found.</p>
<p>Figure 16: Filament Fusion Test (Bom et al.,2020,p.10, Fig. 4).</p> 	<p>Extrudability: Extrusion Uniformity</p> <p>Printing accuracy: Resolution, Printng Fidelity</p>	<p>Evaluates the merging and spreading behaviour of printed filaments. By printing a meandering pattern with closely spaced parallel strands, the test determines the minimum distance needed to prevent fusion between filament segments. A smaller distance corresponds to a higher resolution (Schwab et al, 2020;Bom et al, 2022) (Figure 16).</p>



2.4. PRINT OPTIMIZATION

The print quality of a print can be improved by two main strategies: (1) by optimizing the rheology behaviour of the ink, (2) by optimizing the printing parameters, or (3) by in-situ and post-treatments. This Section discusses these strategies.

2.4.1 RHEOLOGY OPTIMIZATION

A primary challenge in controlling the quality of DIW lies in effectively controlling the flow behaviour and extrusion parameters to attain the desired structural integrity and dimensional accuracy. For an ink to be suitable for printing without solidification by temperature change or rapid chemical reaction, it needs to possess specific rheology properties. Therefore, rheological concepts play a crucial role in DIW.

The rheological properties of the ink, including shear thinning behaviour, viscoelasticity and thixotropic recovery directly influence the extrusion process, ink flow, and necessary post-processing steps (Schwab et al., 2020). These rheology concepts are discussed below. Though no researchers have been able to create a holistic method on how to precisely formulate an Ink with the ideal rheology for DIW, there are some general criteria that can be used regarding the preferred rheology properties of DIW inks and their overall influence on the print quality.

2.4.1.1 VISCOSITY & SHEAR THINNING BEHAVIOUR

Shear thinning behaviour is a fundamental rheological concept in DIW that significantly affects the extrusion and flow properties of inks. In shear-thinning materials, the viscosity decreases as the shear rate increases, allowing for smoother extrusion through the nozzle and improved control over the ink flow. Shear-thinning behaviour is needed for achieving precise deposition, preventing discontinuous extrusion and reducing the chances of nozzle clogging. (Del-Mazo-Barbara & Ginebra, 2021 ; Li et al, 2019).

Because of the shear thinning properties, a paste with a relatively high zero-shear viscosity can be formulated for printing, allowing for better shape retention after printing, without the need for extremely high extrusion pressures. Thus, good shear thinning behaviour can allow for the use of smaller nozzles which means higher printing resolution and smoother surface finish (Schwab et al., 2020; Romberg et al., 2021).

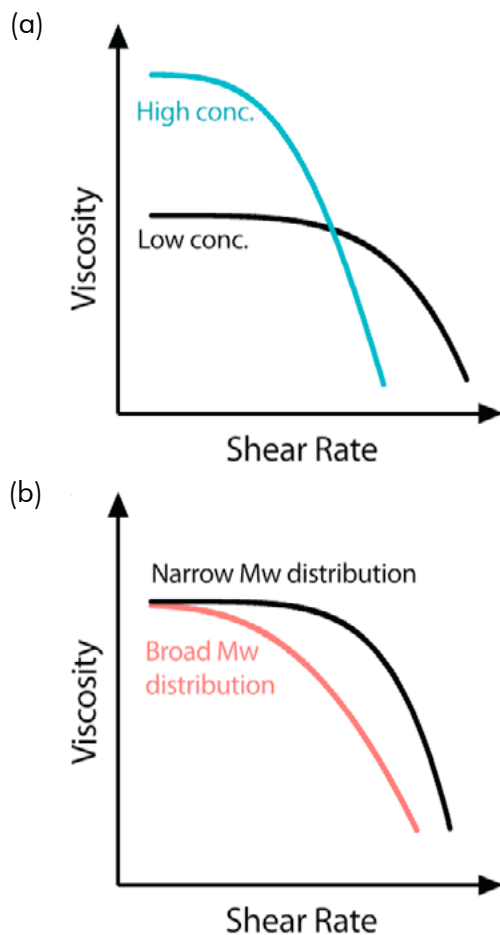
The shear thinning behaviour of ink is strongly influenced by its solid-volume fraction, particle shape and sizes, the composition of filler, the use of dispersant agent, the ageing time, the pH, and the use of rheology modifiers (Del-Mazo-Barbara & Ginebra, 2021).

Cooke and Rosenzweig (2021) state that increasing polymer percentage causes an increase in zero-shear viscosity and a reduction of the shear rate required to induce shear-thinning.

In addition, increasing the polymer content results in a faster decrease of viscosity in relation to the shear rate (Figure 17a). Cooke and Rosenzweig also mention the effect of the molecular weight (M_w) of polymers on the shear-thinning behaviour. Materials with a broad M_w diffusion show a less extreme shear thinning behaviour compared to those with a narrow distribution (Figure 17b)

Regarding the viscosity of a material at rest, high zero-shear viscosity inks, result in better print accuracy and shape retention. However, with increased viscosity, higher shear stress is required for extrusion. The amount of extrusion pressure that can be generated is thus a limiting factor. On the other hand, lower viscosity inks can reduce nozzle clogging but have worse printing accuracy and shape retention (Cooke and Rosenzweig, 2021; Schwab et al., 2020).

Figure 17: The effect of polymer percentage (a) and Molecular weight (b) on viscosity and shear-thinning effect. (Cooke and Rosenzweig, 2021, p.3)



2.4.1.2 VISCOELASTICITY

In addition, Inks for DIW need to show viscoelasticity. viscoelasticity refers to the ability of the material to exhibit both elastic and viscous properties when subjected to stress. When an ink displays viscoelastic behaviour, it is able to return to its original or near-original viscosity after shear-thinning has occurred.

Two key parameters used to characterize the viscoelastic behaviour are the storage modulus (G') and the loss modulus (G''). These moduli are measures of the material's resistance to deformation and its ability to dissipate energy and display viscous flow, respectively (Li et al., 2021; Amorim et al., 2021). When the ink is extruded, the ink should flow easily, meaning the loss modulus G'' needs to be higher than the elastic modulus G' . However, as soon as the ink leaves the nozzle, the ink should return to its higher viscosity to retain its shape. Thus, the loss modulus G'' needs to be lower than the elastic modulus G' after extrusion. Figure 18 visualizes the desired viscoelastic behaviour.

The ratio of G'' to G' , is known as the loss tangent ($\tan\delta$). It provides insights into the energy dissipation characteristics of the ink. A high loss tangent indicates a more viscous behaviour, while a low loss tangent indicates a more elastic behaviour. To achieve good print quality, a good balance between G'' and G' needs to be found (Bom et al., 2022). A study by Gao et al. (2018), correlated a high loss tangent with improved uniformity of extrusion and a lower tangent with better structural stability.

Furthermore, to achieve good stability of ink after extrusion, the value of G' for DIW inks must be practically constant under low shear stress. This feature of a material is called the linear viscoelastic region (LVR) (Li et al, 2019; Saadi et al., 2022). Li et al. (2019) state that the G' within the LVR should exceed 10^3 Pa to support a stable multiple-layer 3D structure with a large enough difference between G'' and G' , meaning a low $\tan\delta$. They suggest a $\tan\delta$ of 0.8 or lower.

2.4.1.3 YIELD & FLOW STRESS

The yield stress (σ_y) of a material determines the minimum stress that is necessary to induce the shear thinning behaviour. The flow stress (σ_f) is the stress required to switch from a solid to liquid-like behaviour and is reached at the cross-over point where $G' = G''$ (Figure 18) (Del-Mazo-Barbara & Ginebra, 2021).

Yield behaviour in viscoelastic materials can thus be seen as having a flow transition zone (FT-zone) between the yield onset point and the flow point. The flow transition index (FTI) is defined as σ_y / σ_f . The closer this value is to 1, the higher the tendency of the material to show brittle fracture (Amplitude Sweeps Anton Paar Wiki, n.d.).

To gain good printing results with DIW, inks require a sufficient yield stress for self-support of multiple layers, while also displaying a high shear thinning effect when this stress is reached to allow for good flow and reduced clogging prevention (Romberg et al., 2021; Li et al, 2021; Bom et al., 2021).

Research by Mouser et al. (2016), proved that inks with high yield stresses and high shear thinning result in good extrudability, printing accuracy and shape retention.

Thus, a high storage modulus and yield stress can reduce an ink's deformation after it is deposited, which avoids the collapse of the 3D-printed structure. However, a low flow stress reduces the pressure required for extrusion through the nozzle. Since both parameters correlate with each other, a balance needs to be found.

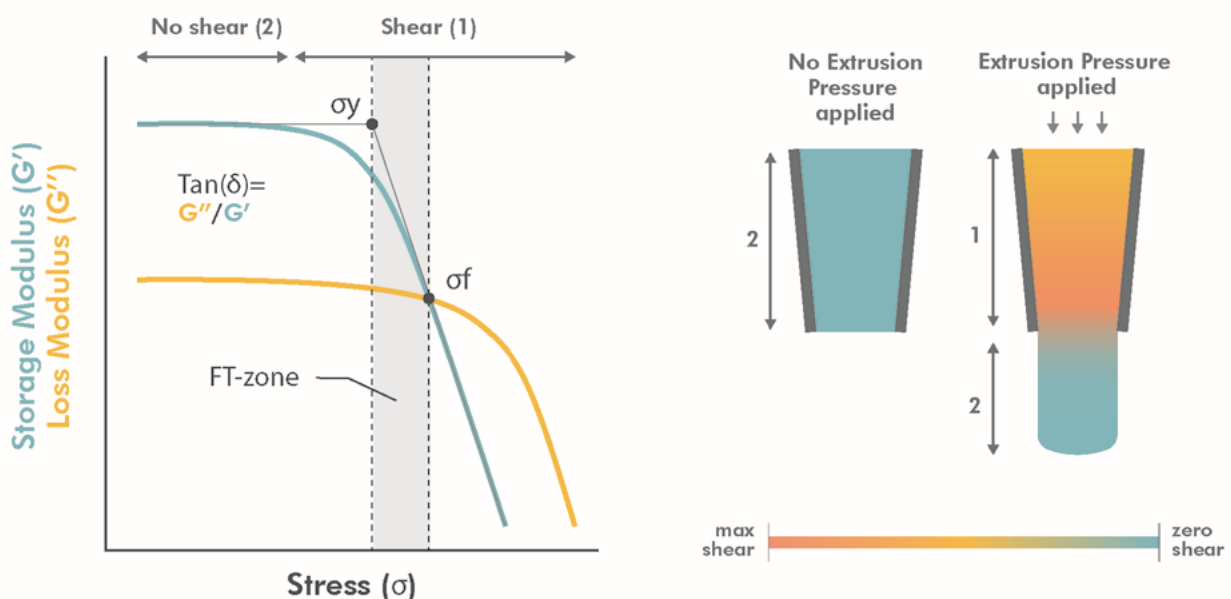
2.4.1.4 THIXOTROPIC RECOVERY BEHAVIOUR

Thixotropy refers to the time-dependent recovery behaviour of viscoelastic materials. In thixotropic materials, the viscosity recovers to its original state after a certain recovery time (Wilt et al., 2021).

In the application of DIW, the recovery time highly influences the shape fidelity of a print. The aim is to formulate materials with short recovery times and a high enough restored modulus to ensure high shape fidelity even when multiple layers are stacked onto each other (Cooke & Rosenzweig 2021; del-Mazo-Barbara & Ginebra, 2021).

The optimal ink for DIW printing would not show thixotropic behaviour, instead, its properties would only be affected by the sudden rate at which it is sheared.

Figure 18: Viscoelastic behaviour of DIW inks. 1 = shear region, 2 = no shear region.



Unfortunately, the properties of most inks are affected by shear history and thus show a delayed recovery response (Tagliaferri et al., 2021; Saadi et al., 2021; Vittadello & Biggs, 1998).

How quickly a material recovers depends on its composition, but no holistic guidelines can be given for the formulation of quick recovery inks and pastes. Research from del-Mazo-Barbara & Ginebra (2021), showed a reduction of restored storage modulus (viscosity) with increasing ceramic content in ceramic pastes.

Figure 19 shows how the ink position in the printing process correlates with the shear strain. When Extruded through the nozzle in a vertical downward direction the shear increases (2), with a maximum shear occurring at the nozzle tip (3). After which the shear strain quickly drops (4).

Figure 19: Shear strain throughout the DIW printing process (del-Mazo-Barbara & Ginebra, 2021, p.26, Fig. 10).

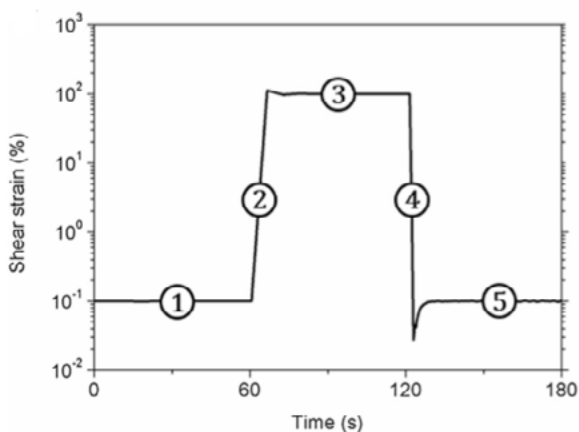
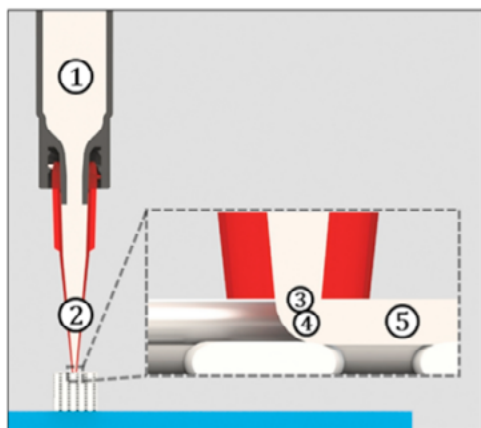
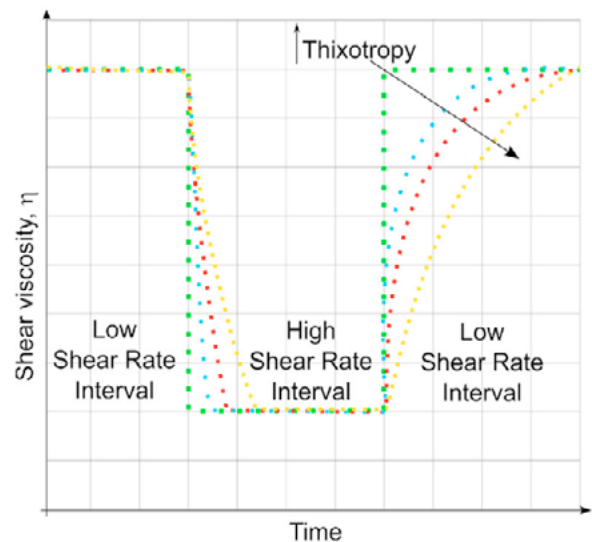


Figure 20, shows the thixotropic response of viscoelastic inks when subjected to strains corresponding with this extrusion process. The green dotted line shows the ideal viscoelastic response for DIW printing; A thixotropic response that resembles this line as closely as possible is thus preferred.

Figure 20: Thixotropic response of viscoelastic inks (Amorim et al., 2021, p.6, Fig. 4)



2.4.1.4. RHEOLOGY PROPERTIES RELATION TO PRINTABILITY AND PRINT QUALITY

Printability in DIW consists of two different concepts: (1) good extrudability and (2) shape retention/dimensional accuracy.

Summarizing the effect of the rheology concepts discussed, this requires DIW inks to exhibit shear-thinning behaviour when a force is applied and display a quick thixotropic recovery of a high enough Storage Modulus (G'_{LVR}) to support multiple layers and allow for spanning. (del-Mazo-Barbara & Ginebra, 2021; Bom er al, 2022; Tagliaferri et al., 2021; Corker et al; 2019)

Rheology characterisation techniques, using a rheometer, can serve as a medium to predict the printability and print quality of inks and help tweak formulations for better performance.

The rheology of formulations can be changed by adjusting component ratios or by the addition of rheology modifiers.

Noteworthy, however, is that properties gathered from rotational rheometers will often differ from the actual rheology properties during extrusion. Though they can give valuable insights into the effect of changes in material formulation, the true printability can only be evaluated by printing.

Table 2 shows a summary of the rheology parameters that influence the printability and print quality including the rheology test that can be used to evaluate them.

All of the tests discussed in the table were used in this research to evaluate the rheological behaviour of the final best- and worst-performing recipes and correlate the found values with their performance in terms of print quality.

2.4.2 PRINT PARAMETER OPTIMIZATION

Apart from the formulation of inks and their resulting rheology characteristics, both in-situ and post-print parameters have a large effect on the print quality of prints.

In this section, The literature focused on print parameter optimisation is shortly discussed. By fine-tuning these printing parameters the final print quality of materials can be further enhanced.

2.4.2.1. IN-SITU PRINT PARAMETERS: PRINTER SETTINGS

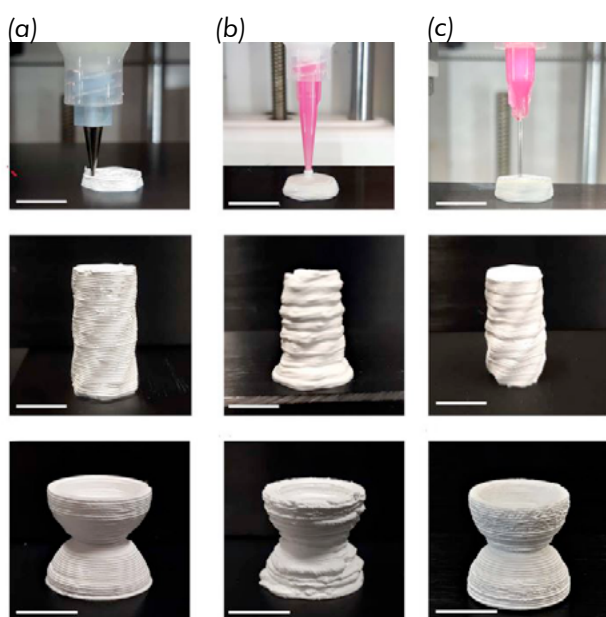
Printer settings can have a significant effect on the resulting print quality of prints. Some of the key parameters are the nozzle geometry, layer height extrusion pressure, infill and print speed (Bom et al.,2020; Buj-Corral et al,2020).

Table 2: Rheology parameters influencing the printability and print quality of DIW inks

Predictor of	rheology parameter	Significance	Characterization Technique
Extrudability	Flow stress (σ_f)	Stress required to make ink flow. (At Cross-over point where $G' = G''$)	Amplitude Sweep
	Flow Behaviour index (n)	Helps to determine the shear-thinning effect	Flow Sweep
Shape retention/ dimensional accuracy	Storage modulus in LVR (G'_{LVR})	Stiffness of the ink after extrusion	Amplitude Sweep
	Loss tangent; G''/G' ($\tan\delta$)	Relation between the viscous and elastic behaviour of an ink	Amplitude Sweep
	Yield stress (σ_y)	Maximum stress before ink's deformation becomes irreversible	Amplitude Sweep
	Thixotropic Recovery times	Time required to recover the elastic behaviour after extrusion	Three interval thixotropy test
	Thixotropic Recovery Percentage	Recovered percentage of the G'_{LVR}	Three interval thixotropy test

The ink's flow behaviour and print resolution are closely tied to the geometry of the nozzle. Decreasing the nozzle diameter can improve resolution, but it may also increase the likelihood of clogging. In a study conducted by Guo et al. (2023), three different nozzle shapes were tested for their impact on print quality: a conical nozzle (b), a cylindrical nozzle (c), and a conical nozzle with a cylindrical tip (a) (see Figure 21). The conical nozzle resulted in the poorest print quality due to inconsistent extrusion velocity. The cylindrical nozzle offered good print quality thanks to its more consistent extrusion velocity, but dead zones within the nozzle, where material flows less, raised the risk of clogging. In contrast, the hybrid nozzle design (b) reduced dead zones while maintaining a consistent extrusion velocity at the tip, combining quality with clogging risk reduction.

Figure 21: Printing tests from Guo et al (2023, Fig 8) using three different nozzle geometries: (a) Conical nozzle with cylindrical tip, (b) Conical nozzle, (d) Cylindrical nozzle.



Layer height is often considered, as it can affect the dimensional accuracy, shape fidelity and precision of prints (Bom et al., 2022). According to research by Naghieh et al. (2019), layer height correlates with line width. By adapting the layer height, a wide range of layer widths can be reached. Smaller layer heights result in wider lines, yet improve the resolution and thus the surface finish.

In DIW, too large layer heights can lead to non-continuous printing, whereas too small heights can hinder proper inflow or lead to the pushing down of the structure (Naghieh et al., 2019; Bom et al., 2022).

2.4.2.2. IN-SITU PRINT PARAMETERS: SOLIDIFICATION TECHNIQUES

Increasing the solidification rate can be a valuable way of improving the shape fidelity and accuracy of prints. While the desired viscoelastic behaviour of DIW inks already causes the ink to thicken and hold its shape, the ink is not yet solidified directly after extrusion and is thus susceptible to movement. In literature, multiple methods are found to improve the solidification rate and thus the structural stability of the prints during printing. Xu et al. (2022), categorise these solidification mechanisms into thermal-assisted, solvent assisted and UV-curing.

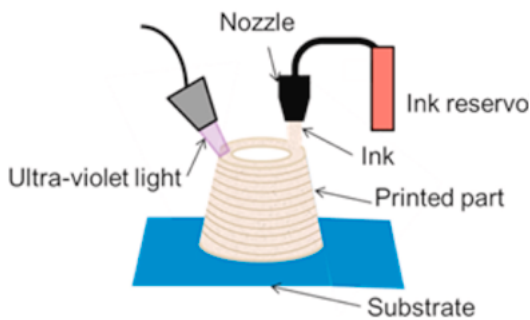
Among the three categories presented, solvent-assisted solidification stands out as the least energy-intensive method. While water-based inks are the most environmentally friendly, the water evaporation rate is relatively slow. To achieve better stability at higher printing speeds, solvents with higher vapour pressure are often employed. Ethanol is an example of such a solvent, as it evaporates quickly and thus speeds up the solidification process after extrusion. However, faster evaporation can lead to uncontrollable and nonuniform shrinkage, ultimately reducing print accuracy and precision (Xu et al, 2022). Striking a balance between quicker solidification and more controlled shrinkage is thus key to attaining good print quality when using this solidification mechanism.

In thermal-assisted solidification, heat is applied to facilitate the solidification or curing of the printed material. By subjecting the print to controlled temperatures, the material undergoes a faster and more controlled curing process, resulting in improved shape stability, accuracy and mechanical properties of the final print. However, it has some drawbacks. First, this solidification mechanism is the most energy-intensive of the ones

presented. second, some materials in the ink may degrade or exhibit undesirable behaviour when subjected to elevated temperatures. Third, rapid or uneven drying through heating can lead to warping in the printed structure, especially if there are variations in material composition or thickness (Xu et al., 2022).

Out of the three main mechanisms, UV-curing allows for the quickest solidification and as a result, for the quickest print speeds. UV curing utilizes UV light to solidify inks through photopolymerization (Figure 22). Compared to thermal processing, it is a less energy-intensive method, but still more energy-intensive than solvent-based techniques. The advantage of using UV curing is that it allows for enhanced control over the solidification process, resulting in less brittleness and improved shape fidelity and accuracy of prints. However, it does have some limitations. Rapid curing can prevent layers from melding together properly, resulting in anisotropic mechanical properties arising due to a lack of strong inter-layer bonding.

Figure 22: Schematic representation of the UV-curing in DIW (Balani et al., 2022, Fig 6)



Second, the printing nozzle can easily clog when the UV-curing process spreads to the nozzle during printing (Xu et al., 2022). In addition, some materials may not be compatible with UV curing, which may limit their use in certain applications (Balani et al., 2021; Xu et al., 2022; Wilt et al., 2021).

An additional noteworthy solidification method, developed by Badr et al. (2022), is the in-situ crosslinking of sodium alginate-based prints through a CaCl₂ crosslinker mist. Higher mist flow rates led to better gelation and affected the mechanical properties and

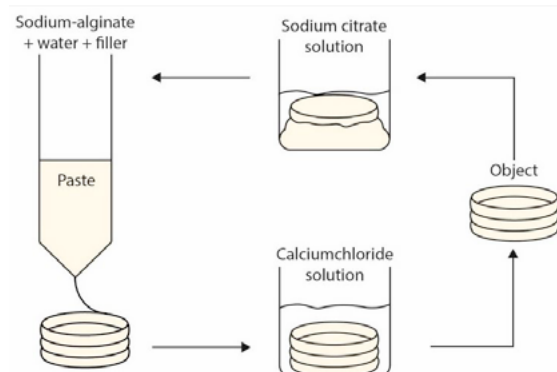
shape stability of the printed constructs. However, too high flow rates resulted in over-gelation, poor interlayer bonding and reduced dimensional accuracy. Closely controlling the mist flow rate is crucial for high-quality printing. Other crosslinking mechanisms can also be applied for in-situ solidification (Shahbazy & Jäger, 2021).

2.4.3 POST-PROCESS OPTIMIZATION

Lastly, post-print treatments can help to improve the final mechanical properties, stability, and functionality of the printed object. Post-treatments can be categorized into three main groups: thermal treatments, chemical treatments, and mechanical treatments. Thermal treatments involve processes like sintering and thermal annealing to enhance structural integrity and mechanical properties. Chemical treatments, such as cross-linking, focus on modifying the molecular structure of the printed material to improve mechanical properties or functionalities such as water insolubility. Mechanical treatments encompass processes like surface smoothing and polishing which improve the surface finish and overall shape accuracy of the printed object.

A good example of a post-process treatment to enhance the functionality of a print is the research of Sauerwein et al. (2020). Within this research, alginate-based prints were crosslinked with CaCl to achieve water insolubility and reverse crosslinked with Na-citrate to allow for reprintability (Figure 23).

Figure 23: Water Insolubility and Reprintability process based on ion cross-linking (Sauerwein et al, 2020, Fig 3)



2.5 CHALLENGES AND LIMITATIONS

While DIW offers promising capabilities for printing with biobased materials at room temperature, there are still significant challenges that limit its large-scale adoption. This chapter discusses these challenges and limitations.

3.3.1. LOW EFFICIENCY

One of DIW's main limitations is its lower print resolution and speed compared to other commercialised manufacturing methods. Printing large structures with high-resolution details would require infeasible production times. Especially when taking into account the time spent on ink formulation and parameter optimization (Saadi et al., 2022; Rocha et al., 2020; Shahbazi & Jäger, 2020).

3.3.2. INTERFACE INTEGRITY & MECHANICAL PROPERTIES

In addition to DIW's already relatively slow printing speeds, print speed also negatively correlates with interface integrity. Because of DIW's layer-by-layer deposition, printing at higher speeds results in poorer bonding between layers. This paradox is an important limitation of DIW and has an especially big influence on the printing of large-scale structures (Saadi et al., 2022).

Moreover, structural defects such as trapped gas or other paste irregularities are common in DIW and can cause poor bonding between layers (Saadi et al., 2022; Rocha et al. 2020; Shahbazi & Jäger, 2020). Additionally, non-treated natural waste sources can have high percentages of extractives (e.g. fats and waxes) that can negatively affect the interface integrity. Pre-treatment of these materials might be necessary to gain sufficient interface integrity for the desired mechanical properties of the final print (De Prá Andrade et al, 2021)

3.3.3. STRUCTURAL DEFORMATION

Printing high structures, overhangs, or bridging features in DIW poses a significant challenge due to its reliance on the post-extrusion (low shear) viscosity of the material to maintain its structure before solidification. This often leads to the self-weight of a structure causing structural deformation or failure. Printing stable structures requires precise material formulation based on its rheology. However, even with optimized rheology, there are inherent limitations to the achievable features (Saadi et al., 2022; Rocha et al., 2020). When the rheology requirements for shape retention can not be met, secondary processes such as curing, drying and cross-linking can be adapted to achieve the required results (Wilt et al., 2021).

Additionally, water-based bio-composites for DIW printing are extremely sensitive to shrinkage. Especially when organic fillers are used (Sauerwein et al., 2020)

3.3.4. NOZZLE CLOGGING

The susceptibility of DIW to nozzle clogging is another main limitation of this method. Clogging frequently occurs since the length of reinforcement fibres in DIW inks is comparable to the nozzle diameter. Clogging can be caused by varying mechanisms near the nozzle tip, such as the accumulation of misaligned fibres and fibre entanglement. These mechanisms are influenced by parameters such as the fibre length, volume fraction and nozzle geometry (Croom et al., 2021). However, Gudipaty et al (2011) found that even when fibre fractions are low, clogging can still be caused by the clustering of particles on the nozzle wall. Hence, minimizing nozzle clogging requires appropriate processing of the material and effective control of material flow through the optimization of printing parameters and nozzle design (Saadi et al., 2022).

Guo et al. (2023), for example, showed that optimizing the geometry of the nozzle can play a crucial role in preventing clogging.

By identifying the “dead-zones” where material flow is compromised, they were able to propose a redesign with an improved flow path. Reducing the chances of entanglement or accumulation of fibres.

3.3.5. MATERIAL FORMULATION & PRINTING CONDITIONS

Even though DIW’s flexibility in the use of different material types, the printability of these materials highly depends on their rheology characteristics. DIW asks for a material that flows easily during extrusion yet maintains its shape after deposition. To achieve this, precise rheology criteria have to be met which makes developing inks from novel materials a challenging and time-consuming task. Additionally, Different materials, with differences in rheology have to be extruded under different conditions (Rocha et al, 2020; Saadi et al.,2022).

As of today, no general guidelines or holistic methods have been developed that can help formulate inks for optimized rheology or translates the material’s rheology to its optimal printing conditions. Hence no models exist that can relate the rheology properties to the print performance (Saadi et al.,2022). Currently, material development for DIW, especially with novel materials, is a trial-and-error-based process.

Additionally, natural resources used in these bio-inks, especially waste-stream materials, can have different properties depending on their batch and their origin. The weight percentage of components in Pecan shells, for example, can differ greatly depending on the country of origin (De Prá Andrade et al., 2021).

3.3.6. POST-PROCESS SUSTAINABILITY

Though the energy demand of DIW is significantly lower than that of other AM methods and most traditional manufacturing methods, prints often require additional processing to achieve the desired quality.

Hence, the additional environmental impact and production cost of solidification methods such as curing, drying, cross-linking and sintering need to be taken into account. (Rocha et al, 2020; Saadi et al.,2022).

3.3.7. STATIC COST OF PRODUCTION

Similar to other AM methods, the cost of producing a single unit stays the same even with increased batch size. Hence, when larger batch sizes are required, DIW will not be cost-competitive with traditional manufacturing methods. Its low amount of initial investment does allow it to compete with other methods when batch sizes are small (Saadi et al.,2022).

2.6 KNOWLEDGE GAP

The exploration of new methods and materials for 3D printing, driven by the need for sustainable manufacturing, has led to innovative approaches utilizing unused waste sources and room-temperature printing. This approach holds promise in significantly mitigating the environmental impact of 3D printing, yet the current literature underscores substantial challenges in establishing these methods and materials as viable alternatives.

2.6.1 PRIMARY RESEARCH QUESTIONS

Achieving satisfactory print quality remains one of the most persistent challenges. Most current research using bio-materials and ambient printing predominantly focuses on the field of tissue engineering, where biocompatibility and cell viability are put higher on the priority list than print quality. While studies like those by Faludi et al. (2019) and Sauerwein et al. (2020) have expanded the scope to wider applications, they highlight the importance of enhancing print quality to match the standards set by conventional 3D printing materials.

The struggle to improve the print quality of bio-material printed at ambient temperatures highlights a gap in the understanding of the complex relationship between ink formulation, print parameters and print quality.

In trying to understand these relationships, many researchers do point out the significant influence of rheology characteristics. However, none have managed to translate this data to general guidelines or holistic methods that can help formulate inks for optimized rheology.

With all of this in mind, the identified gap has prompted the formulation of the following research question that will be addressed throughout this research:

1. What is the effect of ink formulation, print parameters and environmental factors on the resulting print quality of biowaste-derived materials fabricated under ambient conditions?

1. How does varying the composition and preparation of the ink formulation impact the print quality?
2. How do adjustments in print parameters (e.g. speed, layer height, jerk) influence the print quality?
3. To what extent do environmental factors play a role in the print quality achieved?

2. What are the specific rheology characteristics that need to be considered when formulating inks for optimized print quality?

2.6.2 SECONDARY RESEARCH QUESTION

Although it is not the main focus of this thesis, the literature highlights some additional limitations and advantages of water-based Bio inks with solvent-assisted solidification that are worth exploring. These bio-inks are often

water-soluble, which can significantly reduce their durability. However, this characteristic can also be considered an advantage, as it can enhance the biodegradability and reprintability of the material. This leads to an interesting research question regarding the print quality and reprintability of these materials:

3. To what extent does reprinting biobased materials at ambient temperatures affect the print quality across successive printing cycles and what factors contribute to maintaining or degrading print quality over these multiple cycles?

Some researchers are working on developing materials that are both reprintable and water-insoluble to overcome their limited durability. For example, Sauerwein et al. have successfully created an alginate-based material that is both water-insoluble and reprintable through post-process reversible crosslinking.

Unfortunately, alginate-based recipes exhibit relatively high shrinkage and lower print quality. In summary, the development of materials with good print quality, water insolubility, and reprintability remains a challenge. This has led to the exploration of the following research question, albeit with lower priority:

4. How can the print quality of alginate-based recipes be improved to create a material with good print quality, reprintability, and water resistance?

Through systematic investigation, each phase of this research addresses key aspects of the research questions, contributing to a comprehensive understanding of how these factors can be optimized for sustainable and high- print quality ambient printing with biowaste-derived materials.



3. EXPERIMENTAL EXPLORATION

During the preliminary research phase, various ink compositions were tested by drawing on previous research and knowledge from literature. The primary aim was to discover new compositions that displayed promising printability through tinkering. This helped to deepen the understanding of the material's behaviour and provided answers to the research question:

How does varying the ink formulation's composition and preparation affect the print quality? (RQ.1.1)

By doing so, it established a strong foundation for further optimization of the ink formulation and print parameters in the Subsequent phase (Chapter 4).

3.1 INGREDIENT SELECTION

To begin, biobased ingredients suitable for room-temperature extrusion needed to be selected. Prior research and insights from the literature were used to identify candidate ingredients. The objective was to gather ingredients that aligned with the principles of sustainability, were compatible with the room temperature printing process, and had the potential for achieving high print quality. As was explained in Chapter 2.2, materials for room-temperature printing consist of the following main ingredients: Fillers, Binders and solvents. Additionally, additives can be used to improve the behaviour of the material and add additional functionalities.

3.1.1 FILLER SELECTION: PECAN SHELLS

Apart from formulating a biobased material that can be printed at room temperature, one of the other goals of this research was to use an unutilized waste source as a filler material. Though there are many unutilized waste sources, the choice was made to keep the filler material consistent throughout the tinkering and development process. The choice of filler material was based on the size and availability of the waste source, its potential future growth, the suitability of its composition and morphology and its previous performance in additive manufacturing. Based on these criteria pecan shells were selected as the most suitable waste source for the filler material (Figure 24).

Figure 24: Pecan in Shell, (Southeastern Reduction Company, n.d.).



3.1.1.1 A LARGE AND GROWING WASTE SOURCE

The United States is the world's largest pecan-producing country, contributing to 80-90% of the global production (Mordor Intelligence, 2023)

In 2022, the US produced approximately 265 million pounds of pecans (National Agricultural Statistics Service (NASS) et al., 2023). With 50% of the pecan's weight coming from the shell (De Prá Andrade et al., 2021), this corresponds to 132.5 million pounds of pecan shell waste; a large amount of waste which can be used for other applications.

While pecan shell waste is already being repurposed for the manufacturing of cereal bars, as a nutritional supplement and as a replacement for activated carbon, a significant amount remains unused. Research indicates that in 2011, approximately 55 million kilograms of pecan shells in the US still ended up as waste (Littlefield et al., 2011). More recent numbers on the amount of waste could unfortunately not be found.

Though the production has been relatively stable over the past years, research predicts an increase in pecan production due to rising demand fuelled by higher consumption of vegan food and growing nutritional awareness among consumers (Mordor Intelligence, 2023).

3.1.1.2 DESIRABLE COMPOSITION & MORPHOLOGY

The composition of a filler can play a large role in the quality of the final material. Pecan nut shells (PNS) are composed of holocellulose, lignin, ash, and extractives. Among these components, holocellulose plays a pivotal role in determining the mechanical properties of the pecan shell, while lignin significantly contributes to its thermal stability. However, an excess of lignin content can lead to undesired brittleness in composites (De Prá Andrade et al., 2021).

In determining the ideal Pecan Nut Shell (PNS) for a specific application, it is essential to consider the desired material properties. For room-temperature printing, where mechanical strength takes precedence over thermal stability, selecting Pecan shells with a higher cellulose content is desirable.

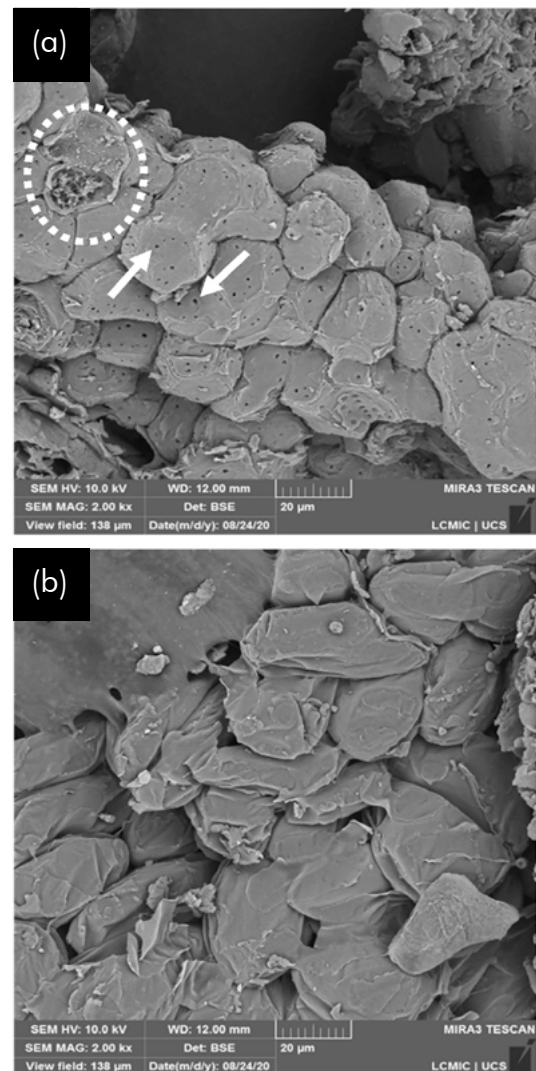
The composition of PNS can vary based on factors such as climate, geographical location, and harvest year (De Prá Andrade et al., 2021). When selecting pecan shells for high-end production, this can be taken into account. For this research, however, the selection of PNS was determined based on availability.

Another factor influencing the print performance of PNS is its morphology. Microscopic images of PNS show irregularities and pores (Figure 25a). These features can improve the physical interaction with other materials, such as matrix materials, providing anchor points for mechanical interlocking. Extractives (e.g. fats, waxes and proteins), however, can interfere with these physical interactions between fibres and matrix. Figure 25b, shows how these extractives can cover the surface of cells leading to reduced irregularities and pores for materials to latch onto.

When extractive levels are high in PNS, it can thus be valuable to use a pre-treatment to remove them (De Prá Andrade et al., 2021). Sánchez-Acosta et al. (2019), found that in untreated PS, fatty acids acted as a lubricant agent which decreased the filler-polymer interaction. Polymers with treated PS showed higher densities, flexural moduli, impact strengths, storage moduli and crystallinity.

However, extractives such as polyphenols and proanthocyanins are recognized for their antioxidant activity and serve to protect from bacterial and fungal decay, which keeps the fibre properties consistent over time. Removing these extractives using heat treatment could result in faster decay of mechanical properties over time. Both the advantages and disadvantages of pretreatments thus need to be considered.

Figure 25: SEM images of irregularities and pores in PNS-surface (a) compared to PNS surface covered by extractives (b) (De Prá Andrade et al., 2021, p.2232, Fig. 1)



Another advantage of using Pecan Nut Shells (PNS) in DIW printing lies in their oval-shaped cells. When PNS is ground to pecan shell flour (PSF) for ink formulation, these oval-shaped shells improve the flowability of the material (Southeastern Reduction Company, n.d.).

Additionally, these cells are sclereid, which means they are dead at maturity (i.e. when the pecan falls off the tree), meaning no decay occurs from the death of live cells, making their properties more consistent.

3.1.1.3 PSF USE IN THIS RESEARCH

Concluding, The large amounts of pecan shells wasted in combination with their mechanical, thermal and morphological properties, make it a valuable source as a filler.

While it may be argued that this source is not indigenous to the Netherlands and therefore less sustainable for the creation of printable paste materials predominantly used in this area, it should be noted that such negative effects would be eradicated if the material were produced and utilized in the United States. PNS was thus selected for use in this study.

For all experiments, pre-ground pecan shell, also known as pecan shell flour (PSF) was gathered from the South-eastern Reduction Company (Figure 26). 99.9% of the utilised PSF had a particle size of lower than 149 μm , and 98.2% was lower than 44 μm . The PSF received contains 80% insoluble fibres (lignin and holocellulose), small amounts of fat (<4%) and protein (<3%) and approximately 4.5% polyphenols and 10% proanthocyanins. Its ash content is less than 2% (Southeastern Reduction Company, n.d.). More specific data on the composition was unfortunately not available.

Figure 26: Pecan Shell Flour received from the South-eastern Reduction Company



3.1.2 BINDER SELECTION

Another important ingredient in the ink formulation is the binder, also referred to as the matrix material. The binder serves as a matrix for the other ingredients to latch onto. Without a proper binder, formulations would have no structural integrity. The selection of suitable binders for ink formulation was guided by the following criteria:

1. The materials' solidification mechanisms are not driven by temperature change or other high energy-consuming mechanisms (e.g. UV-curing)
2. The materials are non-toxic and biodegradable
3. The materials are commonly accessible

Previous results on print quality with the potential binders were also taken into consideration and materials found in the lab were evaluated on their potential for use in the recipes. Ideally materials selected were from natural and abundant resources, however, some synthetic sources were also chosen for testing due to their good performance in previous research and their availability at the lab. In addition, the use of synthetic binders will most likely result in improved mechanical properties. Though improving the mechanical strength of the print materials was not the aim of this research, experimenting with some of these materials was deemed valuable.

Table 3 gives an overview of the natural and Table 4 of the synthetic binders selected for in-depth tinkering. The tables include the process of deriving the material and the sources of the materials used in this research.

Table 3: Natural binders used in the tinkering phase. Including the extraction/production process and the source of the specific binders used.

All Binder (AB)	Casein (Cas)	Arabic Gum (AG)	Guar Gum (GG)
			
<ul style="list-style-type: none"> Derived from sources like corn, wheat and/or potatoes. Source: Honig. 	<ul style="list-style-type: none"> Manually extracted from skim milk. Source: Campina's "elk melkpowder." 	<ul style="list-style-type: none"> Derived from the sap of Acacia trees. Source: Voordeelkruiden.nl 	<ul style="list-style-type: none"> Derived from Seeds of the Guar Plant. Source: Voordeelkruiden.nl
Natural Latex (NL)	Calcium Lignosulfonate (CL)	Sodium Alginate (SA)	
			
<ul style="list-style-type: none"> Derived from the Amazonian rubber tree. Source: Laguna 	<ul style="list-style-type: none"> Derived from wood/plant through sulphite pulping process. Source: Lignostar, Starling CA 	<ul style="list-style-type: none"> Derived from brown seaweeds. Source: Unique Products Alginate, Oldenhof.nl 	

Table 4: Synthetic binders used in the tinkering phase. Including the extraction/production process and the source of the specific binders used.

All Purpose Glue (APG)	Sodium Silicate (SS)	Polyvinyl Alcohol (PVA)	
			
<ul style="list-style-type: none"> n/a Source: HEMA 	<ul style="list-style-type: none"> Fusion of sodium carbonate and silica sand (quartz) at high temperatures. Source: 	<ul style="list-style-type: none"> Polymerization of vinyl acetate, a petrochemical-derived monomer Source: 	

3.1.2.1 ALL BINDER: “ALLES BINDER”

“Alles binder” is a popular food thickener commonly used in culinary applications. It contains natural starches, typically derived from sources like corn, wheat or potatoes, making it safe for consumption and, thus non-toxic and biodegradable.

Additional benefits are that it is readily available and low in cost. However, part of the sustainability of All Binder depends on the way it is sourced; either sourced from waste or a dedicated crop. When sourced from agricultural waste streams, it notably reduces the environmental impact associated with resource-intensive practices like water, fertilizer, and pesticide usage, thus aligning it with a more environmentally sustainable choice for a binder. No data could be found on whether all binder used in this research is sourced from waste.

Previous students following the Advanced Prototyping Minor at the TU Delft gained good results using this binder as an ingredient in their material formulation (Barrow et al., 2022 [unpublished]) (Figure 27).

Figure 27: Prints of Advanced Prototyping Minor students using All Binder (Barrow et al., 2022, [unpublished]).



3.1.2.2 CASEIN

Casein is a natural protein derived from milk, found in the curds that form during milk coagulation. Due to its natural origin, casein biodegrades well.

Due to its good binding properties and rheology characteristics, casein was a key ingredient in traditional casein paints and has even been used to create bioplastics. The fact that it has been used for the manufacturing of paints makes this binder interesting for this application. The thixotropic behaviour necessary for paints is very similar to that needed for room-temperature 3D printing; The material needs to flow (or smear) when under shear and hold its shape (not drip) when shear is removed. This is further substantiated by the use of casein by Liu et al. (2019) in 3D food printing.

Though casein shows great qualities regarding rheology, some concerns are worth stating. Firstly, dairy farming can be very resource-intensive and the extraction of casein requires the “wasting” of a valuable food source. Casein is not a waste product unless it is extracted from leftover dairy. Additionally, shelf-life might offer a problem. Casein-based materials can go “bad” relatively quickly and are sensitive to moisture (Bonnaillie et al., 2014).

In this research, casein was manually extracted from skim milk powder by adding water followed by the next steps: adding vinegar for curdling, straining to separate curds from whey, and naturalisation of the PH-value through the addition of baking soda. The ratio of ingredients used was: 5 water: 1 milk powder: 1 Vinegar: 0.25 Baking Soda. The resulting casein was used in the formulation of recipes during tinkering. When recipes proved to not mix well, some additional baking soda was added in the tinkering process.

3.1.2.3 ARABIC GUM

Derived from the sap of Acacia trees, Arabic gum is a natural binder and thickening agent that finds use in the food, pharmaceutical, and cosmetic industries for its stabilizing and thickening properties. This entirely natural ingredient is biodegradable and sourced from renewable sources. Again, its degree of sustainability depends on the harvesting practices used.

Arabic gum was successfully used in a recipe of previous students following the advanced prototyping at the TU Delft (Barrow et al., 2022 [unpublished]). However, only in combination with All Binder (Figure 28). No literature shows research that has successfully formulated inks with AG as a binder alone, and it is mainly used as a rheology modifier. For this reason, it was only used in combination with All Binder in this research.

Figure 28: Prints of Advanced Prototyping Minor students using Arabic gum in combination with All Binder (Barrow et al., 2022 [unpublished]).



3.1.2.4 GUAR GUM

Guar gum is a natural binder material derived from the seeds of the guar plant, which is primarily cultivated in India and Pakistan. It is used as a thickening and stabilizing agent in various industries. Guar gum is considered safe for consumption and is biodegradable. Just as with the other naturally won resources, the degree of sustainability in guar gum production depends on responsible sourcing and farming practices. In terms of additive manufacturing, Guar Gum has been used in bio-inks and composites for uses such as tissue engineering. It is mostly used in combination with other binders.

3.1.2.5 NATURAL LATEX

Natural latex is a biodegradable binder sourced from the rubber tree's sap, it is primarily harvested in regions such as Southeast Asia, Africa, and South America. It finds applications in adhesives, latex paints, and latex foam products.

Being an entirely natural ingredient, it is considered non-toxic and environmentally friendly. Again, sustainability in natural latex production is closely tied to responsible sourcing, tapping methods, and land management practices.

Kim & Choi (2021), showed relatively good printability using Natural Latex, though their formulations using only natural latex without the addition of synthetic latex, did show less dimensional accuracy.

Additionally, previous students from the advanced prototyping minor successfully used natural latex as well. This in combination with its availability in the lab resulted in this binder being used in the tinkering phase.

3.1.2.6 CALCIUM LIGNOSULFONATE

Lignosulfonate is a by-product of the sulphite pulping process, which is a method used in the paper industry to separate cellulose from lignin in wood. Lignosulfonates have a history of use in various products, including road surfaces, pesticide formulations, and animal feedstock. Studies have been conducted to assess their environmental impact, concluding that properly manufactured and applied lignosulfonates are safe for the environment. They are considered non-toxic to plants, animals, and aquatic life (LignoStar Group BV, 2020). An additional benefit of calcium lignosulfonate is that it can enhance soil health. It does this by improving the soil structure, water retention, and nutrient availability.

In their research, Gluewitz et al. (2020), show the potential of using lignin-derived materials in formulations for DIW (Figure 29).

Figure 29: Lignin based ink for DIW by Gluewitz et al. (2020)



Previous results in combination with calcium lignosulfonate being an environmentally friendly by-product/waste product, made it a valuable binder for the tinkering phase.

The Calcium lignosulphonate used in this research was donated by LignoStar, under the name of Starling Ca.

3.1.2.7 SODIUM ALGINATE

Sodium alginate is a natural binder and thickening agent derived from brown seaweed. It is used in various industries, including food, textiles, pharmaceuticals, bio-inks and cosmetics. Being entirely natural and biodegradable, sodium alginate is considered environmentally friendly. Again, Its degree of sustainability largely depends on harvesting practices.

Though sodium Alginate has previously been shown to not yield very good print quality, it was still incorporated in the initial tinkering phase, since it does have great potential for making the final print water insoluble in a reversible manner. This would mean that the final prints can be made water-insoluble for use, after which they can be returned to their water-soluble state for reprintability.

Sauerwein et al. (2020) have successfully proven this principle by creating a water-resistant and reprintable material from mussel shells and sodium alginate through cross-linking. They also developed a recipe using alginate and walnut shells (Figure 30), which can be compared to pecan shells to some extent.

Figure 30: 3D prints by Sauerwein et al. (2020. Fig 6.) with a variety of fillers, from left to right: mussel shell, eggshell, walnut shell, olive pomace, cacao shell, and maple sawdust.



However, it should be noted that these prints did display significant shrinkage, with a 26% reduction in height and a 12% reduction in line width.

3.1.2.8 ALL PURPOSE GLUE

All-purpose glue, a versatile adhesive used in various repairs and crafts, typically contains synthetic components that might not align with sustainability goals. Its production often involves chemicals and may not be biodegradable under normal circumstances, raising concerns about its environmental impact.

The composition of all-purpose glue can vary among manufacturers. The specific components used in its production can differ, making it challenging to ascertain the environmental impact or sustainability of a particular product.

Yet, all-purpose-glue was chosen for initial tinkering, since it was previously used by advanced prototyping students (Alexeev et al., 2021 [unpublished]) and showed promising results in terms of printability (Figure 31).

Figure 31: Pecan Shell Flour and All Purpose Glue Print by Alexeev et al. (2021, [unpublished])



3.1.2.9 SODIUM SILICATE

Sodium silicate, also known as water glass, is typically manufactured through the fusion of sodium carbonate and silica sand (quartz) at high temperatures. It is used for many purposes, among which as a binding agent in adhesives and sealants, which makes it valuable for this application.

Sodium Silicate has also shown previous promising results. Van Sice et al. (2019 [unpublished]) developed a printable paste with both Mica and microcrystalline cellulose fillers with Sodium silicate as a binder (Figure 32). Previous graduation student Ennio Donders (2022) used Sodium Silicate in combination with eggshells to create a printable paste.

Figure 32: Mica and Sodium Silicate print (a) and microcrystalline cellulose and Sodium Silicate print (b) by Van Sice et al. (2019 [unpublished])



However, while versatile, SS poses some sustainability concerns. Its production demands significant energy and relies on raw materials like silica sand and soda ash, often mined with environmental impacts. In addition, in some cases, the release of sodium silicate into natural environments, particularly aquatic ecosystems, can have negative effects on aquatic life due to changes in pH and alkalinity (PubChem, 2023).

3.1.2.10 POLYVINYL ALCOHOL

Polyvinyl alcohol (PVA) is a synthetic polymer used as a binder in various applications. It is typically produced through the polymerization of vinyl acetate, which is a petrochemical-derived monomer. While it is generally non-toxic and considered biodegradable under specific conditions, its sustainability is limited because of its use of non-renewable resources. It is not a natural material and its production involves energy-intensive processes and the use of petrochemical feedstocks, contributing to environmental concerns, including greenhouse gas emissions.

Elmer's school glue was used in the tinkering phase of this research. This glue has PVA as its main ingredient. Previous students successfully used Elmer's glue in formulations for room-temperature printing.

3.1.2 SOLVENTS

The solvents used in this research were limited to a combination of water and ethanol. Though only using water as a solvent would be a more sustainable choice, the addition of ethanol can strongly improve the print quality of the material. The higher evaporation rate of ethanol allows the material to solidify quicker after extrusion, thus decreasing the chances of the print collapsing.

The sustainability of ethanol as a solvent varies depending on factors such as feedstock choice and production methods. Ethanol can be produced from renewable resources, such as sugarcane, corn, or cellulosic biomass as well as from petrochemical feedstock. To minimize the environmental impact a renewable feedstock is thus desirable. Yet, in both cases, the production is likely still water and energy-intensive.

In terms of material formulation, finding the right ratio between water and ethanol is crucial. Too much ethanol would result in too rapid drying of the material before extrusion, increasing the chances of clogging and uneven deposition of material. On the other hand, too little ethanol can reduce the drying rate to an extent that causes the print to collapse after a few layers if a constant print speed is used. An added benefit is the fact that Ethanol and water have different solubility properties. Combining them allows for the dissolution of a wider range of materials.

Within this research, 96% Ethanol from TechSolv Sigmaldrich was used.

3.2 INITIAL TINKERING

Following the selection of ingredients for the material formulation, the next crucial step was to assess the compatibility of these ingredients by formulation of initial recipes. This assessment included two main aspects: compatibility with the printing process itself and compatibility among the chosen ingredients.

The objectives of this stage were to:

1. Find a composition of ingredients that mixes well and creates a homogenous ink
2. Find an ink composition that is extrudable and holds its shape after extrusion

3.2.1 METHOD & MATERIALS

TRIAL-AND-ERROR TINKERING APPROACH

While formulating initial recipes with the selected materials (Chapter 3.1), a structured approach was taken to guide the trial-and-error process:

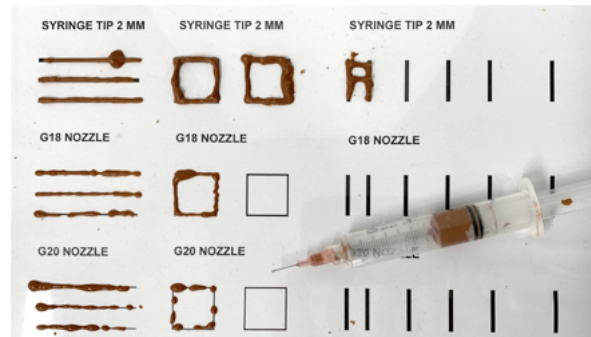
1. If known, existing filler-to-binder-to-solvent ratios from previous research were used as a starting point for formulations.
2. If initial ratios did not perform well, the water-to-solid ratio was gradually adjusted until the desired viscosity for extrusion and shape retention was achieved.
3. When steps 1 and 2 resulted in a sufficiently performing recipe, meaning the material extruded showed uniformity and shape retention, binder-to-filler and water-to-ethanol ratios were fine-tuned for further improvement of the printability and shape retention.

The printability and shape retention of the initial recipe and the adjustments made (steps 1-2) were tested using hand extrusion tests with a 10 ml syringe with Luer Lock.

For all recipes, 3 different extrusion diameters were tested; 2 mm (no nozzle), 0.81 mm

(18 gauge nozzle) and 0.64 mm (20 gauge nozzle). All nozzles that were used had a tip length of 12.7 mm (1/2 Inch). The template shown in Figure 33 was used to guide the hand extrusion test.

Figure 33: Hand Extrusion test template



During step 3, the recipes were printed using the Eazao bio with a pressure control box (Figure 34). To better assess any minor adjustments made, a machine-printed sample was deemed necessary. The use of a printer allowed for consistent extrusion pressure, speed, and layer height, which is impossible to achieve by hand extrusion. Consequently, this provided a more accurate basis for evaluating any modifications.

Both single- and double-walled cubes of 20x20x10 mm were printed for evaluation. A layer height of 0.6 mm was used for all cubes and speeds of 5, 6 and 7 mm/s were tested to see the potential effects of speed on the print quality.

Figure 34: The Eazao Bio with Pressure Control Box.



The extrusion pressure was determined separately for each print since small differences in material and environmental factors were found to influence the necessary pressure for good extrudability. The pressure was adapted until the extruded material showed no signs of under-extrusion or over-extrusion (Figure 35). The extrusion pressure was determined per recipe variation but kept constant during the printing. No fans were used while printing in this phase of the research.

Figure 35: Under- and over-extrusion signs

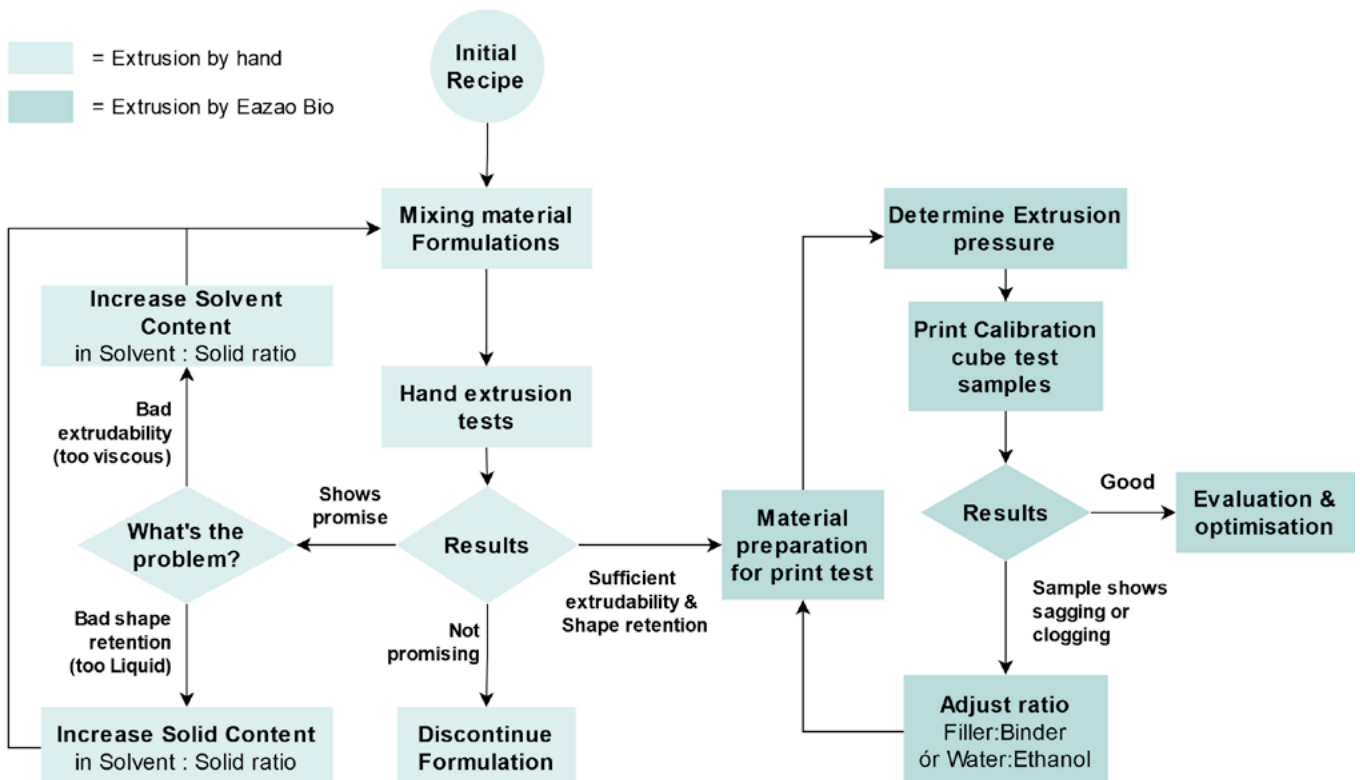


Figure 36 shows the flow diagram of the trial-and-error approach described. It is worth noting that this flow diagram served as a tool to support tinkering not as a strict method to follow.

MATERIAL PREPARATION

The choice of mixing method is essential in shaping the properties of ink formulations. Key ink attributes, such as rheology, material homogeneity, and stability, hinge on the quality of the selected mixing technique. A not properly mixed material can increase the chances of clogging or cause non-uniform extrusion. However, achieving the desired ink properties extends beyond the mixing method alone. Ink formulation not only encompasses the selection of the mixing method but also the precision in measuring ingredients, the order of ingredient addition, and the methodical filling of the printer. Each of these steps contributes significantly to the quality and performance of the ink.

Figure 36: Flow diagram of the trial-and-error tinkering approach



During the tinkering process, a KERNdem scale with a precision of 0.001 was used for weighing all the ingredients. Mixing was done using a laboratory mixer (RW17basic from IKA Lbrotechnik) (Figure 37).

The formulations were mixed for 5 minutes at approximately 360 RPM to ensure consistent shear history across the samples. If a mixture did not achieve homogeneity after the initial 5 minutes, the mixing time was extended accordingly and documented.

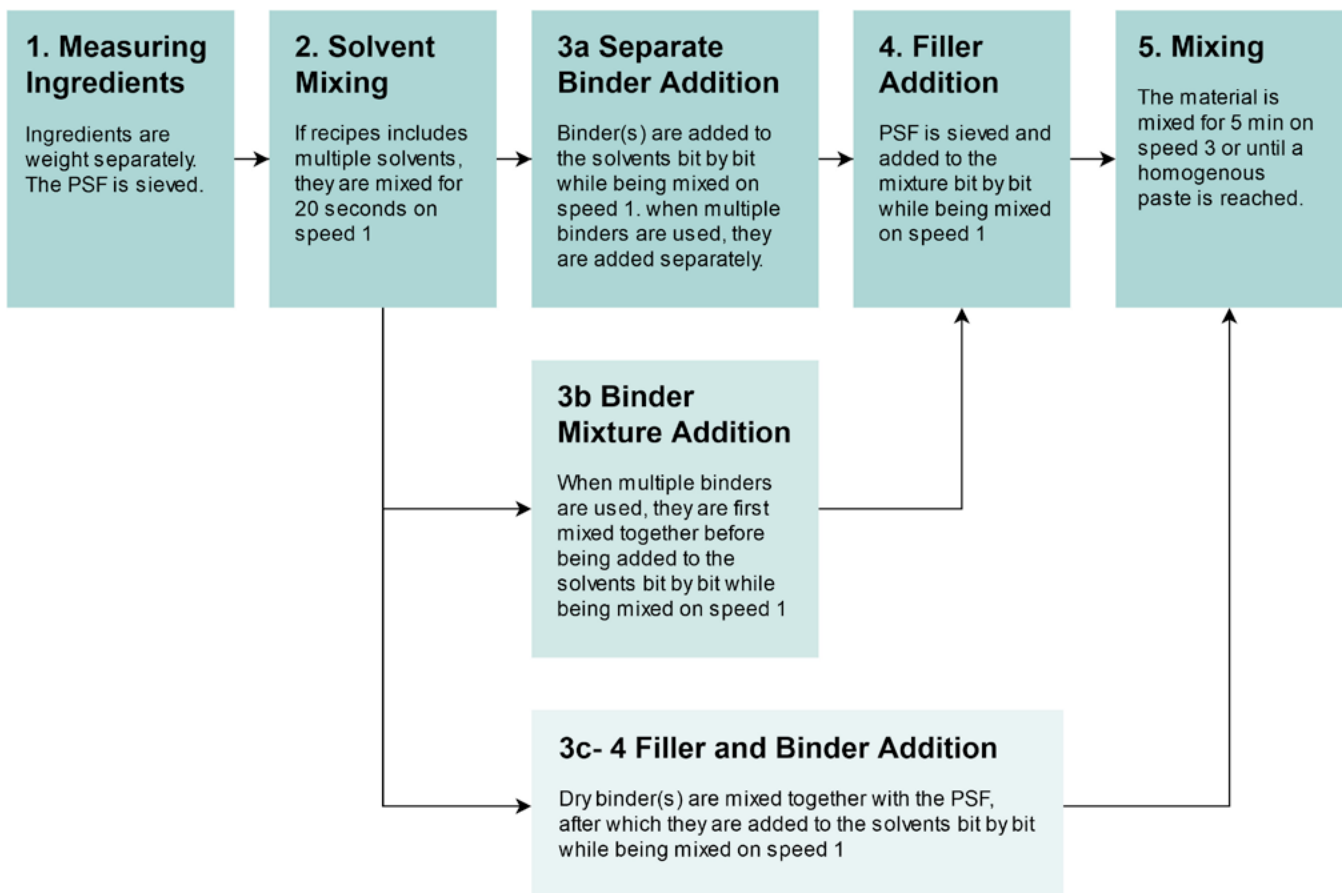
The order of ingredients was varied during the tinkering process to find the optimal mixing method for each recipe.

Figure 38 shows a flow diagram of the mixing procedure, including the variations that were tried out.

Figure 37: Material mixing setup



Figure 38: Material mixing procedure, including the variations experimented with



3.2.2 RESULTS

Table 5 provides an overview of the binders and binder combinations that were tested using the previously outlined approach and preparation method. The table displays the number of ratio variations attempted, along with the outcomes. Each outcome was evaluated using a subjective scoring system ranging from 1 to 5. A score of 1 indicates that the materials and ratios tested exhibited

no compatibility, while a score of 5 indicates that the recipe demonstrated excellent printability.

The different ingredients and mixing variations tested, resulted in four formulations demonstrating excellent extrudability and sufficient shape retention (marked green in Table 5). Within the range of variations tested and the available time, none of the other binders yielded promising results.

Table 5: Overview of the binders and binder combinations tested

Binder(s)	Recipe based on	Adaptations	# Variations	Score	Outcome notes
All Binder (AB)	Barrow et al., 2022 [unpublished]	Pecan instead of Walnut shell	10	5	Good extrudability and shape retention
Casein (Cas)	Trial-and-error	n/a	12	2	Bad Extrudability: non-uniform extrusion
Guar Gum (GG)	Trial-and-error	n/a	4	1	Bad mixability: non-homogenous ink
Natural Latex (NL)	Kim et al.,2021	PSF-filler; different source NL	9	2	Quick clogging
Calcium Lignosulfenate (CL)	Trial-and-error	n/a	8	5	Best surface finish; Improved stability with increasing print speed.
Sodium Alginate (SA)	Sauerwein et al.,2020	Pecan instead of walnut shell; different source SA	3	3	Sufficient shape-retention; bad repeatability; high shrinkage and warping
All Purpose Glue (APG)	Alexeev et al. 2021, [unpublished]	Different source APG;	11	4	Low shrinkage; water resistant to some extent; quick clogging
Sodium Silicate (SS)	Faludi et al.,2019	Different source SS	12	1	Bad Extrudability: non-uniform extrusion
Polyvinyl Alcohol (PVA)	Trial-and-error	n/a	6	2	Clumps form in the mixture.
Sodium Alginate & All Binder (SA+AB)	Trial-and-error	n/a	8	5	Reduced shrinkage and warpage compared to SA
Sodium Alginate & Calcium Lignosulfenate (SA+CL)	Trial-and-error	n/a	4	1	CL and SA are not compatible
All Binder & Arabic Gum (AB+AG)	Barrow et al., 2022 [unpublished]	Different source AG	6	3	Difficult to extrude with smaller nozzles without causing non-uniform extrusion or bad shape retention

3.2.2.1 MIXING PROCEDURE

Among all variations tested, a notable variability in the effectiveness of different mixing approaches and mixing times was found. This suggests that no universally superior approach exists. Rather, the choice of mixing technique appears to depend on the composition of the formulation.

Take for example the All Binder and Sodium Alginate recipe. First Mixing the AB and SA before adding them to the solvents in the formation of a paste in just 10 minutes, an improvement compared to the approximately 30 minutes or more required when SA was first mixed with the solvents. Interestingly, this approach resulted in a rougher surface finish but showed better quality in corners (Figure 39). This suggests potential variations in ingredient interactions and, potentially, even differences in mechanical properties.

Figure 39: Surface finish and corner differences with varying mixing procedures applied in the AB+SA recipe.



These findings emphasize the necessity of customizing mixing protocols to suit the distinctive attributes of the ingredients used in the formulation and the desired outcomes. Just like with the formulation of a recipe, the finding of the optimal mixing procedure is a trial-and-error process. Nevertheless, it was noted that in all recipes tested, the mixing

of (dry) binders and fillers before solvent addition led to suboptimal mixtures (Step 3c-4 in Figure 38). Despite the intent to improve mixing efficiency and achieve a more uniform particle distribution, this approach yielded less consistent and reproducible results across the board.

3.2.2.2 COMPATIBLE FORMULATIONS

The four formulations with good compatibility between the ingredients and the printing process are discussed in this section. Table 6 shows the final composition of the recipes developed in this phase, including the mixing order which showed the best results.

ALL BINDER-BASED RECIPE

Figure 40 shows samples printed with AB during the tinkering process. Other filler-to-binder ratios were tested, however, they showed immediate problems when extruded and are thus not shown.

Only double-walled samples showed sufficient stability. Additionally, a speed of 5 mm/s led to over-extrusion even when the extrusion pressure was kept low. No difficulties such as clogging occurred during printing with AB-based formulations when the right formulation was found. However, of all promising recipes, this recipe showed the most sensitivity to changes in extrusion pressure. Small adjustments resulted in under or over-extrusion fairly quickly. Luckily, over the span of a print, there was no need for adjustments to the extrusion pressure once the right pressure was determined.

Table 6: Final Tinkering Recipes

Recipe Name	Recipe Formulation (weight %)	Mixing Order
AB	20 PSF, 48 AB, 20 Water, 12 Ethanol	Solvents – AB - PSF
CL	32 PSF, 32 CL, 25 Water, 11 Ethanol	Solvents – CL – PSF
AB+SA	17 PSF, 43 AB, 3 SA, 25 Water, 12 Ethanol	Mix AB and SA – Solvents -PSF
APG	40 PSF, 22 APG, 11 Water, 27 Ethanol	Solvents – APG - PSF

In terms of mixing, first dissolving the all binder in the solvents before adding the PSF showed the best results. A homogenous paste was reached within the 5-minute mixing time. It was however noted that achieving a uniform mixture using the laboratory mixer showed some difficulties. Without intervention, no singular cohesive mass was achieved through mixing, resulting in portions remaining unmixed within the beaker. Consequently, human intervention was needed for proper mixing.

CALCIUM LIGNOSULFONATE-BASED RECIPE

Figure 41 shows some of the samples printed with CL. Again, only double-walled samples showed sufficient stability. While tinkering with CL, some noteworthy observations were made.

First of all, the use of CL as a binder resulted in improved efficiency of the mixing process.

Mixtures with CL reached a homogenous paste quicker than the other successful recipes. This is coherent with CL's use as a dispersant agent in other applications. Practically no human intervention was needed to reach a homogenous paste.

Secondly, CL showed improved shape fidelity at the higher print speeds (7 mm/s) compared to the lower print speeds (5 and 6 mm/s). This brought forward the hypothesis that with an increasing shear rate either the percentage of recovered viscosity or the recovery time improves. Yet, CL does not perform better at the highest speed tested when compared to the other recipes. If the CL-based recipe is able to print with good quality up to a higher speed, is further investigated in Chapter 4.

Additionally, CL-based recipes show the smoothest and glossiest surface finish of all recipes tested.

Figure 40: AB-based recipe samples



Figure 41: CL-based recipe samples with improvement in shape fidelity when print speed is increased.

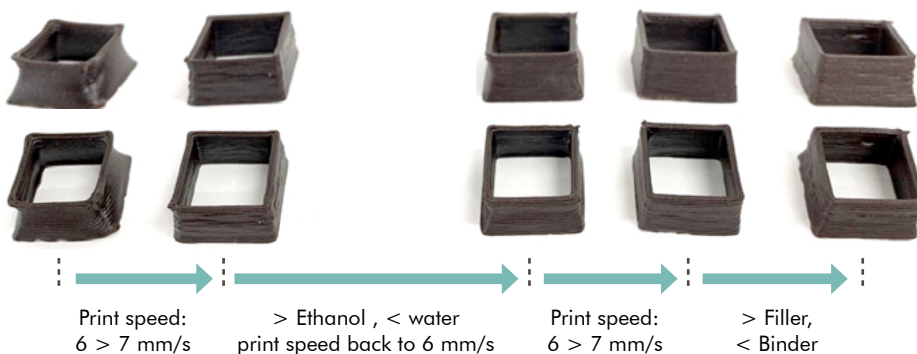
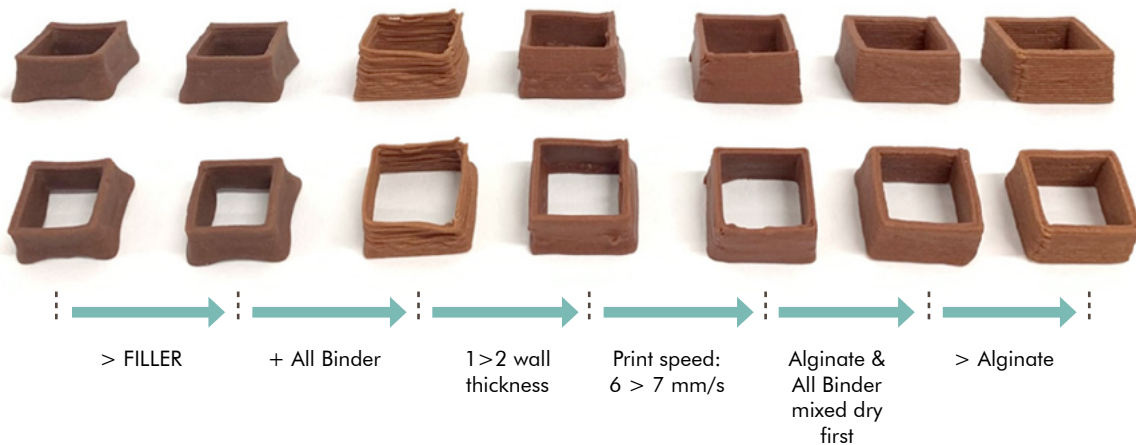


Figure 42: SA+AB-based recipe tinkering samples. First two samples do not include AB.



SODIUM ALGINATE & ALL BINDER-BASED RECIPE

Figure 42 shows samples printed using a combination of SA and AB during the tinkering process. Initially, it was observed that SA alone yielded suboptimal results. Although a formulation was identified to achieve satisfactory shape retention, the samples exhibited significant warping, shrinkage, and cracking. To mitigate these undesirable effects, formulations incorporating additional CL or AB were explored. While CL demonstrated poor compatibility with SA, the addition of AB yielded promising outcomes.

As discussed in Chapter 3.2.1.7 SA was chosen as a binder for tinkering due to its capacity for achieving water insolubility through cross-linking. With the introduction of AB into the formulation, the question remains if cross-linking of SA can still result in water insolubility.

In terms of mixing, first mixing the AB with the AG showed the best overall results (as discussed). though it had a slightly negative effect on the surface quality, this method allowed for quicker dissolving of the binders and improved corner quality.

In the course of experimentation, it was further observed that SA only exhibited solubility in water and not in ethanol. Formulations exclusively comprising SA demonstrated suboptimal outcomes when ethanol was

added as an additional solvent. Notably, upon extrusion of these formulations, ethanol appeared to segregate from the remainder of the mixture, leaving a lump of material within the syringe (Figure 43).

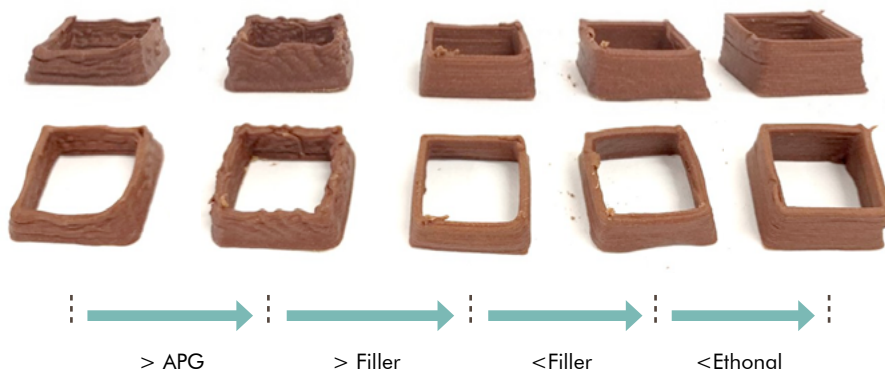
Figure 43: Ethanol segregating from the remainder of the mixture, leaving a lump of material within the syringe.



However, with the inclusion of AB, ethanol demonstrated compatibility with the formulation, suggesting that AB was capable of dissolving in ethanol and establishing a cohesive bond with the in-water-dissolved SA.

Lastly, the biggest disadvantage of this recipe is its sensitivity to procedural errors or changes, making it more difficult to get consistent results. Slight changes in the mixing process resulted in large differences in print results.

Figure 44: APG-based recipe tinkering samples



ALL PURPOSE GLUE-BASED RECIPE

Figure 44 shows samples printed with APG in step 3 of the tinkering method. APG's main limitation was its sensitivity to clogging and the need to change the extrusion pressure throughout the printing process. Both of these limitations are likely caused by the hardening rate of the APG within the formulation.

Noteworthy, however, is the fact that when thrown in water, the APG samples did not immediately deteriorate, which was the case for the other recipes developed. The reason for this resistance to water is the solidification process of glues. Most glues work by creating chemical bonds between molecules, and once they dry, these bonds are generally irreversible. Adding water to the material with dried glue thus does not cause it to form a paste again. This also means turning the dried prints into a reprintable paste will not be as easy as adding water to the grinded-up prints. This is supported by previous research by students not succeeding in generating a reprintable paste from prints with APG (Alexeev et al., 2021 [unpublished]).

Finally, among all the promising recipes, those incorporating APG are anticipated to yield the most favourable results in terms of mechanical properties. However, given that this aspect falls outside the scope of this research, it has been assigned a lower priority and has not been subjected to testing. Moreover, it is

worth noting that replicating the results from previous students using an APG-based recipe was unsuccessful. When printing with the recipe developed in this research, clogging was observed to occur almost instantly. This phenomenon may be attributed to potential variations in the composition of the all-purpose glue used, or potentially the method of extrusion. In this research, the extrusion relied on air pressure rather than pressure generated by a piston. If air pressure-driven extrusion can lead to quicker clogging could be a valuable topic for future research. One plausible hypothesis is that the continuous influx of air with lower moisture content may speed up the evaporation of solvents within the syringe, potentially increasing the likelihood of clogging.

3.2.2.3 INCOMPATIBLE FORMULATIONS

Of all the binders tested, some showed incompatibility with the other ingredients in the formulation or with the printing process. While prior studies have explored the utilization of PVA (Elmer's glue) SS, it was observed that these binders exhibited incompatibility with both the PSF and the solvents employed in this particular study. Notably, both formed lumpy and non-uniform pastes which proved to not be extrudable.

Natural Latex, too, demonstrated incompatibility, yielding predominantly clumpy paste across various attempts.

Although a uniform paste was eventually achieved, it was observed that the natural Latex vulcanized quickly, consequently causing rapid clogging within the nozzle.

The discrepancies in results with previous research may stem from the differences in the source of the binders and fillers or their potential status as residual materials from the laboratory, possibly having exceeded their designated shelf life. Moreover, it is worth noting that the variations conducted were limited, leaving the possibility that alternative ratios might still yield compatible results.

Regarding the experimentation involving casein, it may be advisable to explore the use of commercially sourced casein as opposed to manually extracted casein. The casein extracted from skim milk manually proved challenging to dissolve within the formulation, leading to a non-homogenous paste. It is anticipated that employing commercial casein powder would eliminate this issue.

3.2.3 CONCLUSION TINKERING

Tinkering resulted in the development of 4 recipes with each their advantages and disadvantages. In terms of print quality, further evaluation is necessary to properly compare them. However, some interesting conclusions can be drawn regarding their sustainability, process efficiency and repeatability.

The sustainability of a material depends not only on the sourcing of the material but also on factors such as its durability and end-of-life scenario. This introduces a notable paradox in the findings. On one hand, the APG-based recipe offers water resistance and likely superior mechanical properties, enhancing durability. However, samples containing APG cannot be easily reprinted, likely require special conditions for biodegradability and are less sustainably sourced. In contrast, recipes using more sustainably sourced materials like AB and CL, offer more potential for reprintability and biodegrade easily. The choice between these materials ultimately depends on the specific application.

Formulations that incorporate SA may present an intriguing middle ground, offering both water resistance and reprintability through reversible crosslinking. This could bring added value to the recipe. However, this possibility requires further investigation.

Another significant conclusion to draw from the study pertains to process efficiency. CL-based recipes demonstrate superior efficiency, characterized by rapid mixing with minimal human intervention, resulting in the formation of a homogeneous paste in a short period. Both APG and AB-based recipes show inefficiencies primarily due to the mixer's limitations in accessing specific areas within the beaker. Should production be scaled up, a redesigned mixer could rectify this issue.

In the case of SA-based recipes, the most prominent challenge lies in the extended time required for SA dissolution, which is likely to remain a limiting factor. Additionally, SA-based recipes displayed difficulties in terms of repeatability of the results. This is a problem that would have to be further investigated and solved if this material is adopted.

3.3 INITIAL EVALUATION OF PRINT QUALITY

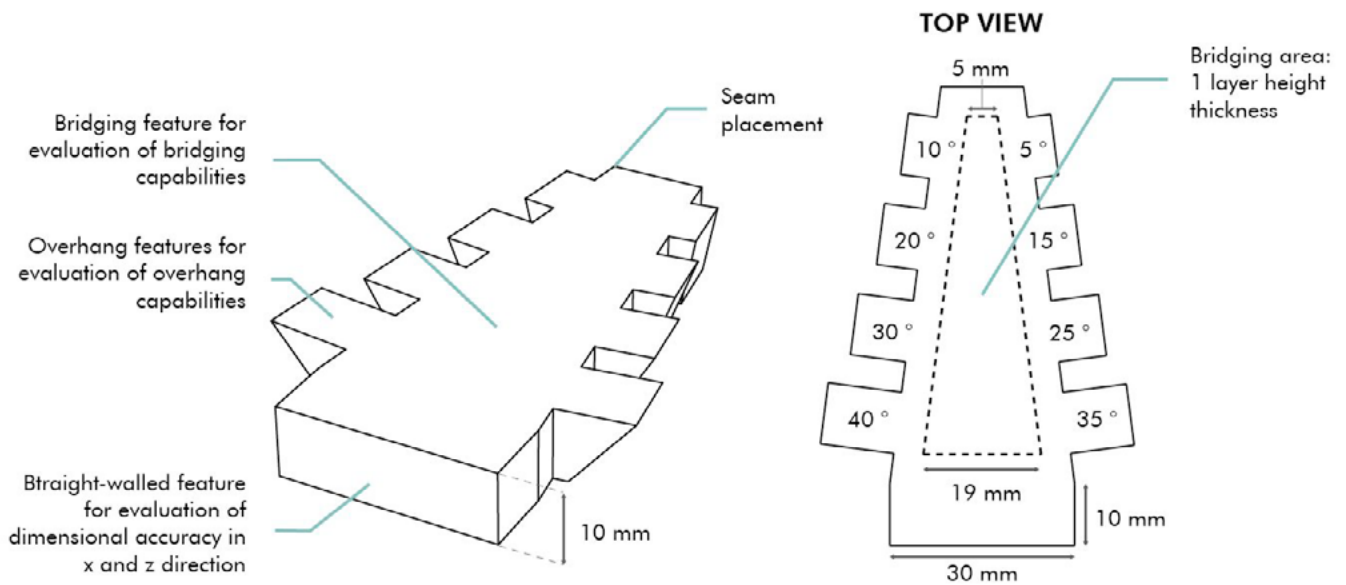
To allow for a good starting point for further optimisation, the objective of this part of the research was to assess the print quality of the most promising recipes from the initial exploration phase (Chapter 3.2). Based on this, a well-substantiated choice could be made on what materials to move forward with and which aspects of them needed to be optimised.

3.3.1. METHOD & MATERIALS

3.3.1.1 EXPERIMENTAL SETUP

Using a specially designed model for checking the print quality (Figure 45), the dimensional accuracy, bridging, overhang and surface finish were assessed.

Figure 45: Print quality assesment model



The model was printed on the Eazao Bio with a commercial fan pointing at the print bed (Figure 46). One print was made for each of the recipes. The seam of the print was placed in a corner that would not disrupt any measurements.

Figure 46: Eazao Bio with commercial fan setup

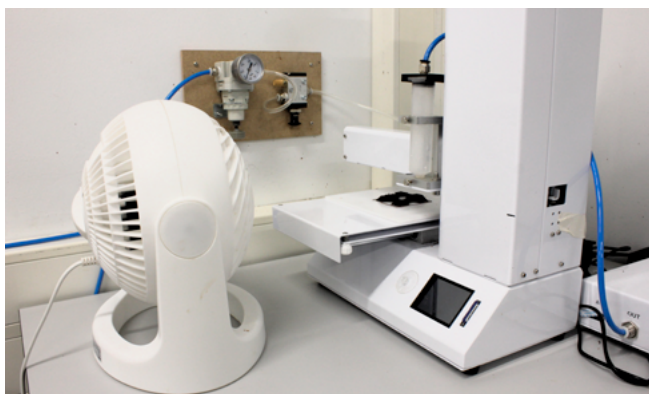


Table 7 shows the printer setting used. Settings were kept constant between recipes for better comparison. These specific settings were chosen since all well-performing recipes showed good results with them in the initial tinkering phase. The necessary extrusion pressures were determined per model.

Table 7: Printer settings of the initial quality assesment in the tinkering phase

Printer settings	Value
Nozzle Inner diameter	0.81 mm
Layer height	0.6 mm
Layer width	0.81 mm
Print speed	7 mm/s

3.3.1.2 QUALITY METRICS

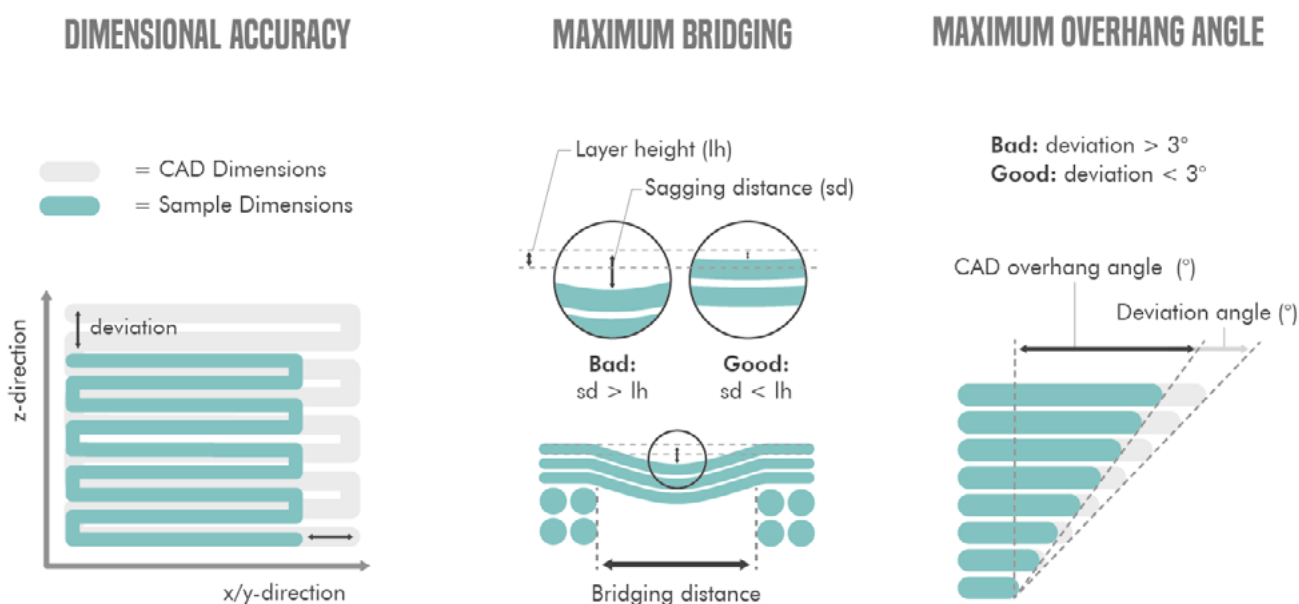
Table 8 shows the criteria used for the evaluation of the main quality aspects. Additionally, extra attention was paid to defects detected in the prints, such as gaps and accumulation of material.

Figure 47 shows a visual representation of the quality measurements and criteria used for the objectively measured quality metrics. The quality assessment method for bridging presented in Chapter 2.3.4 was slightly adapted as no suitable measurement tools for measuring the deflection were available.

Table 8: Criteria for the evaluation of the initial quality assesment tests from the tinkering phase

Quality Metric	Measurements & Criteria	Measurement tool	Precision
Dimensional Accuracy	Deviation from CAD-model dimensions in the X-Y and Z plane (%)	Digital Calliper	0.01 mm
Maximum bridging distance	Max distance bridged (in mm) that meets the following criteria: Sagging distance of the bridge is < the layer height	Digital calliper & Digital length gauge (heidenhaim MT 2500)	0.01 mm
Maximum overhang angle	Max overhang that meets the following criteria: The deviation of the overhang compared to the CAD-model is < 3°	Swing arm protractor	5° for max overhang max; 1° for deviation
Surface finish	Subjective comparison between samples.	Own judgement	n/a

Figure 47: Visual representation of the assesment of the quality criteria of dimensional accuracy, maximum bridging and maximum overhang angle



3.3.2. RESULTS

Measurements were done on each of the quality samples printed. Table 9 summarizes the results. Figure 48 shows the quality assessment samples of each recipe.

Unfortunately, the bridging feature in the AB sample broke before a picture could be taken, and the CL sample was accidentally dropped, resulting in a broken corner.

The APG-based recipes show the least amount of shrinkage with 0.3% in the xy plane and

3.0% in the z plane. Followed by AB with 7.5% in the xy plane and 3.1% in the z plane. CL performs the worst in terms of dimensional accuracy (9.8% xy-plane, 6% z-plane). In all case, the dimension accuracy in the z-plane is better than in the xy-plane, which suggest most shrinkage happens in the directions parallel to the print bed. The dimensional accuracy in the z-direction seems to be mostly affected by the sagging of the prints due to gravity.

In terms of bridging, recipes including AB show the best results. The AB-only recipe shows high-quality bridging up to 15.6 mm, which is the largest distance bridged in the model. The SA+AB recipe shows good bridging up to a bridging distance of 14.8 mm. Of the non-AB including recipes, the APG-based recipe did not show any bridging with sufficient quality and the CL-based only managed to reach a bridging distance of 5.1 mm.

All recipes were able to print overhangs up to 40 degrees, the maximum overhang

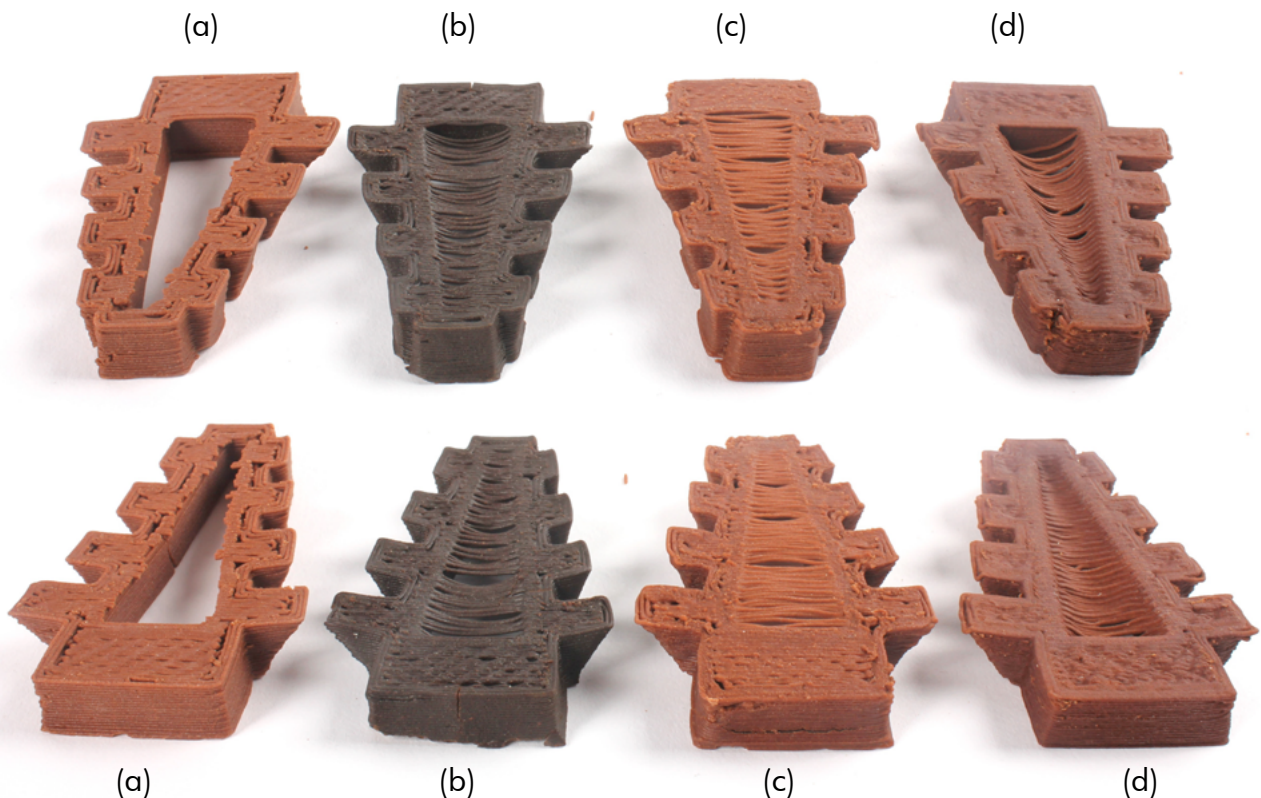
measured in the model. When taking into account the deviation of the overhang angles, the CL-based recipe did show a deviation higher than 3° when an overhang of 40° was printed. Thus, CL showed to only print with sufficient quality up until 35° according to the criteria.

Though CL performs badly on most metrics, it does appear to yield the smoothest surface finish, followed by the AB+SA-based recipe, the AB-based recipe, and finally, the APG recipe.

Table 9: Print quality assesment results

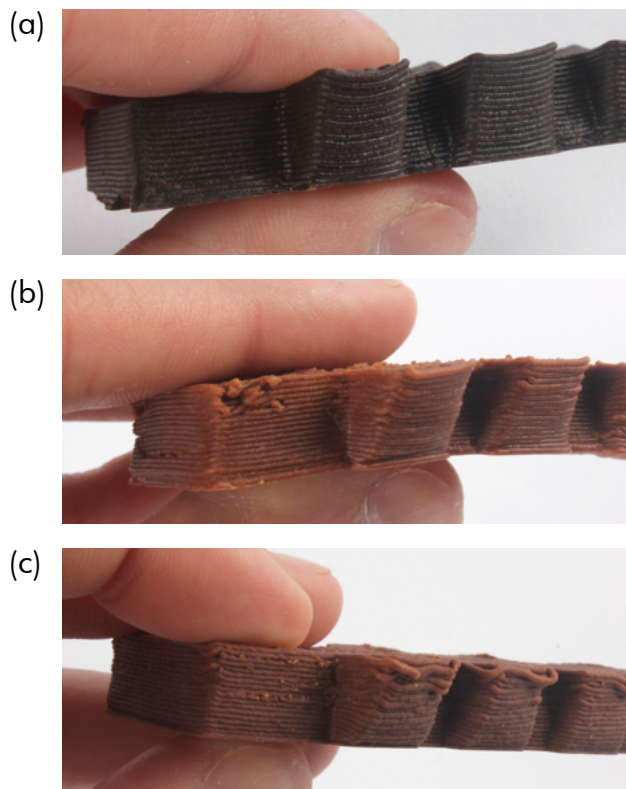
Recipe	Dimensional deviation in the xy-plane (%)	Dimensional deviation in the z-plane (%)	Maximum bridging distance (mm)	Maximum acceptable overhang (°)	Surface finish
AB1	7.5	3.1	15.6	40	+
CL1	9.8	6.1	5.1	35	+++
SA+AB1	7.7	3.3	14.8	40	++
APG1	0.3	3.0	-	40	-

Figure 48: Quality assesment samples of (a) AB1, (b) CL1, (c) SA+AB1, (d) APG1 shown from two different viewpoints



Regarding print defects, all recipes, except for the CL-based one, exhibit instances of excess material in certain spots and occasional gaps within the print (Figure 49). The CL-based recipes does show a more pronounced curling up of the corners of the model.

Figure 49: CL1 (a) AB+SA (b) and APG (c) comparisson of defects and curled up corners



3.3.4. CONCLUSION INITIAL PRINT QUALITY

Based on the results, it is evident that the tested recipes all exhibit great potential in different aspects.

The recipe for all-purpose glue results in the least amount of shrinkage, particularly in the XY-direction, and is anticipated to yield superior mechanical qualities. Yet, it falls short in bridging distances and may suffer from frequent clogging of the nozzle due to the drying out of the glue. The surface finish of these prints also feels the roughest.

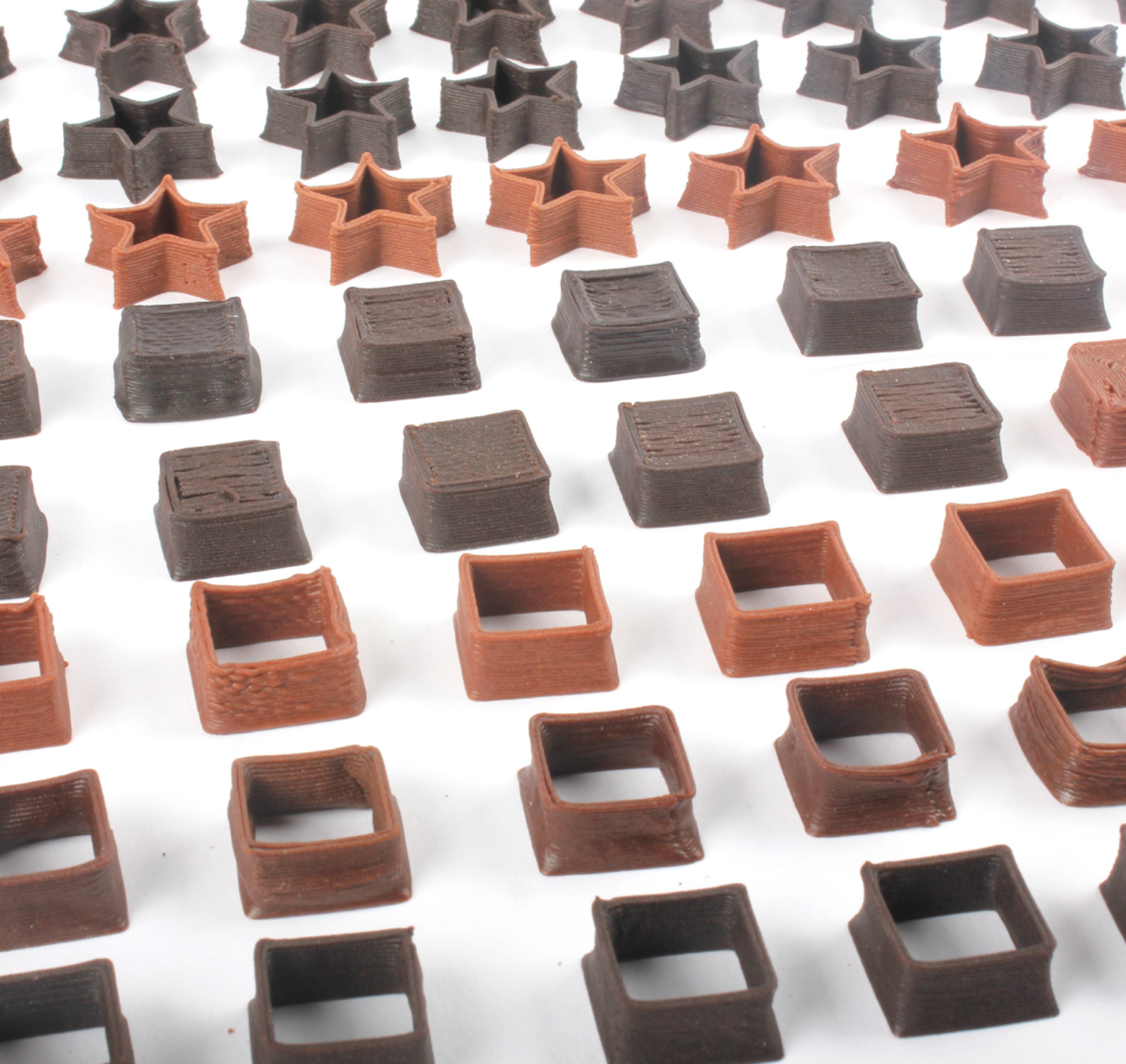
Both recipes with all binder show the best capability of bridging unsupported distances

during printing. Although they exhibit worse shrinkage than the APG recipe, they perform better than the CL recipe. Compared to the APG recipe, they also have a better surface finish. Additionally, the incorporation of SA might prove to be of great potential for possible reversible water insolubility, as previously discussed.

The CL recipe performed worst on all features except for the surface finish. The surface finish of this recipe showed superior smoothness and had a nice gloss. Additionally, the CL seemed to show improved quality with increasing print speed (Chapter 3.2). This was deemed as a valuable feature, since it enables the achievement of superior quality without sacrificing speed, ultimately enhancing overall efficiency. The difference in the overhang capability of CL compared to the other sample is only small and might be caused by other parameters than the recipe formulation.

To conclude, all used binders seem to have their own valuable effects on print quality. All binder-based recipes show the best bridging, the APG-based recipe shows the least shrinkage and CL gives a nice surface finish and has the possibility to increase overall print efficiency. Therefore, the decision was made to further develop these recipes by combining binders to possibly combine different positive effects in one recipe. In the case of the AB+SA-based recipe, its value mainly depends on its potential for water insolubility since it does not show superiority in any of the quality measurements.

Before further optimisation, it was thus deemed necessary to check if the crosslinking of SA in this recipe would still lead to water insolubility. As a result, tests were conducted to check the SA+AB recipe's water insolubility after cross-linking. Unfortunately, crosslinking did not lead to water insolubility. Multiple additional tinkering steps were undertaken to improve the quality of SA-only-based recipes to still achieve reversible water-insolubility, but no sufficient print quality was achieved within the limited time span. Additional tinkering steps included the pre and in-situ cross-linking of Sodium alginate. All tests and results can be found in Appendix A.



4. PARAMETER OPTIMISATION

Building upon the insights gained from the experimental exploration (Chapter 3), the focus shifts to refining the recipes and print parameters for optimal performance. This phase encapsulated the process of balancing material properties, ensuring compatibility with the printing process, and finding the most efficient and best-performing print parameters. The main objective was to unlock the material's potential for high-quality prints.

It helped to further answer research questions:

1.1 *How does varying the composition and preparation of the ink formulation impact the print quality?*

1.2 *How do adjustments in print parameters (e.g. speed, layer height, jerk) influence the print quality?*

4.1 RECIPE & PRINT PARAMETER OPTIMISATION

Building upon the recipes that exhibited promising printability and quality attributes in the tinkering phase, this phase focused on ink formulation and print parameter optimisation. The goal was two-fold:

1. To unlock the full potential of synergistic effects between ingredients that showed promising results in the tinkering phase, by capitalising on their individual strengths in a single formulation.
2. To identify the optimal print parameters for peak performance.

Ultimately, the goal was to find the perfect combination of recipe ingredients and print settings. Most of the tests in this phase of the research were carried out by Christophe Raynaud as part of his internship at the TU Delft.

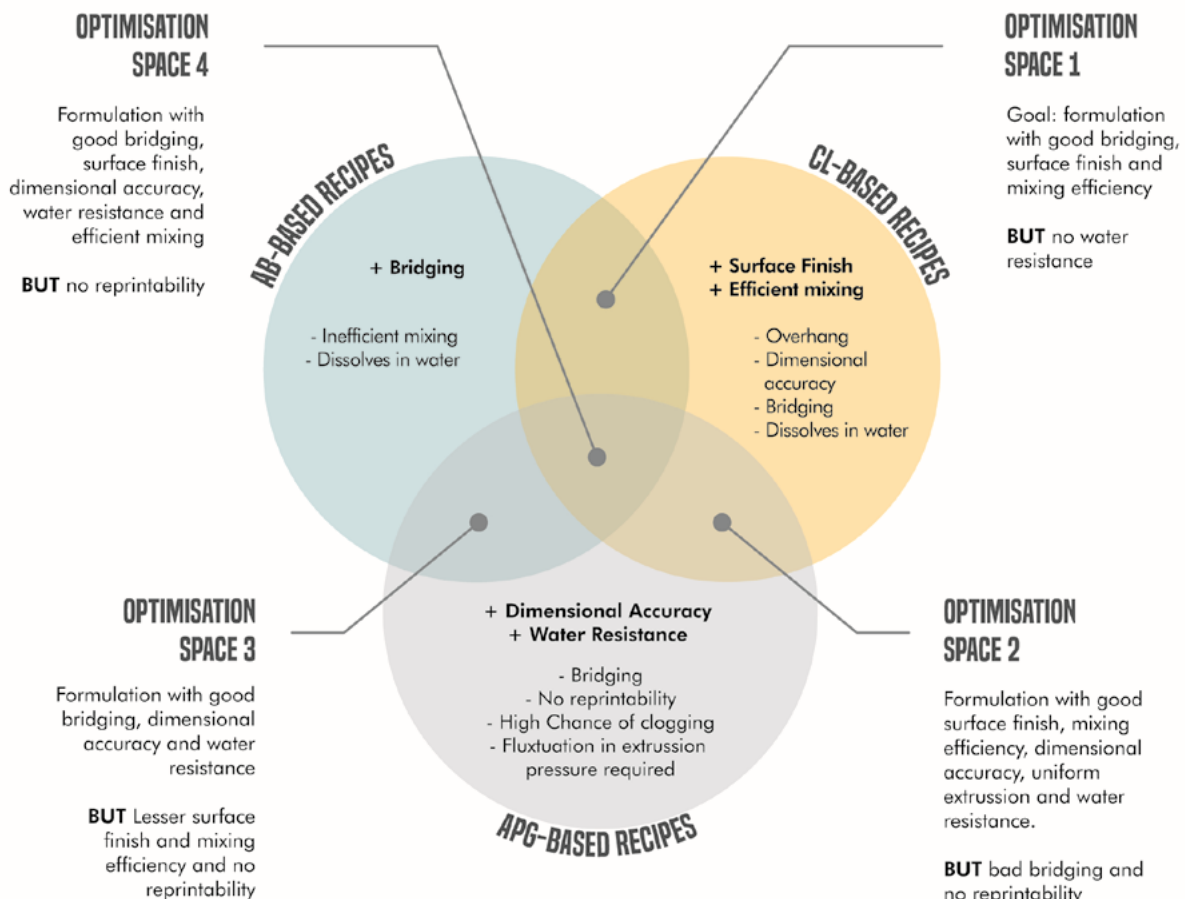
4.1.1 METHOD & MATERIALS

4.1.1.1 RECIPE OPTIMISATION

As concluded in Chapter 3.3.4, the binders CL, APG, and AB each have unique strengths. To maximize these strengths, experiments were conducted to combine them in various ways. The Venn diagram displayed in Figure 50, illustrates the potential optimization spaces that were explored by combining these binders.

Creating a formulation that combines different binders to produce positive synergies requires careful consideration. It is not possible to simply extract the positive qualities from each binder. Instead, a balance must be struck to ensure that the strengths of one binder complement the weaknesses of another. This optimisation process involved assessing factors such as binder compatibility and different ingredient ratios.

Figure 50: Venn diagram of possible areas for optimisation



Ideally, balancing these factors results in a formulation that outperforms each individual binder, ultimately producing a final print with a desirable mix of print quality traits.

Among the optimization spaces depicted in Figure 5200, space 2 remained largely unexplored. This decision stemmed from the expectation that both CL's and APG's bad performance in terms of bridging would lead to inadequate bridging quality when combined.

Since Spaces 1 and 3 only combined two binders, they were explored before space 4.

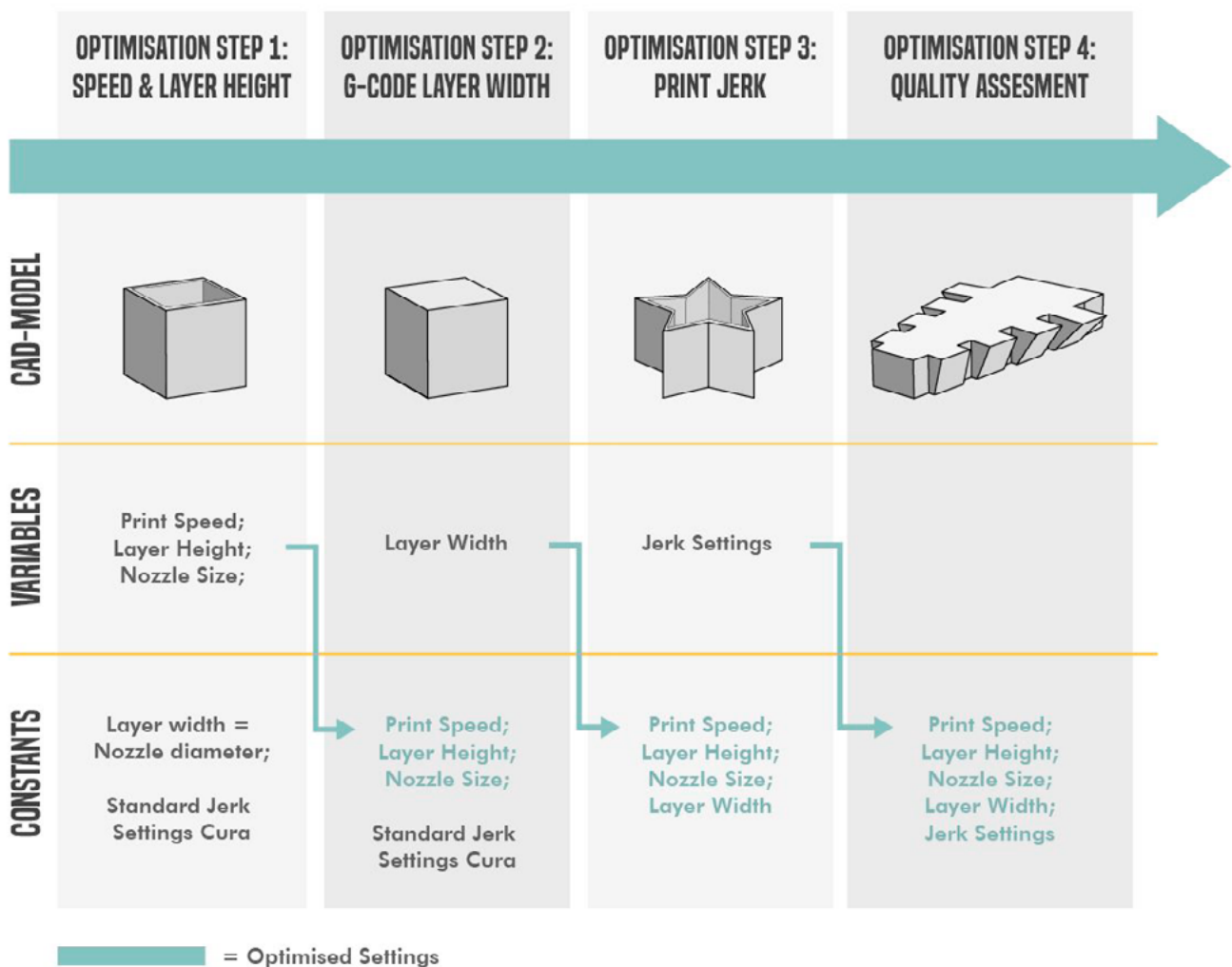
Ingredients that were used in this phase had the same sources as the materials used in the tinkering phase (Chapter 3.1.2, Tables 3 and 4).

4.1.1.2 PRINT PARAMETER OPTIMISATION

Each recipe adaptation that showed good extrudability was put through a four-step print setting optimisation process to find the optimal printer settings (Figure 51). Parameters changed included: print speed, layer height, nozzle size, layer width and print jerk. the steps consisted of:

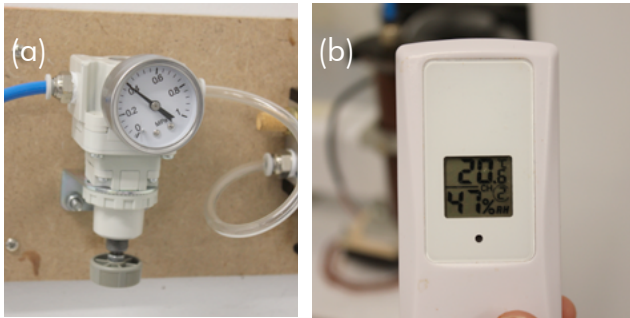
1. Determining the optimal print speed and layer height combination.
2. Determining the optimal settings for layer width.
3. Determining the optimal jerk settings
4. Printing a quality assessment model to evaluate the effectiveness of the optimisation.

Figure 51: Four-step print setting optimisation process



The necessary extrusion pressure, air humidity and room temperature were monitored during the printing process and documented for each sample. This was done with a humidity and temperature sensor and the pressure valve of the EazaoBio (Figure 52).

Figure 52: Eazao Bio Pressure valve (a), Humidity and temperature sensor (b)



In **step 1** of the optimisation, a matrix was used to test different layer height and print speed combinations (Figure 53). Tests were conducted with both an 18 and 20-gauge nozzle. Combinations in the light-grey columns and rows were only carried out when the combination above or below them showed promising results.

Figure 53: Step 1 print speed and layer height optimisation matrix

		Layer height (mm)					
		18 gauge nozzle			20 gauge nozzle		
		0.6	0.55	0.5	0.45	0.4	0.35
Print speed (mm/s)	6	S1.1	S1.2	S1.3	S1.4
	7			
	8						
	9						
	10						



A printability map was generated for each recipe by color-coding the combinations based on their resulting print quality. A colour gradient from red to green was used to represent varying levels of print quality, with red indicating lower quality and green denoting higher quality.

The settings from step 1 showing the most promising result (bright green) were used for further optimisation in **step 2**. In this step, the matrix in Figure 54 was used to determine the optimal layer width setting in combination with the optimal speeds and layer heights from step 1.

Figure 54: Step 2: step 1 settings and G-code layer width optimisation matrix

		Layer width(mm)					
		18 gauge nozzle			20 gauge nozzle		
		0.70	0.75	0.8	0.55	0.60	0.65
Step 1 setting	S1.#	S2.1	S2.2	S2.3	S2.4
	S1.#			
	Etc						

When adjusting the layer width settings in slicing software, such as Cura, it is important to consider the amount of overlap between printed lines. While some overlap is necessary for strong layer adhesion, excessive overlap can result in material buildup and reduced accuracy in the final print.

Printing a cube with 100% infill is a valuable technique to verify whether the print lines are appropriately spaced. This method could be seen as an expansion of the fusion filament test (Chapter 2, Table 1). The presence of visible gaps between the printed lines indicates that the programmed layer width is larger than the actual layer width and must be decreased. Conversely, if the printed cube reveals material buildup due to excessive overlap, it means that the programmed layer width is too small and should be increased.

In **step 3**, the jerk settings were optimised while keeping the previously found optimal settings constant.

In Cura, the jerk signifies the maximum instantaneous velocity change of the print head. A higher value means faster movement, while a lower value implies slower motion. This setting thus allows you to control how quickly the print head decelerates before changing directions. Especially when printing corners, the jerk settings can become crucial.

Printing a star-shaped 3D structure allowed for a good inspection of the effect of jerk settings on the printed corners and the overall shape fidelity.

Tests were conducted using both the standard jerk setting from Cura, as well as jerk settings with a range of values both higher and lower than the print speed used. Figure 55 shows the optimisation matrix used in step 3.

Figure 55: Step 2 settings and jerk setting optimisation matrix

		Print jerk (mm/s)				
		print speed -2	print speed -1	Same as print speed	print speed +1	print speed +2
Step 2 setting	S2.#					
	etc					

The last step, **step 4** encompassed the printing of a quality assessment sample (Chapter 3.3, Figure 45) for the recipes showing sufficient shape fidelity. In this step, the optimised settings from steps 1, 2 and 3 for each recipe were used.

Recipes were compared using the same criteria and methods as described in Chapter 3.3, Table 8.

4.1.2 RESULTS

4.1.2.1 RECIPE OPTIMIZATION

The recipe optimisation process led to multiple recipe variations being tested based on the proposed optimisation areas as described in Chapter 4.1.1.1. Table 10 summarizes the variations tried and how many showed successful shape fidelity for print parameter optimisation.

Table 10: Recipe variations tried for each optimisation space, including the number of variations with sufficient shape fidelity

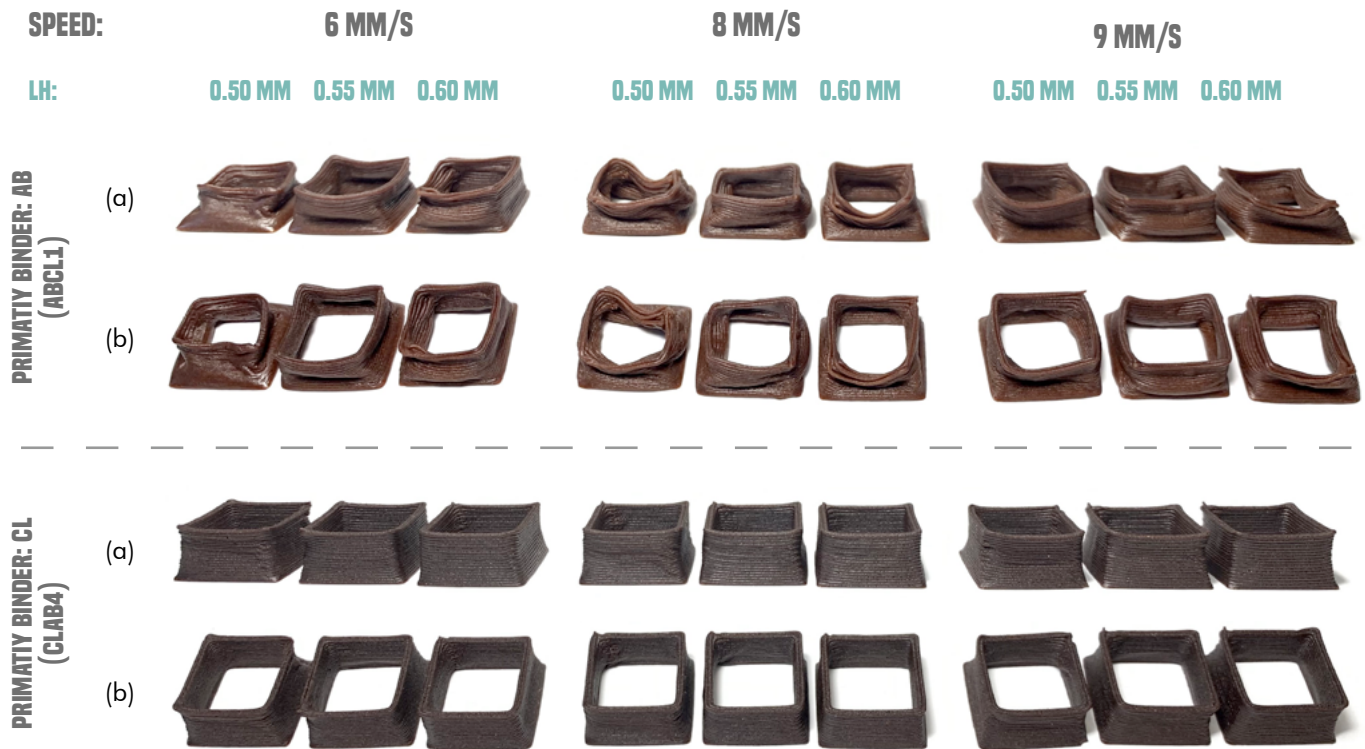
Optimisation space		Variations tried	Sufficient shape fidelity
1	AB + CL (main binder: AB)	8	3
	CL + AB (main binder: CL)	4	4
2	CL + APG	3	0
3	APG + AB	4	0
4	AB + CL + APG	0	n/a

Table 11, shows the composition of the recipes that showed sufficient quality and were used for print parameter optimisation. The final recipes from the exploration phase (Chapter 3) AB1 and CL1 were also put through print parameter optimisation. The APG recipes was not included as too many problems with clogging occurred.

Table 11: Recipe variations used in print parameter optimisation

Optimisation space 1: AB & CL					
Recipe name	Ingredients (weight %)				
	PSF	AB	CL	W	E
Base recipe AB1	20	48	0	20	12
Base recipe CL1	32	0	32	25	11
CLAB1	29.5	8.3	29.5	22.9	9.8
CLAB2	27.3	15.2	27.3	21.2	9.0
CLAB3	29.0	12.9	25.8	22.6	9.7
CLAB4	28.6	14.3	25.4	22.2	9.5

Figure 56: Side (a) and top (b) view of ABCL1 samples with AB as their primary binder and CLAB4 with CL as their primary binder. Samples were made in step 1 of the print parameter optimisation process.



OPTIMIZATION SPACE 1: AB + CL

Within the time constraints, only compatible formulations with sufficient shape fidelity were achieved in optimisation space 1. The AB and CL configurations experimented with can be categorized into recipes using either CL or AB as the primary binder.

Configurations with AB as the primary binder demonstrated greater difficulty in the optimisation process and led to insufficient results either in terms of shape fidelity or maximum print speed. Out of the eight different variations that were tested, five of them exhibited poor shape fidelity, while the others displayed slow maximum printing speeds. It was observed that print speeds higher than 7 mm/s could not be achieved with the maximum extrusion pressure available (0.65 Mpa). This suggests that these configurations may exhibit a less pronounced shear thinning effect, have a higher flow point and yield stress, or possibly both. Due to their low maximum print speed, these recipes were not put through further print parameters optimisation steps despite their sufficient shape retention.

On the other hand, Configuration with CL as the primary binder showed the most promising result and all variations tried showed good shape fidelity and better maximum print speeds. Figure 56 compares the shape fidelity of a recipe with AB as its primary binder (ABCL1) with a recipe with CL as its primary binder (CLAB4).

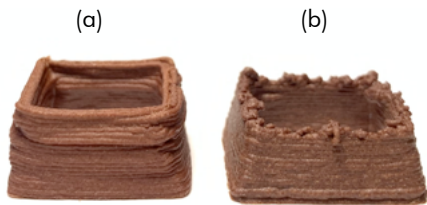
OPTIMISATION SPACE 2 & 3: APG+CL, APG+AB

APG showed insufficient performance with both CL and AB in optimisation spaces 2 and 3. In the APG-only recipe that resulted from Chapter 3, the main issues that were found during printing were bad bridging, fluctuation of the required extrusion pressure throughout the print and a heightened chance of clogging. However, the recipe's water-insolubility was deemed as a valuable feature to further explore. Formulations with additional AB and CL were tried out in the hope of reducing these issues.

By introducing CL, the aim was to enhance particle dispersion, resulting in a more uniform mixture with reduced variation

in extrusion pressure required. While the addition of CL improved mixture uniformity, the problem of inconsistency in the required extrusion pressure persisted. Instead of fluctuating, the required pressure gradually rose during the print cycle. This could indicate the gradual solidification of the material during printing. CL incorporation thus seems to accelerate the curing of the APG, if this is actually the case would require more testing. Yet it could be explained by the reduced percentage of solvent required for achieving the right consistency. Figure 57 compares cubes printed with and without additional CL.

Figure 57: APG samples (a) without additional CL and (b) with additional CL



When APG was mixed with AB, it led to the formation of clumps in the print, rendering the mixture unprintable.

Because of the incompatibility of both CL and AB with APG, combining all three of them (space 4) was not explored.

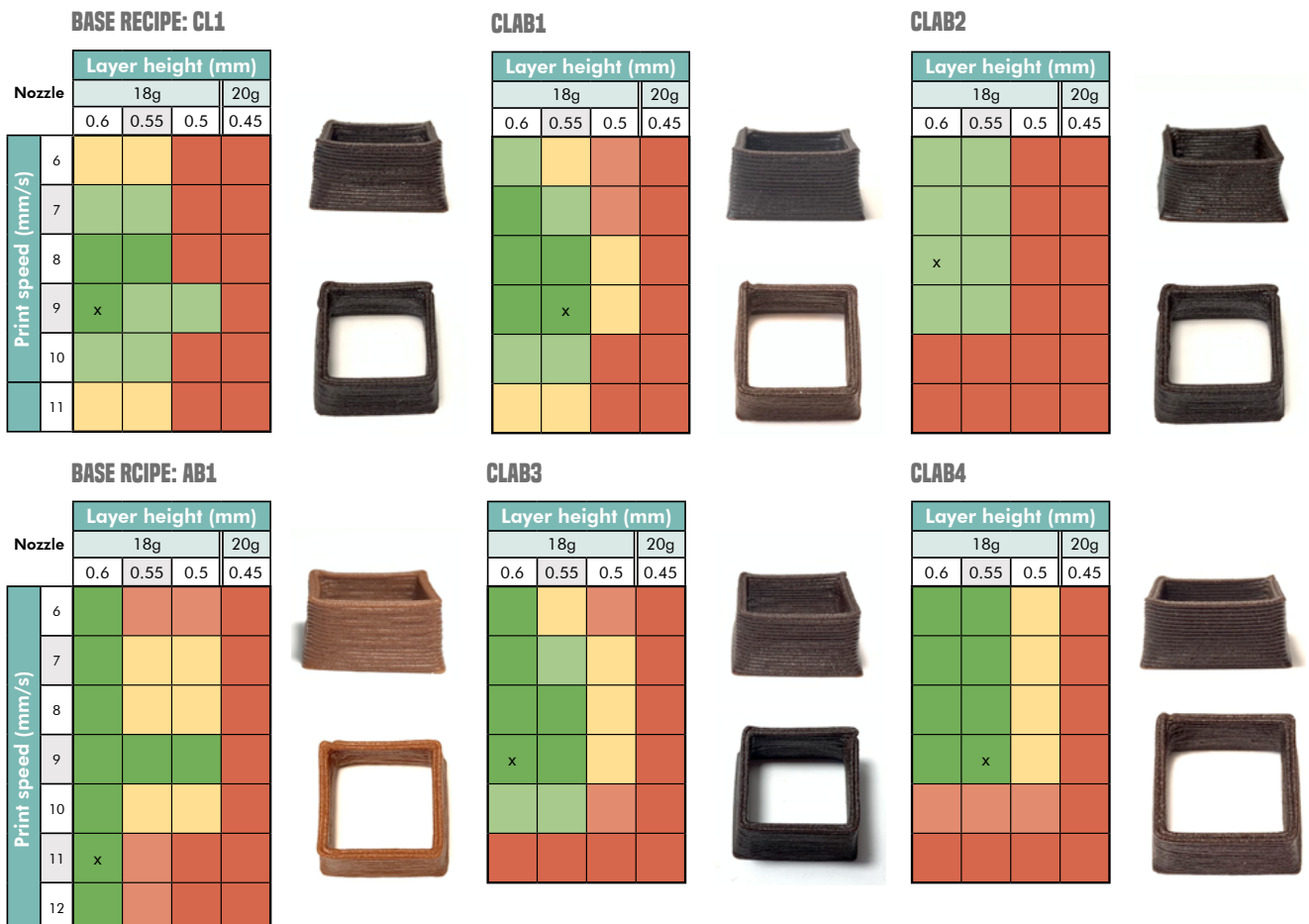
4.1.2.2 PRINT PARAMETER OPTIMISATION

All successful recipes underwent the print parameter optimization process (Figure 51). This section delves into the most notable findings and the outcomes.

STEP 1: PRINT SPEED & LAYER HEIGHT

For each recipe, a printability map was created to visualise the range of print speed and layer height settings in which the quality was sufficient (Figure 58). Included are pictures of the best-performing samples.

Figure 58: Printability matrixes of print speeds vs layerheight for the recipe variations with sufficient shape fidelity. Pictures of of the best quality samples are included for each matrix and marked with an x.



Not all combinations in the grid were tested, therefore some of the coloured-in squares are based on estimates that were derived from looking at the surrounding results in the grid. Looking at the printability maps, we can see a clear difference in printability ranges. AB1 and CLAB4 show the best overall printability ranges and shape fidelity within this range.

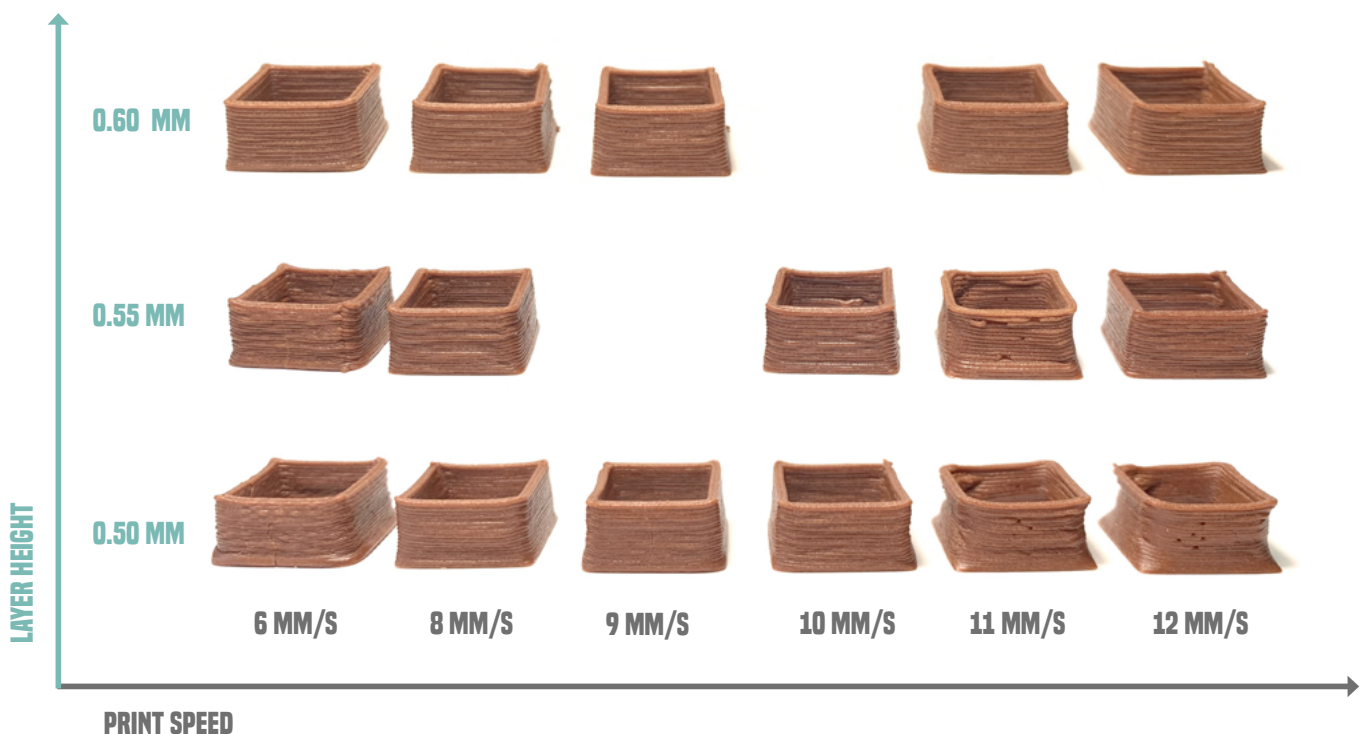
The primary advantage of AB1 lies in its exceptional printability across a wider speed range, from 6 mm/s to 12 mm/s. This is attributed to its lower extrusion pressure requirement compared to alternative formulations. AB1 seems to exhibit a superior mix of shear thinning properties, yield stress and recovery behaviour. This translates to a viscosity that sufficiently decreases for smooth extrusion under shear, while swiftly returning to a high enough viscosity after extrusion for accurate shape retention. Figure 59 shows the AB1 samples printed. Though the range of print speeds with good quality is high, AB1 does show a reduction of quality when printed with a lower layer height at higher speeds.

In AB1 the low-pressure requirement also results in slight over-extrusion at lower speeds (6mm/s) with smaller layer heights (0.55 and 0.50 mm) and thus a more “bumpy” surface.

Looking at the CL+ AB configuration, CLAB1, CLAB3 and CLAB4 show a good range of print speeds and layer heights that result in sufficient quality. However, their maximum print speeds are less compared to AB1. In CLAB1 the maximum print speed is limited by the walls slightly warping due to nozzle movement which suggests its yield stress is too low to withstand this movement. whereas, In CLAB4 and CLAB3 the printed walls are less sensitive to movement, However, their higher pressure requirements do limit the maximum printing speed to 9 mm/s (CLAB4) and 10mm/s (CLAB3). Of these recipes, CLAB4 differentiates itself from AB1 by showing good quality at lower layer heights in a wider range of speeds. The previously shown Figure 56 includes the samples of CLAB4 printed at different layer heights and speeds.

When looking at the effect of the changes made to recipes, the addition of AB to the CL1 recipe mainly seems to have improved the stability of the material when printed at lower speeds. When comparing AB1 with the CLAB4 recipes, the combination of AB and CL seems to reduce the sensitivity of the material to the movement of the printer head at lower layer heights. This does come with the added disadvantage of a limited speed at which can be printed due to pressure limitations.

Figure 59: Printability range of the AB1 recipe



In terms of layer height, we can see a similar trend in all recipes. A layer height of 0.6mm with the 18g nozzle, seems to not cause any quality-related problems. However, it does result in a lower resolution of prints and a smaller layer height is thus preferred when aiming for better surface finish and detail in prints. Though a layer height of 0.55 mm can be printed with good quality in all of the recipes, this is in most cases, except for CLAB4, only possible in a small range of print speeds. A layer height of 0.50 in most cases results in too much obstruction of the shape fidelity. Thus, depending on the desired outcome of the print, the best combination of speed and layer height needs to be chosen. For example, when printing with AB1, the best layer height to go with is 0.6 mm if a fast printing time of 12 mm/s is desired, while if a higher resolution is desired, it's best to print at a layer height of 0.55 or 0.5 mm with a slightly lower speed of 9 mm/s to avoid the movement of the head pushing and pulling the walls.

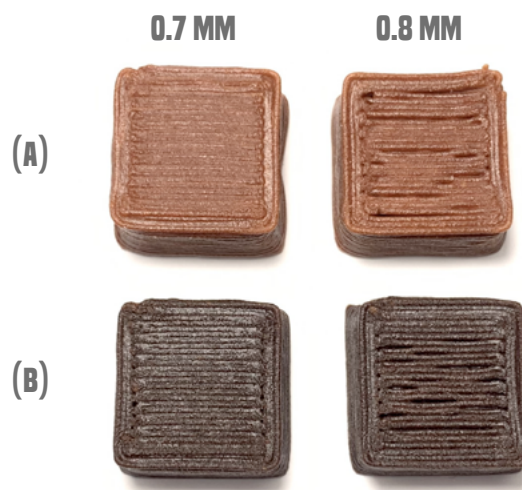
Interestingly to also mention is the fact that the improved print quality of CL-based recipes with increasing speed as hypothesised in chapter 3.2.2.2, seems to be only partly substantiated by these results. The fidelity of prints having the highest amounts of CL (CL1 and CLAB1) improve with speed in the range of 6 mm/s to 9 mm/s. However, at higher speeds, these prints lose stability due to the movement of the printer head. Using CL to allow for higher print efficiency is thus not very valuable since the quality improvement with increasing speeds stops before a speed is reached at which it outperforms AB1. Additionally, CL-containing formulations that have enough shape fidelity show an overall lower limit in print speeds being able to be reached with the available pressure.

Lastly, none of the recipes were able to print with the smaller 20g nozzle with an inner diameter of 0.64 mm. In most cases, the nozzle clogged immediately. The particle sizes of the PSF filler used are likely too big for printing with this nozzle.

STEP 2: LAYER WIDTH

Within the tests performed in optimisation step 2, no clear differences were found in layer width settings required for good-quality prints between recipes. With all recipes, a layer width setting of 0.7 mm resulted in the best-quality prints (with a nozzle size of 0.81 mm). Higher layer width settings resulted in gaps in the top surface of the cubes, while smaller layer width settings resulted in lines overlapping and expansion of the print in the xy-plane (Figure 60).

Figure 60: layer width optimisation of (a) AB1 (b) CLAB4



Theoretically, it was anticipated that samples printed with a smaller layer height would exhibit a slightly larger layer width. However, the disparity between the samples printed at 0.6 and 0.55 mm layer heights was barely noticeable. Among the tested layer widths (0.7, 0.75, and 0.8), the optimal performance was observed at 0.7 mm for all samples.

During this optimization step, it did become evident that the standard infill with wall overlap setting in Cura was set too high, resulting in outwardly pushed walls. Consequently, this overlap was adjusted from 0.12 mm to 0.105 mm for subsequent prints in this study. These new values facilitated good wall-to-infill adhesion without compromising the print's shape fidelity.

Figure 61: Jerk setting samples of AB1 at print speed 11 mm/s with different jerk settings

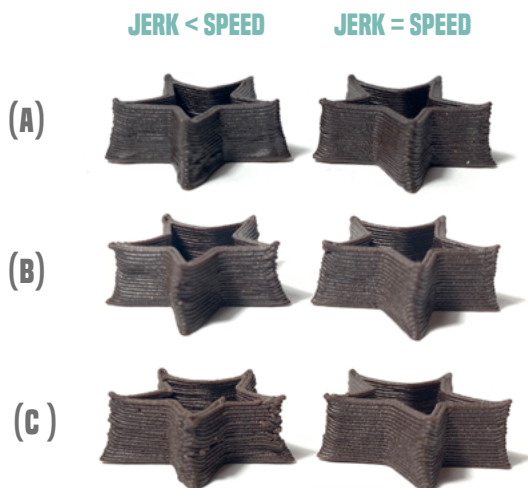


STEP 3: JERK

When printing the star models using the recommended settings from steps 1 and 2, it became clear that both the speed and jerk settings significantly affect the quality of sharp corners. A consistent trend emerged in the optimal jerk settings for AB1. All samples showed improved corner sharpness when the jerk was set to the same value as the print speed. Figure 61 shows AB1 samples printed with various jerk settings. When the jerk was set lower than the print speed, corners exhibited signs of over-extrusion (Figure 61 Column 2).

CL-containing recipes showed a less strong reaction to changes in jerk (Figure 62). A possible reason for this might be the lower speed at which they were printed.

Figure 62: Samples of CL (a), CLAB2 (b) and CLAB4 (c) printed at different jerk settings.



Besides jerk settings, another significant factor affecting corner quality was found: print speed. Samples printed at higher speeds tend to pull corners inward, resulting in warped corners in the z-direction. Figure 63 illustrates this difference by comparing AB1 star models printed at 8, 9 and 11 mm/s. All samples were printed with jerk settings matching their respective print speeds.

Figure 63: Effect of speed on corner quality. speed (blue), Jerk (grey). The dotted lines show the ideal 90° angle of the corners



Even though AB1 displayed excellent quality at high speeds during optimization step 1, it is important to note that printing sharp corners at this speed can lead to reduced quality. When printing models with corners sharper than 90°, it is necessary to lower the print speed.

STEP 4: PRINT QUALITY ASSESSMENT

As a final step of the optimisation process, quality assessment models were printed for each of the recipes. the print settings for the model were chosen based on the previous

optimisation steps. Table 12 shows the optimised settings for each of the recipes.

For most recipes except for CLAB1 and CLAB2, models with both the 0.6 mm and the 0.55 mm layer height were printed with their respective optimal print speeds. Though AB1 could be printed at 12 mm/s a speed of 9 mm/s was chosen to get better results in corner sharpness.

For CLAB4, samples were printed at a speed of 8mm/s instead of the maximum speed of 9 mm/s identified in step 1. The CLAB4 batch designated for printing the quality samples required a higher extrusion pressure than in step 1. This difference could be caused by variations in environmental conditions within the lab or inconsistencies in ingredients.

Figure 64 displays the quality assessment prints for each recipe, while Table 13 presents the corresponding results.

Table 12: Optimised settings used for printing quality assessment samples.

Recipe	Print Speed (mm/s)	Layer Height (mm)	Layer Width (mm)	Jerk (mm/s)
AB1.1	9	0.60	0.7	9
AB1.2	9	0.55	0.7	9
CL1.1	9	0.60	0.7	9
CL1.2	8	0.55	0.7	8
CLAB1	9	0.55	0.7	9
CLAB2	8	0.60	0.7	8
CLAB3.1	9	0.60	0.7	9
CLAB3.2	9	0.55	0.7	9
CLAB4.1	8	0.60	0.7	8
CLAB4.2	8	0.55	0.7	8

Figure 64: Quality assessment models of different recipes and settings corresponding to Table 12.



Table 13: Quality assessment measurements of optimised recipes. The best results of each quality metric are marked in blue, the worst in light grey.

Recipe	Dimensional deviation in the xy-plane (%)	Dimensional deviation in the z-plane (%)	Maximum bridging distance (mm)	Maximum acceptable overhang (°)	Surface finish
AB1.1	7.0	3.1	14.33	35	+
AB1.2	2.8	3.8	13.90	40	+
CL1.1	10.1	7.0	11.20	40	+++
CL1.2	10	7.8	13.11	35	+++
CLAB1	10.7	9.6	13.26	40	++
CLAB2	10.3	9.3	6.90	35	++
CLAB3.1	8.2	7.0	8.84	35	++
CLAB3.2	7.5	8.2	11.22	40	++
CLAB4.1	8.9	6.5	14.28	40	++
CLAB4.2	7.1	7.8	14.22	40	++

Based on these outcomes, it is evident that AB1 outperforms other formulations across most quality metrics. The exception lies in surface finish, where formulations containing CL exhibit an advantage over AB1. Of all recipes combining CL with AB, only CLAB3 and CLAB4 significantly reduced dimensional deviation in the xy plane compared to the CL1 recipe. no clear differences were found in the z-direction.

Though AB was added to the CL1 recipe to improve its bridging, the post-optimization print of CL1 demonstrates better bridging compared to the sample printed in Chapter 3. This suggests that either the recipe performance is sensitive to environmental changes in the lab or that the optimisation of the print setting has had a large effect on the final print quality. Still, an improvement in bridging can be seen in CLAB4, which, in conjunction with AB1, exhibits superior bridging capabilities.

When comparing samples printed with a 0.60 mm and 0.55 mm layer height, a few interesting things can be noted. In the case of AB1, a smaller layer height seems to result in less dimensional deviation in the xy-plane. This trend is also noticeable in other

AB-containing recipes, albeit to a lesser degree. However, in all these cases, the deviation of the model in the z-direction seems to increase with a smaller layer height. If these findings are significant can not be said and more testing would be required to prove these statements.

4.2 CONCLUSION

In conclusion, this phase of the research aimed to refine both the recipe formulation and print parameters. Consequently, two recipes, AB1 and CLAB4, emerged as the most promising candidates for further evaluation in Chapter 5.

While attempting to combine the strengths of various binders proved challenging, the combination of CL and AB yielded successful recipe formulations. After thorough testing and parameter optimization, both the original recipe AB1 and the newly developed CLAB4 exhibited superior overall print quality.

Regarding print parameter optimization, AB1 demonstrated a broader range of viable speed settings that maintained sufficient quality. Although CLAB4 also displayed a commendable range, it was constrained by

the maximum extrusion pressure available. Both recipes proved capable of producing prints at layer heights of 0.6 mm and 0.55 mm with satisfactory quality. Notably, CLAB4 exhibited good quality at a wider range of print speeds when using a 0.55 mm layer height.

None of the recipes could be successfully printed with a nozzle smaller than the 18-gauge nozzle without encountering clogging issues. In all cases, the 18-gauge nozzle with a layer width setting of 0.7mm yielded the best results.

Furthermore, it was observed that all recipes achieved optimal performance when the jerk setting was aligned with the speed at which they were printed. Particularly in the case of AB1, lower jerk settings led to over-extrusion in corners, whereas CLAB4 demonstrated greater resilience to this issue.

Taking into account the comprehensive results, both AB1 and CLAB4 emerged as the top-performing recipes. AB1 excelled in terms of dimensional accuracy and bridging and was capable of achieving high-speed prints of sufficient quality.

On the other hand, CLAB4 exhibited a superior surface finish and jerk resistance compared to AB1. though in most quality print aspects, AB1 outperforms CLAB4, CLAB4 did show improved dimensional accuracy and bridging when compared to CL1 and other CL+AB variations tested. This suggests that some of the strengths of the AB binder have transferred to this recipe.

Consequently, it was decided to advance both AB1 and CLAB4 into the evaluation and optimization stage (Chapter 5) for a more in-depth investigation into the quality and potential advantages of each recipe over the other.

4.3 DISCUSSION

Several noteworthy points emerge for discussion. Firstly, while combining different binders to enhance properties shows promise, it introduces complexity. Exploring binder

interactions could yield positive synergies, but understanding optimal ratios and compatibility between binders is crucial for refining the optimization process and achieving more effective combinations in future research.

Secondly, bigger ranges of print parameters showing good quality could mean the printability of a material is less influenced by print conditions such as the available print pressure, environmental conditions and slight differences in material composition. Designing formulations that perform well under multiple conditions can help advance the quality of these materials further.

Thirdly, Even with materials that can print sufficiently at high speed, higher speeds have their limitations, especially when printing sharp corners. The fact that these materials do not dry completely during printing, increases their sensitivity to movement of the printer head, which can significantly impact the quality at higher speeds. If high-speed printing is desirable, it is worth looking into methods for in-situ solidification.

Lastly, the printer setup used in this research possibly limits the maximum corner quality that can be reached. The Eazao Bio required manual regulation of extrusion pressure. This meant that the extrusion pressure was kept constant during printing. Low jerk settings, causing slower deceleration thus led to over-extrusion as the amount of extruded material per second remained the same. To prevent over-extrusion, the deceleration in corners thus had to be quick. Jerk settings that corresponded to the speed therefore showed the best results. However, when printing at high speeds, this quick deceleration causes more force to be exerted on the print, which can cause walls to warp more easily. For future research, it thus seems valuable to look into regulating the extrusion pressure throughout a print. By allowing the extrusion pressure to drop at corners, a slower deceleration (lower jerk) can be applied, which makes it possible to print at higher speeds without walls warping easily.



5. EVALUATION & VALIDATION

The successful formulation and optimisation of two waste-based recipes for room-temperature printing marks a crucial step in reducing the environmental footprint of additive manufacturing processes. The two developed materials, AB1 and CLAB4, have the potential to reduce the overall energy use of the process and offer a way to make good use of the large waste source generated by the pecan industry.

However, before further development into materials that can be adopted in a market, it is essential to evaluate and validate the current recipes on their current quality.

This chapter delves into the evaluation and validation of the two most promising pecan shell-based DIW recipes that have been developed; AB1 and CLAB4.

The evaluation encompasses an assessment of print quality, precision, rheological behaviour, and reprintability. In doing so it helps to answer the research questions:

1.3 To what extent do environmental factors play a role in the print quality achieved?

2. What are the specific rheology characteristics that need to be considered when formulating inks for optimized print quality?

3. To what extent does reprinting biobased materials at ambient temperatures affect the print quality across successive printing cycles and what factors contribute to maintaining or degrading print quality over these multiple cycles?

5.1 PRINT QUALITY & PRECISION EVALUATION

The successful development of the two materials shows potential for more sustainable additive manufacturing. However, as mentioned in the literature review, gaining good print quality with these materials and methods is one of the main challenges in the field. The combination of precise rheology requirements; high sensitivity to environmental factors; and the wide range of natural ingredients' properties make it difficult to gain good quality with good precision.

This section focuses on the evaluation of the print quality and precision of the developed materials; AB1 and CLAB4. The objectives are to assess both materials' overall quality and precision. The precision of a recipe measures to what extent the quality is repeatable with each new batch of the material. It also addresses the material's sensitivity to slight changes in environmental conditions.

5.1.1. MATERIALS & METHODS

5.1.1.1 EXPERIMENTAL SETUP

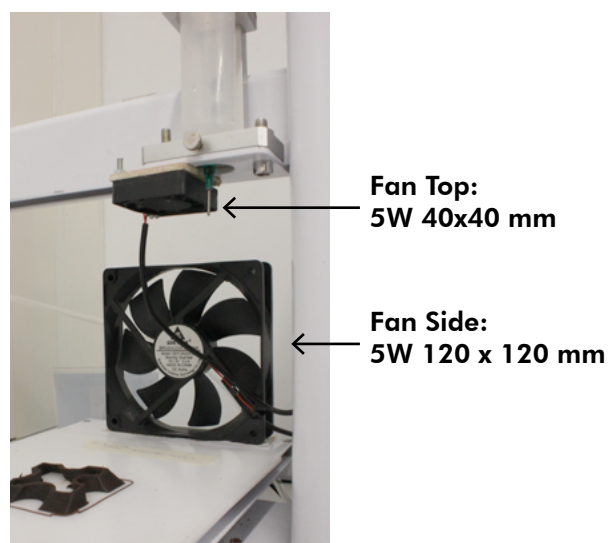
AB1 and CLAB4 were mixed using the best-performing mixing procedure described in Chapter 3.2.1. To evaluate the print quality and precision, 9 quality assessment prints (Chapter 3.3) for each recipe were printed using the printer settings that were found to perform best for both prints in Chapter 4.

Table 14 shows the print settings used for each of the recipes. While AB1 can print at a higher speed of 12 mm/s when the environmental conditions allow for it, it was decided to print all samples at the same speed for comparison. Figure 65 shows the printer setup used while printing these samples. To achieve the best print quality possible, two fans blowing from each side of the print were added. One small fan directly above the nozzle offered a more localised airflow.

Table 14: Print setting quality assesment

Printer settings	Value
Nozzle Inner diameter	0.81 mm
Layer height	0.55 mm
Layer width	0.7 mm
Print speed	8 mm/s
Jerk Settings	8 mm/s
Fan Sides	2x 5W 120x120 mm
Fan top	1x 5W 40 x 40 mm

Figure 65: Printer and fan setup for quality assesment prints



The extrusion pressure was determined for each print separately since small differences in material and environmental factors were found to influence the necessary pressure for good extrudability.

To improve the overall print quality of the model, a few extra changes were made to the Quality assessment print used in Chapter 3.3:

- A z-hop during travel moves of 0.4 mm was added to prevent the nozzle from touching and dragging already printed material.
- The infill overlap with the wall was reduced from 0.12 mm to 0.105 mm since the large overlap caused inconsistencies in the wall surface, as described in Chapter 4.1.2

5.1.1.2 QUALITY METRICS AND DATA COLLECTION

Both recipes were rated by evaluating several quality aspects using the quality assessment prints. Table 15 shows an overview of these aspects and the criteria used for evaluation. Compared to the quality measurements done in Chapter 3.3, the additional quality metrics of warpage and corner sharpness were evaluated.

Corner sharpness and surface finish were both rated subjectively since no measuring tools for accurate measurements were available within short notice at the IDE faculty. The necessary extrusion pressure, air humidity and room temperature were monitored during the printing process and documented for each sample.

The statistical analysis of the results was performed using IBM SPSS. This software was employed to determine the significance of differences observed between the recipes using boxplots, as well as to explore potential correlations between temperature, humidity, and specific quality metrics.

Scatterplots were employed to investigate potential correlations between environmental conditions and specific quality metrics. To assess the significance of these correlations, the Pearson correlation test was conducted for all correlations involving scale variables. When examining correlations between scale variables and ordinal variables with equal intervals (such as the maximum overhang angle), the Spearman correlation test was utilized.

5.1.2. RESULTS

This section presents the results of the print quality assessment of the two developed materials; AB1 and CLAB4.

One test sample of CLAB4 was left out of the analysis since it proved to be an outlier in all metrics analysed. This was likely caused by the use of a different batch of Calcium Lignosulfonate that showed visibly different behaviour compared to previous batches.

Table 15: Criteria for the print quality assesment of AB1 and CLAB4

Quality Metrics	Measurement & criteria	Measurement tool	Precision
Dimensional accuracy	Deviation from CAD-model dimensions in the X-Y and Z plane (%)	Digital Calliper	0.01 mm
Maximum bridging distance	Max distance bridged (in mm) that meets the following criteria: Sagging distance of the bridge is < the layer height	Digital calliper & Digital length gauge (heidenhaim MT 2500)	0.01 mm
Maximum overhang angle	Max overhang that meets the following criteria: The deviation of the overhang compared to the CAD-model is < 3°	Swing arm protractor	5° for max overhang max; 1° for deviation
Surface finish	Subjective comparison between samples.	Own judgement	n/a
Warpage	Height of highest point of warpage (mm)	Digital length gauge (heidenhaim MT 2500)	0.01 mm
Corner sharpness	Score 1-5 based on the comparison between samples. (5 being sharpest)	Own judgement	n/a

Figure 66 shows samples printed using AB1 and Figure 67 shows those of CLAB4. Not all samples were photographed since some of

them broke during evaluation or were used for reprintability tests. The best sample of both recipes are shown in Figure 68.

Figure 66: Quality assesment samples AB1



Figure 67: Quality assesment samples CLAB4



Figure 68: Best quality assesment sample of AB1 (a) and CLAB4 (b)

(a)

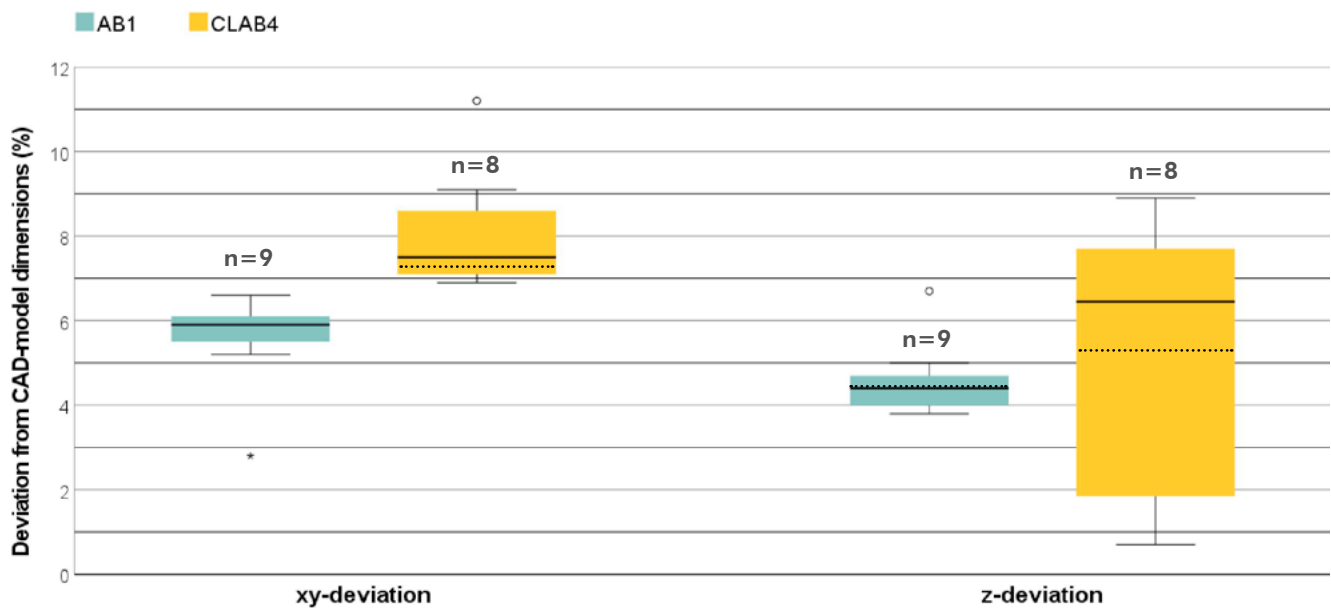


(b)

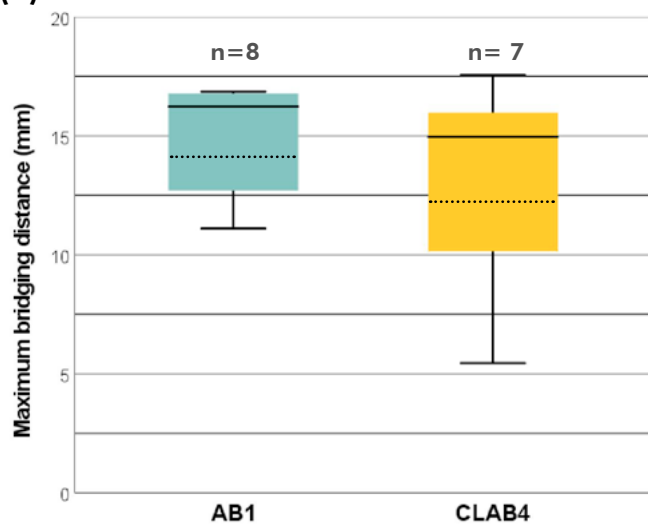


Figure 69: Box plots displaying the distribution of (a) dimensional accuracy, (b) bridging, (c) overhang, and (d) warpage of AB1 (blue) and CLAB4 (yellow). The plot includes: the median (solid line within the box), the mean (dotted line within the box), lower and upper quartiles (bottom and top boundaries of the box, respectively), minimum and maximum values (whiskers), and any outliers (individual data points beyond the whiskers).

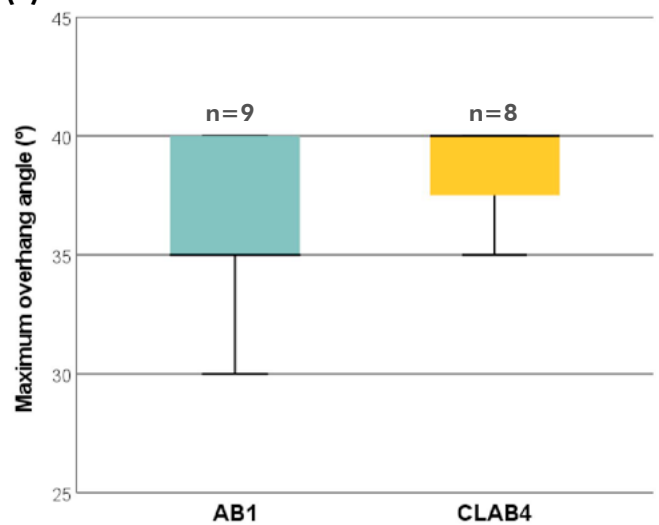
(a) DIMENSIONAL ACCURACY OF AB1 & CLAB4



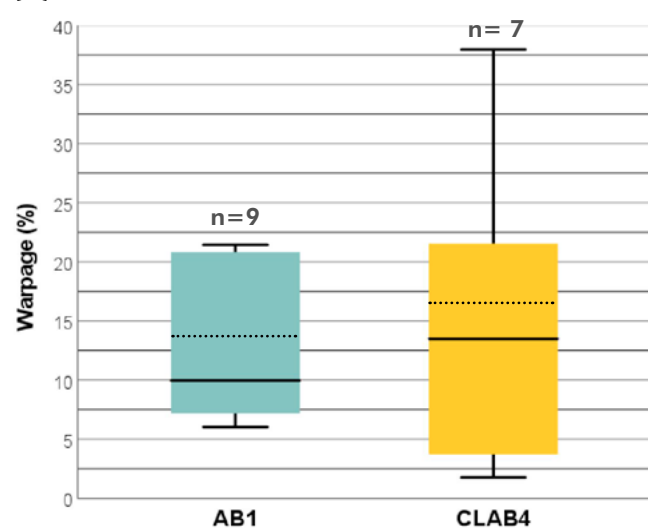
(b) MAXIMUM BRIDGING IN AB1 & CLAB4



(c) MAXIMUM OVERHANG IN AB1 & CLAB4 *



(d) WARPAGE IN AB1 & CLAB4



* measurements were done on an ordinal scale for the maximum overhang angle, but are displayed here as a scale variable for better comparison between quality metrics.

5.1.2.1 DIMENSIONAL ACCURACY

Figure 69a displays the box plots of the dimensional accuracy in the xy- and z-plane of both recipes. The outliers that are visible in the boxplot were excluded from the statistical analysis.

Both regarding dimensional accuracy in the xy and z directions, AB1's performance is significantly better. The AB1 recipe shows a mean deviation in the XY-plane of 5.94% compared to 7.61% in the CLAB4 recipe and a deviation in the z-plane of 4.34% compared to 5.20% in CLAB4. The horizontal solid lines in the boxplots represent the medians of the measurements.

Additionally, CLAB4 shows a bigger standard deviation, especially in the z-direction. This is also well displayed in the boxplots. In the case of dimensional accuracy AB1 shows superior results and superior precision compared to CLAB4.

5.1.2.2 BRIDGING

Figure 69b displays the box plots of the maximum bridging distance of both recipes. For both AB1 as well as CLAB4, one sample could not be included in the measurements due to its breaking.

Noteworthy here is that both AB1 and CLAB4 had samples that showed perfect bridging. In the case of AB1, this happened in 50% of the cases and in the case of CLAB4, this happened in 28.6% of the cases. Due to time constraints, no bigger distances were able to be tested in this research. We thus need to take into account that the maximum bridging of both recipes could be higher with the right conditions. As a result, the calculated means are most likely lower than the actual values.

From analyses, it does become evident that AB1 performs better in bridging with an average maximum bridging distance of 14.93 mm compared to 12.89 mm for CLAB4. When looking at the boxplots in Figure 72b, CLAB4 again shows values with a larger range than those of AB1. Thus, again AB1 shows higher precision.

5.1.2.3 OVERHANG

Figure 69c displays the box plots of the maximum overhang angle of both recipes. The measurements are done on an ordinal scale. Each sample was appointed a group based on the biggest overhang in which the quality was deemed sufficient according to the criteria set (Table 15). The different groups are: 5°, 10°, 15°, 20°, 25°, 30°, 35°, 40°, corresponding to the overhangs in the quality assessment models. No overhangs smaller, bigger or in-between these values were tested.

Both recipes show the possibility of printing the maximum tested overhangs of 40° with good quality if the conditions are right. All samples can print 40° overhangs without collapsing, but most samples do show slight sagging of the layers resulting in some of them not reaching the criteria for sufficient quality.

Based on the results, CLAB4 shows better quality overhangs with a mode value of 40° compared to 35° for AB1. For CLAB4, 75% of the samples met the criteria for good overhang at 40 degrees, compared to 33.3% of the AB1 samples. The possible reasoning behind the significance of these results is further discussed in Chapter 5.1.3.

5.1.2.4 WARPAGE

Figure 69d displays the box plots of the warpage of both recipes. In CLAB4, one sample was not included because it broke during measurements.

AB1 seems to be less influenced by warpage, with a mean warpage of 13.82% compared to 16.50% in CLAB4. CLAB4 again shows more deviation in measurements than AB1 though the differences are smaller. Noteworthy is that warpage seems to mainly be caused by the conditions of drying. The samples that were taken off the build plate and put on a mesh early on in the drying process showed more uniform shrinkage because of consistent airflow on all sides of the print. However, this might also have caused them to warp more. Removing samples from the built plate gives them more axis of freedom to warp along.

5.1.2.5 SURFACE FINISH & CORNER SHARPNESS

Due to the unavailability of proper measuring equipment, this assessment relied on subjective ratings to evaluate the surface finish and corner sharpness of the two recipes.

Findings indicate that CLAB4 seems to yield a slightly smoother surface finish compared to AB1. Most importantly, CLAB4 shows less excess material buildup on the nozzle, resulting in smoother walls. In AB1 material often resulted in worsening of the surface finish (Figure 70). However, It is worth noting that dipping the nozzle in Vaseline strongly reduced this negative effect. The Vaseline created a hydrophobic layer on the nozzle which resulted in less material being stuck to it. When AB1 samples show less material buildup, their surface finish is improved significantly and the difference between CLAB4 and AB1 is less noticeable.

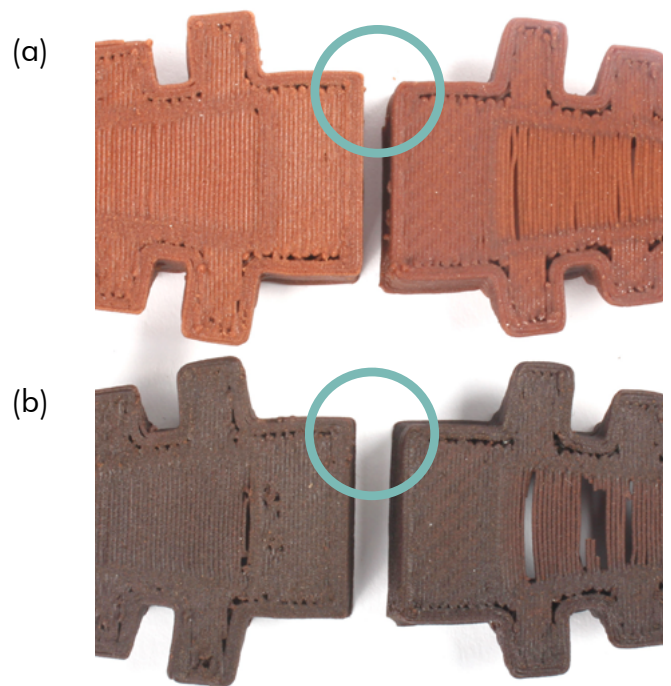
Figure 70: Surface defects due to material buildup on the nozzle with AB1



As discussed in Chapter 4.1.2.2, the sharpness of corners is largely dependent on the printing parameters; especially jerk and speed.

When comparing all samples from both AB1 and CLAB4, no clear differences can be found. Figure 71 shows the best and worst performing samples for both recipes in terms of the sharpness of corners. The fact that the differences between samples from the same material are bigger than when we compare the best and worst-performing samples of each recipe, suggests that the corner sharpness is mainly driven by factors outside of the recipe.

Figure 71: Comparison of worst and best corner sharpness in samples of AB1(a) and CLAB4(b)



5.1.2.6 ENVIRONMENTAL CONDITIONS

The environmental conditions of both humidity and temperature during printing were recorded for all of the samples. To analyse if there were any possible correlations between the quality measurements and the environmental conditions, all objectively measured values were plotted on scatterplots with the quality metrics on the horizontal axis and environmental conditions on the vertical axis. The ones showing signs of a correlation are displayed and discussed here.

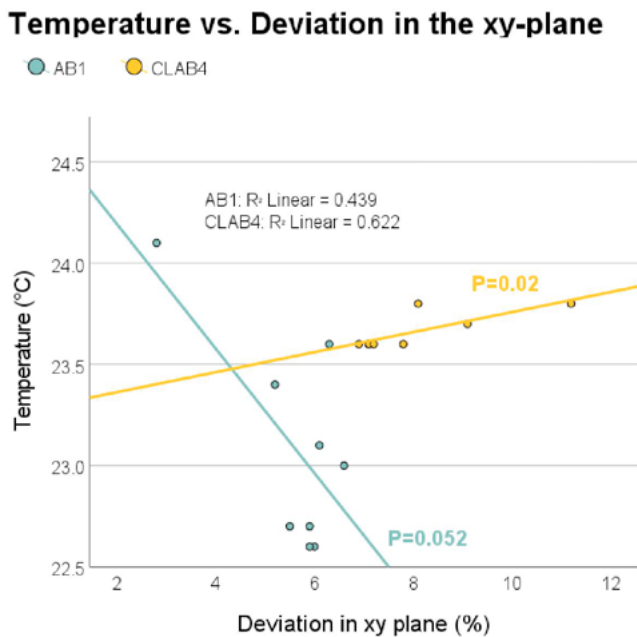
In terms of dimensional deviation in the xy plane, signs of a positive linear regression are found in relation to the measured temperature (°C) in CLAB4 with $r = 0.789$ (Figure 72). The Pearson correlation test yielded a significant result ($p = 0.02$) for CLAB4, satisfying the conventional threshold of 0.05.

With an R^2 value of 0.622, a portion of the data's variability is explained by this trend. However, since it is not an extremely high value, it is likely that temperature is not the only driver for the variance in data found.

In contrast, AB1 did not exhibit a significant correlation ($p = 0.052$) between dimensional accuracy and measured temperature. This suggests that factors beyond temperature exert a more pronounced influence on AB1's dimensional accuracy variance.

No correlation was found between the environmental conditions measured and the dimensional accuracy in the z-plane.

Figure 72: Correlation graph temperature (°C) and deviation in the xy-plane (%)



In terms of warpage, both temperature and humidity seem to influence the warpage in samples to some extent, though they do not seem to be the only factors causing warpage.

With AB1, Pearson correlation shows a significant positive correlation between temperature and warpage ($p=0.041$, $r=0.686$) (Figure 73) as well as between humidity and warpage ($p=0.008$, $r=0.813$) (Figure 74). However, again neither of the correlations found have a very high R^2 value, thus the variance in data found can not be explained by this trend with full certainty.

These results thus need to be taken with a grain of salt and further experimentation would be required to prove if the found trend is correct.

Based on not all variance being explained by this correlation, it is likely that temperature and humidity are not the only drivers causing warpage in AB1. In CLAB4 no significant correlation was found between temperature, humidity and warpage.

Figure 73: Correlation graph temperature (°C) and warpage (%)

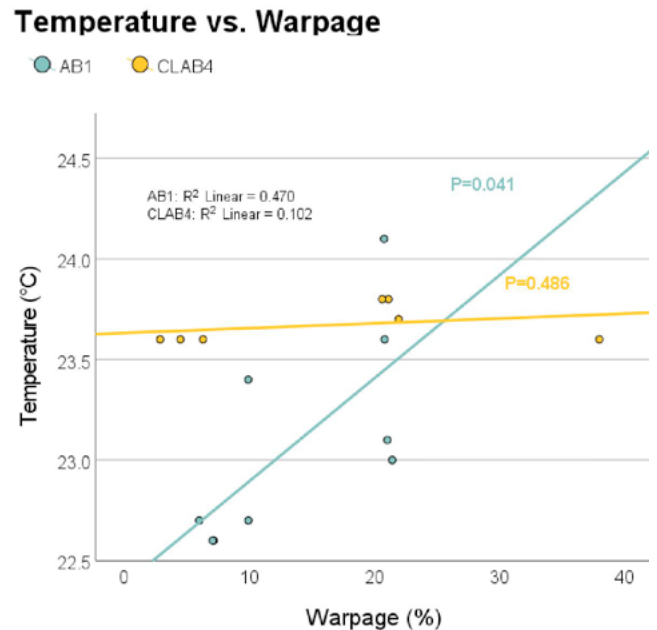
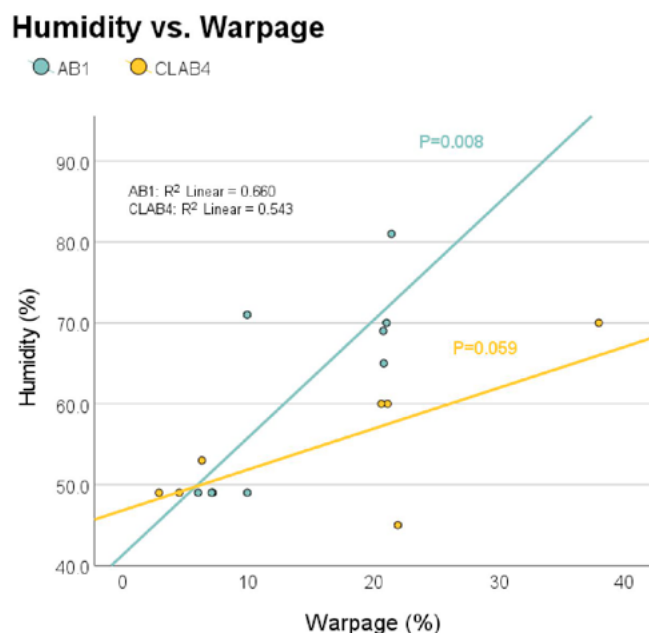
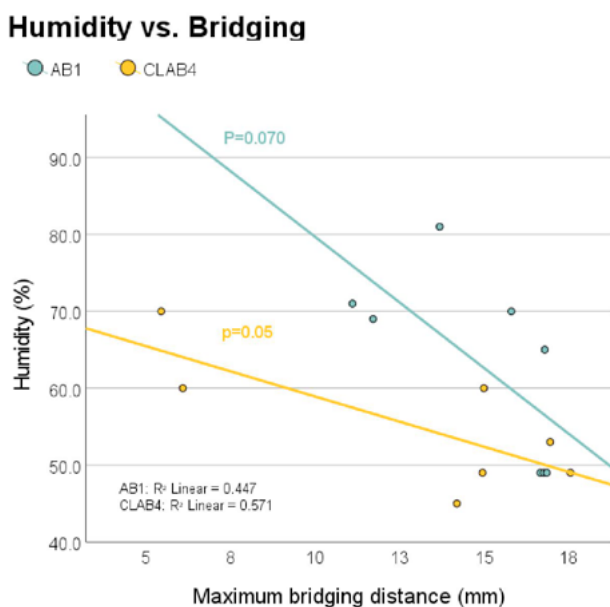


Figure 74: Correlation graph humidity (%) and warpage (%)



Bridging has also shown to be significantly influenced by environmental conditions. The humidity and maximum bridging distance show a significant negative linear regression in CLAB4 ($p=0.05$, $r=-0.755$). In AB1, this correlation has a significance of $p=0.70$ (with $r=-0.668$), which would mean the relationship can not be proven true. However, it should be taken into account here that there was a limit to the maximum bridging distance that could be measured from the model and that in AB1 50% of the samples showed perfect bridging. It is thus likely that the maximum bridging values displayed here are lower than the actual values. When looking at the scatterplot (Figure 75), we can see that a more linear regression would be visible when these values shift more towards higher distances on the x-axis. Hence it is likely that the actual p-value would be lower and may prove to be significant. If the relation is assumed to be significant, AB1 shows a stronger response to humidity than CLAB4 in terms of bridging.

Figure 75: Correlation graph humidity (%) and maximum bridging distance (mm)



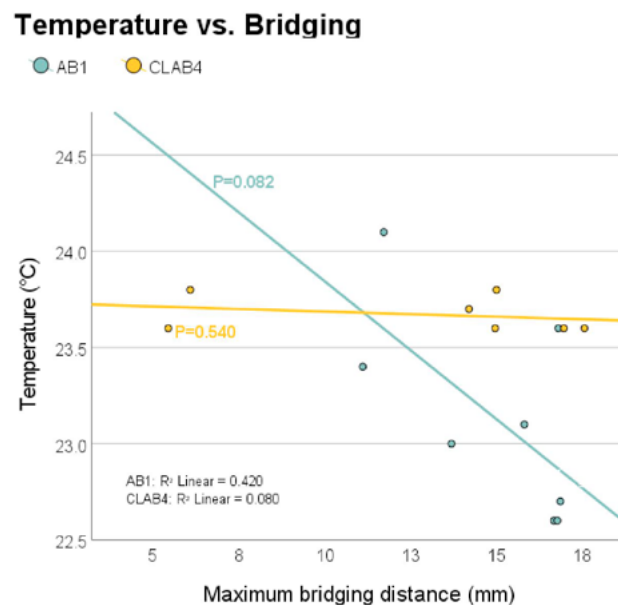
Between the temperature and maximum bridging distance, no significant correlation is found. Yet, with AB1 the Pearson correlation test results in a value relatively close to the significance level ($p=0.082$ with $r= -0.648$). As already explained, this value might be lower due to the limitations of the model

used for testing. It is therefore possible that there still is a significant correlation between temperature and bridging in AB1. The scatterplot for this correlation is shown in Figure 76.

Again the R^2 values of the correlations are not very high, meaning that there are possible other factors driving the variance in data. To prove if these trends are actually true, more precise research and evaluation would be necessary.

In neither recipe, a correlation was found between the environmental conditions and the maximum overhang angle.

Figure 76: Correlation graph temperature (°C) and maximum bridging distance (mm)



5.1.2.7. THE EFFECT OF ENVIRONMENTAL CONDITIONS ON THE EXTRUSION PRESSURE

It was hypothesised that the necessary extrusion pressure for printing is partly influenced by environmental conditions such as humidity and temperature.

Pearson's correlation test shows that this hypothesis could be true. In CLAB4, the temperature has a significant effect on the extrusion pressure needed, showing a positive linear relation ($p<0.001$, $t=0.993$).

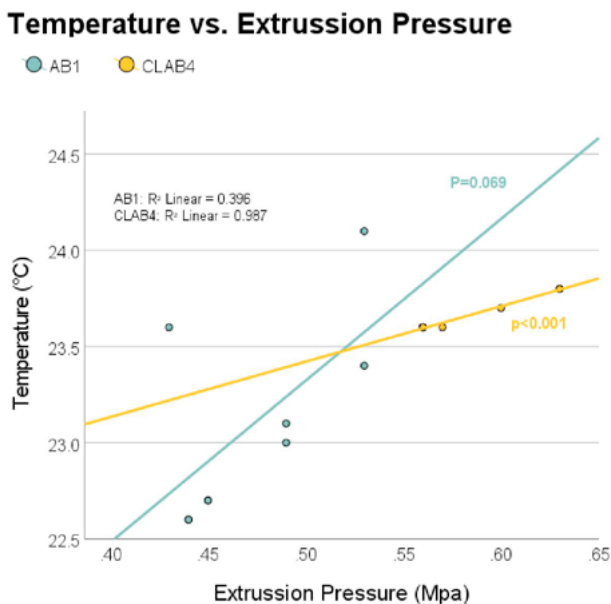
This, however, can not be explained by theory, as it is expected that the required extrusion pressure drops with increasing temperature due to the reduction of viscosity. This discrepancy is further discussed in Chapter 5.1.4.

In AB1, the humidity seems to have a significant effect on the extrusion pressure ($p=0.038$, $t=695$).

No significant relation was found between AB1's extrusion pressure and the temperature, nor between CLAB4's extrusion pressure and the humidity. This does not have to mean that they do not influence the extrusion behaviour at all, the other environmental conditions just contribute predominantly to the change of extrusion pressure.

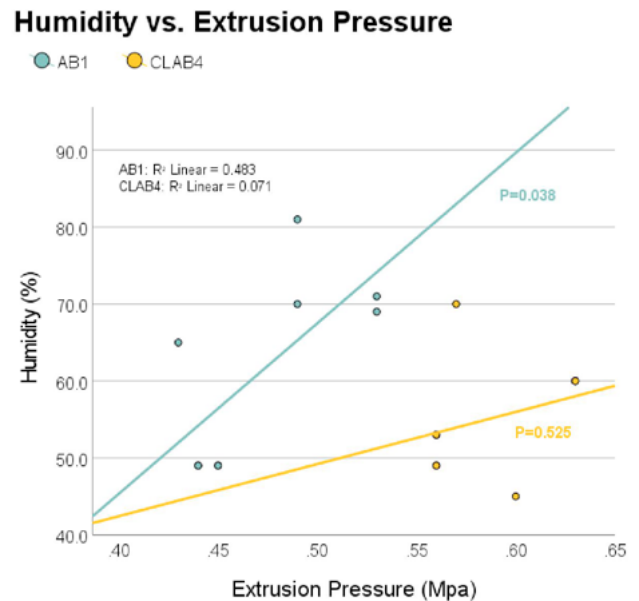
Figures 77 and 78 illustrate the scatterplots depicting the discussed correlations. Once again, it is worth noting the R2 values. With an R2 value of 0.987, the variability in data concerning the correlation between temperature and required extrusion pressure for CLAB4 appears to be predominantly explained by the identified trend. Consequently, we can say with relative certainty that variations in required extrusion pressure for CLAB4 are primarily driven by temperature changes.

Figure 77: Correlation graph humidity (%) and extrusion pressure (Mpa)



On the other hand, the R2 value for the correlation between humidity and extrusion pressure in AB1 is relatively low. This implies that changes in extrusion pressure in AB1 are likely influenced by factors other than humidity to a greater extent. A possibility could be variations within the materials, as the AB used is of lower industrial standard than the CL.

Figure 78: Correlation graph humidity (%) and extrusion pressure (Mpa)



5.1.3. CONCLUSION

PRINT QUALITY AND PRECISION

In terms of print quality, AB1 exhibits the best overall results. It demonstrates superior dimensional accuracy, bridging capabilities, and the least amount of warpage.

CLAB4 performs slightly better in terms of overhangs, but the differences are marginal and might not be significant. Where CLAB4 proves slightly better is in its surface finish. Not only does it yield a smoother finish, but it also shows less material buildup on the nozzle, reducing imperfections on the printed surface. The smoother finish of CLAB4 can be attributed to the use of Calcium Lignosulfonate in the recipe; all formulations with this ingredient exhibited improved surface finishes in Chapter 4.

Concerning the lesser surface finish of AB1, post-treatments could be explored as a means of enhancement. Moreover, further research into potential additives for material formulation might improve the overall surface finish, though this could potentially impact the material's rheology and lead to trade-offs in the other quality metrics.

With AB1, material buildup around the nozzle is a frequent cause of imperfections. Fortunately, there are several ways to prevent this buildup without altering the material composition. Applying hydrophobic coatings to the nozzle surface, for instance, proved effective. In this study, coating the nozzle with hydrophobic Vaseline resulted in reduced adhesion of the material. A permanent coating would further diminish material buildup, as the amount of Vaseline on the nozzle surface decreased during printing. The z-hop added to the g-code also proved to reduce the material buildup.

The inferior overhang capabilities of AB1 may be partly due to material buildup at the nozzle. The material buildup could have exerted downward pressure on overhangs or caused excess material to accumulate, obstructing the measurements. Resolving this issue has the potential to enhance AB1's overhang performance.

Additionally, the enhanced overhang performance of CLAB4 may also be linked to improved interlayer bonding. Making slight adjustments to AB1's rheological behaviour, especially in terms of viscosity as it exits the nozzle, could promote better interlayer flow and adhesion. It is crucial to bear in mind, however, that such adjustments may impact structural stability and other quality metrics.

Thus, AB1 excels in most quality metrics, showcasing superior performance. In the aspect where it falls slightly behind CLAB4, there is potential for enhancement.

Furthermore, AB1 demonstrates notable superiority in precision. Across all assessed quality metrics, AB1 displays reduced variability among prints compared to CLAB4, indicating better repeatability.

Consequently, AB1 emerges as the more suitable choice for larger scale production.

ENVIRONMENTAL CONDITIONS

Environmental conditions seem to affect both AB1 and CLAB4 though based on the gathered results nothing can be proven with enough certainty since all R2 values are relatively low. This means that the chances are high that there are other factors additionally driving the variance in data. These possible other factors could be the drying conditions of the print, the variability within the ingredients and the airflow within the print environment.

However, the correlations that were found suggest some interesting influences:

First of all, the wider range in dimensional accuracy in the xy-plane of CLAB4 compared to AB1 seems to be partly influenced by temperature changes. When temperatures were higher, CLAB4 samples showed less accuracy in the xy plane than when they were lower. This suggests that CLAB4's shrinkage seems to be influenced by thermal stress caused by temperature increase. In AB1, small temperature changes do not have the same effect and thermal stresses seem to have less effect on shrinkage.

AB1's warpage, on the other hand, does show to be slightly influenced by humidity and temperature. R2 values suggest humidity has the more pronounced effect ($R^2 = 0.660$ for humidity and $R^2 = 0.470$ for temperature). However, the increased warpage of AB1 with increasing humidity can not be explained by theory. The increase of warpage with increasing temperatures, on the other hand, can be explained by the higher internal stresses within the material. Though these stresses do not have a strong effect on dimensional accuracy, they do seem to result in more warpage, which could also be seen as an inaccuracy in the production.

When looking at the quality of bridging features, lower humidities seem to have a positive effect on the maximum bridging distances of both recipes. This can be explained by an increase in the solidification

rate due to the bigger differences between moisture content in the print and the air.

All in all, these results suggest that environmental conditions do indeed influence the quality. To what extent and precisely how would however require more research. We can conclude that when further developing these materials for large-scale production, the environmental conditions during printing can play an important role in providing consistency in quality. With controlled environmental conditions, the precision and quality of both recipes could be improved.

5.1.4. DISCUSSION

It is crucial to acknowledge the limitations of this research. Firstly, the models used for testing only assessed bridging up to a certain distance, even though some samples exhibited potential for bridging even greater spans. This introduced a bias in the collected data for the average bridging distances of both recipes and may have resulted in some correlations going undetected.

Secondly, this study solely focused on monitoring temperature and humidity during the printing phase. To gain a more comprehensive understanding of how environmental conditions affect print quality, future research should extend its scope to encompass conditions throughout the entire printing and drying process. This would provide a more accurate depiction of environmental effects, potentially uncovering additional correlations. Ultimately, this could enable quality control through environmental management, which could be a step towards printing with higher precision.

In addition, these values were controlled by the ambient environment, meaning there was no control of the changes in humidity and temperature. In all samples, both the humidity and temperature were variables. To test their true effect, one of them would have to be kept constant while the other is varied. In future research, these variables should thus be controlled to prove the statements made in this research and potentially find other

correlations between environmental factors and print quality.

Lastly, the extrusion pressures measured during testing lacked precision, resulting in a significant margin of error for these measurements. The valve used for these readings had large intervals between markings compared to the pressure differences measured. This increases the likelihood that the observed correlations regarding extrusion pressure may be coincidental. Such coincidences could account for correlations found that are not supported by theory. Therefore, it is strongly recommended to further investigate these correlations using a more precise methodology.



5.2 RHEOLOGY CHARACTERISATION

The rheological behaviour of materials is a fundamental aspect that significantly influences the printability and print quality of materials for DIW printing. Understanding the rheology of the developed materials can be valuable for further optimisation of their print quality. This chapter delves into the rheological characterization of the developed materials, focusing on the investigation of their flow properties and behaviour under different conditions.

By analysing the rheological data of recipes that showed both good and bad results, valuable insights can be gained into why the final two recipes, AB1 and CLAB4, showed superior results and what can still be done to improve their performance in future research.

The rheology characterisation aims to answer the following research (sub)questions:

1. Which rheology characteristics substantiate the superior performance of AB1 and CLAB2 compared to other developed recipes
2. Does the shear rate influence the response time of the developed recipes?
3. To what extent does shear history as referred to by Tagliaferri et al. (2021) play a role in the rheology characteristics and thus printability of the materials?
4. What is the influence of AB and CL on the rheology characteristics of the recipe?

5.2.1 METHODS & MATERIALS

5.2.1.1 MATERIALS

Rheology characterization was carried out for the recipes shown in Table 16.

As concluded in Chapters 4 and 5.1, AB1 and CLAB4 have demonstrated superior print quality. AB1 exhibits the best overall print quality, and precision, while CLAB4 offers a smoother surface finish and reduced material build-up on the nozzle.

ABCL1 was intentionally selected as a poor-performing recipe. This choice aimed to pinpoint rheological behaviours that may account for differences in print quality. Notably, ABCL1 displayed significant shape retention issues.

Additionally, ABCL1, CL1 and CLAB2 served to investigate the effect of CL and AB addition on the rheology changes of a recipe (research sub-question 4). ABCL1 was compared to AB1 to evaluate the impact of CL addition, while CL1 and CLAB2 were used to assess the effect of AB addition.

It is important to note that CL1 showed relatively good structural stability (Chapters 3 & 4) and CLAB2 only showed slight sagging.

All materials were mixed using the previously established method. For detailed descriptions of the materials and their sources, please refer to Chapter 3.1.

5.2.1.2 EXPERIMENTAL SETUP

All rheology tests were conducted using the AR-G2 from TA Instruments 40-mm diameter stainless steel Peltier plate. A gap height of 0.5 mm was used for all samples.

All measurements were performed at a temperature of 25° C. This temperature corresponds to the higher room temperatures measured at the print station.

All rheology tests were initially carried out with 1 sample for each of the material variations. After assessing these results, the decision was made to perform the most valuable test with 5 samples of each material. This was done to assess potential variations in results across different mixed batches. This consideration stems from the insights gained in Chapter 4, indicating that mixing and environmental conditions seem to influence the performance of a recipe, even with consistent ingredient composition.

After preparation, materials were kept in an air-tight container for at least 30 min before usage to account for possible shear history effects from mixing, assuming the zero-shear viscosity of the materials reached a plateau within this timeframe.

After some initial tests with both trimmed and untrimmed samples, the decision was made to not trim the samples, since untrimmed samples showed more consistent results.

Table 16: Recipes used for rheology characterisation and their reasoning for use. In green are the recipes evaluated in Chapter 5.1

Recipe	PSF(g)	Water (g)	Ethanol (g)	AB(g)	CL(g)	Reason for characterisation
AB1	11	11	7	27	0	Best print quality results
ABCL1	11	11	7	27	5	Worst print quality results, Effect of CL addition
CLAB4	18	14	6	9	16	Best print quality results
CL1	18	14	6	0	18	Effect of AB addition
CLAB2	18	14	6	10	18	Effect of AB addition

5.2.1.3 QUALITY METRICS AND DATA COLLECTION

Table 17 summarizes the details and quality metrics evaluated for all tests conducted, including the number of samples tested per recipe. Ranges of shear rates corresponding with the common shear rates in the extrusion process were used for testing (Carnicer et al., 2021; Fig. 1). The TA TRIOS software and Microsoft Excel were used to evaluate the collected data. The procedures for each test are described in more detail below.

FLOW SWEEPS

Flow sweeps were performed for all 5 recipes to evaluate their shear-thinning behaviour and apparent yield stress. The shear rate was ramped down from 10^3 s^{-1} to 10^{-2} s^{-1} with a measuring interval of 5 points per decade. By applying the shear rate from high to low, the sample's history from loading is eliminated and the chances of wall slippage are reduced (TA Instruments, n.d.). The apparent yield stress is determined by averaging the measured stresses before the graph deviates from a horizontal line.

Table 17: Rheology tests conducted and quality metrics evaluated

Rheology test	Details	Quality Metrics	N
Flow sweep	Shear rate ramped down from 10^3 s^{-1} to 10^{-2} s^{-1} with a measuring interval of 5 points per decade.	Evaluation of shear thinning behaviour and apparent yield stress; and the influence of AB and CL on these characteristics	1
Amplitude Sweep	Increasing stress amplitude with a constant oscillation frequency of 1 rad/s.	Evaluation of structural breakdown associated with the yield stress; and the influence of AB and CL on these characteristics	5
Three Interval Thixotropy Test (3ITT)	Shear phases with: lower second phase shear: 1. 200 s shear rate of 10^{-2} s^{-1} 2. 100 s shear rate of 10 s^{-1} 3. 300 s shear rate of 10^{-2} s^{-1} Higher second phase shear: 1. 200 s shear rate of 10^{-2} s^{-1} 2. 100 s shear rate of 20 s^{-1} 3. 300 s shear rate of 10^{-2} s^{-1}	Evaluation of response and recovery behaviours and the effect of shear rate on it; and the influence of AB and CL on these characteristics	5
Three Interval Thixotropy Test with pre-shearing (Pre-shear 3ITT)	Lower second phase shear: 1. 200 s shear rate of 10^{-2} s^{-1} 2. 100 s shear rate of 10 s^{-1} 3. 300 s shear rate of 10^{-2} s^{-1} with a preconditioning step of 10 s^{-1} shear applied for 5 minutes with a 2-minute rest between preconditioning and testing.	Evaluation of response and recovery behaviours and the effect of shear history; and the influence of AB and CL on these characteristics	5

OSCILLATION AMPLITUDE SWEEPS

Oscillation Amplitude Sweeps were performed for all five recipes to evaluate the structural breakdown associated with yielding.

For AB1, CLAB4 and ABCL1, five different samples were tested to check the deviation between different mixes. The elastic storage modulus (G') and viscous loss modulus (G'') for each test were calculated using an increasing stress amplitude and a constant oscillation frequency of 1 rad/s.

The results were used to determine the yield onset point (σ_{onset}), the flow point (σ_{flow}), the flow transition index (FTI), the apparent yield stress (σ_y) and the loss tangent ($\text{Tan}(\delta)$) in the LVR.

The yield onset point, signifying the transition from linear viscoelastic (LVE) to nonlinear viscoelastic (NLVE) behaviour, is characterized by the stress amplitude at which G' and G'' deviate from linearity. In this study, σ_{onset} was determined by identifying the intersection of the tangent lines of the LVR and the initial deformation segment of the G' curve. The stress at which a viscoelastic material fully yields and begins to flow (σ_{flow}) was determined by extracting the stress value at the cross-over point of G' and G'' .

The flow transition index (FTI) was calculated using Formula 1 (Amplitude Sweeps | Anton Paar Wiki, n.d.). Additionally, the Herschel Buckley model was employed to determine **the apparent yield stress** (Formula 2).

$$FTI = \frac{\sigma_{\text{Flow}}}{\sigma_{\text{Onset}}} \quad (1)$$

$$\tau_y = \left(\frac{FTI}{2} \right) * \sigma_{\text{Onset}} \quad (2)$$

THREE INTERVAL THIXOTROPIC TEST (3ITT)

Three Interval Thixotropic Tests were performed for all five recipes to evaluate the response and recovery behaviours of the

materials. This test best resembles the printing process in which the paste is subjected to low shear before extrusion (phase 1), then high shear during extrusion (phase 2), before returning to low shear conditions after deposition (phase 3).

For AB1, CLAB4 and ABCL1, five different samples were tested to check the deviation between different mixes. The 3ITT tests were divided into an initial low shear phase of 0.01 s^{-1} of 200 s, a high shear phase of either 10 or 20 s^{-1} of 100 s, and a low shear phase of 0.01 s^{-1} of 300 s. Each sample was subjected to two different shear rates in the second phase: 10 s^{-1} and 20 s^{-1} . This was done to assess the effect of shear rate on response and recovery times

The results were used to evaluate the initial viscosity, the response and recovery behaviour and the recovered viscosity after shearing.

The original viscosity (η_0) was determined at the 200-second mark in phase 1, just before to the second shear interval.

The phase 2 viscosity (η_2) was derived by averaging the viscosity of the final measured points within the established steady state (maximum 10 points). If a steady state was not attained within 100 seconds of shear, the last measured viscosity was used.

To assess **the initial response rate** of the samples, the slope of the curve during the first second of shear change (from phase 1 to phase 2) was calculated. Additionally, a **levelling time** was determined by recording the duration it took for the viscosity to drop to the final phase 2 viscosity increased by an additional 30 Pa.s. The 30 Pa.s range was chosen since all samples demonstrated an average decrease of approximately 30 Pa.s to reach the final phase 2 viscosity after a linear steady-state decrease was reached.

Concerning the recovery behaviour, all tests exhibited an initial overshoot of viscosity after the removal of the second phase shear. Post-overshoot, the graph no longer displayed a linear relationship; therefore, the response rate could not be assessed using the slope method employed for the response rate.

Instead, **the recovered viscosities after 5 seconds** were compared, as at this juncture, no recipes exhibited any indications of overshoot.

The final recovered viscosity (η_3) was attained from each graph by selecting the final measured point, as the viscosity still exhibited a slight increase beyond the 5-minute mark (after 300 seconds of recovery).

To compare the actual recovery rates between tests with different second-phase shears, **the relative recovered viscosity (η_{3_rel})** was also determined using formula 3.

$$\eta_{3_rel} = \eta_3 - \eta_2 \quad (3)$$

The levelling time in phase 3 was established by identifying the point at which the graph demonstrated a consistent increase, signifying a linear and steady progression of the measured viscosity. This methodology was not applied in phase 2 levelling time, as this segment of the graph exhibited excessive variability, yielding inconsistent results.

THREE INTERVAL THIXOTROPIC TEST (3ITT) WITH PRE-SHEARING

In addition to the standard Three Interval Thixotropic Test, additional Three Interval Thixotropic Tests with a pre-shearing conditioning step were performed for all five recipes to mimic the behaviour of material that has been mixed just before extrusion.

As mentioned by (Vittadello & Biggs, 1998), complex soft materials are influenced by shear history. The internal structure and arrangement of molecules change after shearing. Shear history refers to the cumulative effect of these changes as the material is subjected to different shear forces. A material that has been previously sheared, in mixing for example, can thus react differently to shear than one that has not, especially if the time between the first and

second instance of shearing is short.

The test was divided into an initial low shear phase of 0.01 s^{-1} for 200 s, a high shear phase of 10 s^{-1} for 100 s, and a low shear phase of 0.01 s^{-1} for 300 s. Before the tests, a pre-shear of 10 s^{-1} was applied to the samples for 5 minutes, after which it was left to recover for two minutes before the test started. The two-minute wait time was based on the time it generally takes to fill the printer and start printing after mixing. A pre-shear rate of 10 s^{-1} was chosen since this rate corresponds to the average shears applied in the mixing process (Carnicer et al., 2021; Fig. 1).

For AB1, CLAB4 and ABCL1, five different samples were tested to check the deviation between different mixes.

To quantify the effect of pre-shearing on the initial viscosity, the response and recovery behaviours and the recovered viscosities, the same methods as described in the previous tests were used.

5.2.2 RESULTS

5.2.2.1 FLOW SWEEPS

Unfortunately, the results from the flow sweeps showed bad repeatability. Additionally, most of the apparent yield stresses found did not correspond with those found in the Amplitude sweeps. Table 18 compares the yield stresses found for the initial $n=1$ samples in the flow and amplitude sweeps.

To visualise this discrepancy, Figure 79 shows the flow and oscillation amplitude sweeps of AB1 And CLAB4. With AB1 the yield stresses found are in the same order of magnitude, whereas with CLAB4 the yield stress found in the flow sweep is a lot lower.

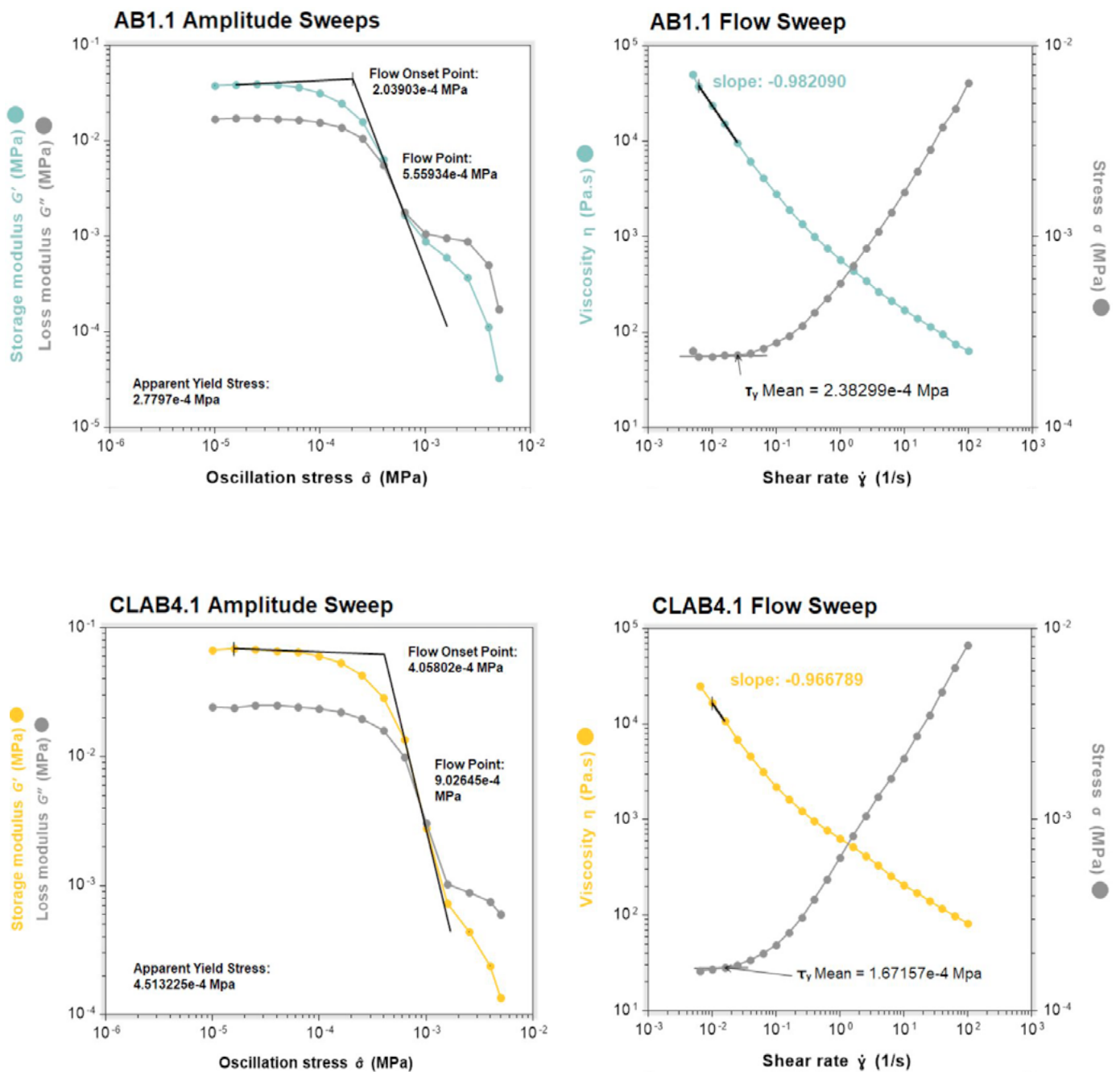
The inaccuracy of results can be attributed to the possible occurrence of wall slippage (TA Instruments, n.d.). Though the chances of wall slippages were reduced by applying the shear rate from high to low, slippage does seem to have occurred.

TA instruments states that wall slippage often arises in conventional flow sweeps when

Table 18: Comparison between yield stress found in flow and amplitude sweeps of n=1 samples

Recipe	σ_y (Pa) - Flow sweep	σ_y (Pa) - Amplitude sweep
AB1	2.38E2	2.78E2
ABCL1	1.89E2	79
CLAB4	1.67E2	4.51E2
CL1	7.84E1	4.76E2
CLAB2	No plateau reached	1.02E2

Figure 79: Yield comparison between amplitude and flow sweeps of AB1.1 (Blue) and CLAB4.1 (Yellow)



higher-viscosity materials such as pastes are used, which is the case for the materials used in these tests. When slippage occurs, measured yield stresses are lower than the actual values. This could be the case in measurements done for AB1, CLAB4 and CL1 as they show higher yield stress when measured with the amplitude sweep. Why ABCL1, however, shows higher shear stresses when measured with the flow sweep, can not be explained. A mistake might have been made in setting up the test or loading the machine.

Based on the inconsistencies in measurements, the flow sweeps were not further used for yield stress evaluation, nor the comparison of different samples. TA instruments advises using oscillatory amplitude sweeps instead for yield analyses, as this test shows more accurate results in paste-like materials such as the ones tested here. Further yield stress evaluation was thus only done using the amplitude sweeps.

Based on the results we can however still conclude that all tested recipes display shear thinning behaviour, which is necessary for printing at room temperature.

5.2.2.2 OSCILLATION AMPLITUDE SWEEPS

Oscillation Amplitude sweeps were used to evaluate the structural breakdown of materials under stress and to evaluate their apparent yield stress.

Table 19 summarises the determined average yield onset point (σ_{onset}), flow point (σ_{flow}), FTI, apparent yield stress (σ_y), and the storage modulus (G'), loss modulus (G'') and loss tangent ($\text{Tan}(\delta)$) in the LVR of all recipes.

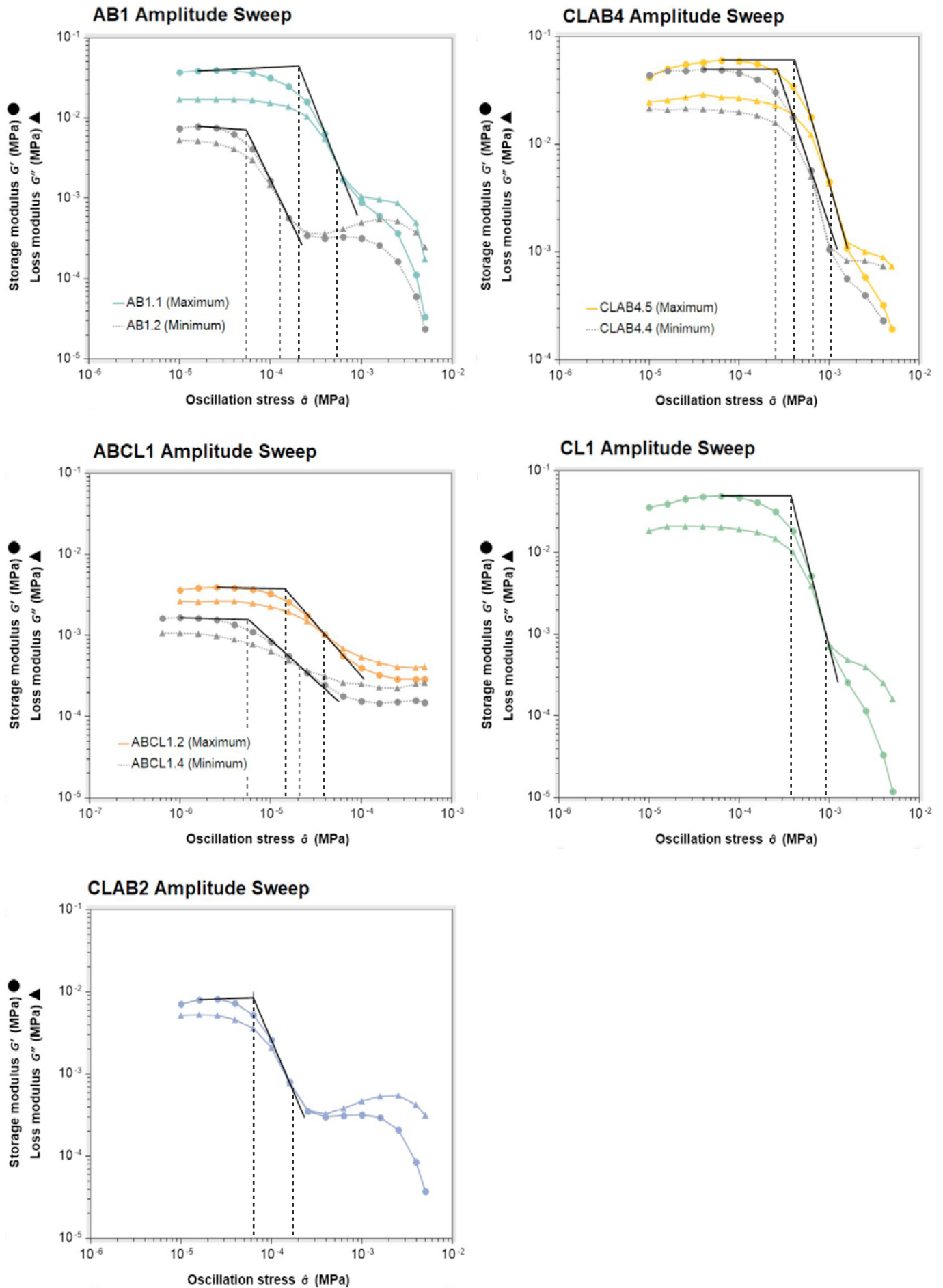
Figure 80 shows the oscillation amplitude sweeps of all recipes. The graphs show a double logarithmic plot of the measured storage modulus (G') and loss modulus (G'') as a function of increasing oscillation stress. For the recipes that were tested using 5 samples, Figure 84 shows the amplitude sweeps of the recipe with the highest and lowest measured values of G' , G'' , σ_y .

One sample (ABCL1.1) of the ABCL1 recipe, exhibited results that significantly diverged from the other values that were measured for this specific recipe. Consequently, it was identified as an outlier and therefore was not taken into consideration during the evaluation process. It is plausible that a material sample from another recipe that was not intended for this particular analysis was utilized in this instance.

Table 19: determined average yield onset point (σ_{onset}), flow point (σ_{flow}), FTI, apparent yield stress (σ_y), storage modulus (G'), loss modulus (G'') and loss tangent ($\text{Tan}(\delta)$) of recipes based on amplitude sweeps

	n	σ_{onset} (Pa)	σ_{flow} (Pa)	FTI	σ_y (Pa)	G' (Pa)	G'' (Pa)	Tan(δ)	Average Extrusion Pressure (Mpa)
AB1	5	127.20 ± 42%	429.95 ± 35%	3.38 ± 23%	214.98 ± 35%	21839 ± 48%	10986 ± 37%	0.54 ± 15%	0.46 ± 7.6% (n=12)
ABCL1	4	7.16 ± 59%	32.99 ± 20%	5.74 ± 37%	16.50 ± 20%	2722 ± 32%	1842 ± 31%	0.68 ± 4%	-
CLAB4	5	388.59 ± 8%	970.31 ± 11%	2.50 ± 5%	485.15 ± 11%	59119 ± 11%	23602 ± 8%	0.40 ± 10%	0.58 ± 5.1% (n=8)
CL1	1	378.43	951.26	2.51	475.63	48824	20812	0.43	0.24 (n=1)
CLAB2	1	63.15	190.37	3.01	95.18	8079	5209	0.64	0.64 (n=1)

Figure 80: Amplitude and flow sweeps of AB1.1 (Blue) and CLAB4.1 (Yellow)



Evaluating the yield stresses of the recipes, CLAB4 ($\sigma_y = 485.15$ Pa), CL1 ($\sigma_y = 475.63$ Pa) and AB1 ($\sigma_y = 214.98$ Pa) have yield stresses in a higher order of magnitude than ABCL1 ($\sigma_y = 16,50$ Pa) and CLAB2 ($\sigma_y = 95.18$ Pa). This correlates with the differences found in their structural stability. ABCL1, which has the lowest yield stress, showed the most extreme sagging of these recipes.

ABCL1's lower quality is also supported by its higher $\tan\delta$ and lower G' . Li et al. (2019) state that the G' within the LVR should exceed 10^3 Pa to support a stable multiple-layer 3D structure. The G' of ABCL1 falls within the 10^3 order of magnitude whereas the well-performing recipes (AB1, CLAB4 and CL1) exceed this with an order of magnitude of 10^4 .

Furthermore, according to Gao et al. (2018), lower loss tangent values indicate better structural stability, while higher values correspond to enhanced extrusion uniformity. The good structural stability of AB1, CLAB4, and CL1 is thus not only substantiated by their higher yield stress but also their lower loss tangents compared to ABCL1 and CLAB2.

There is no indication that the recipes with lower-loss tangents produce unsatisfactory extrusion uniformity. CLAB4, with the lowest measured loss tangent of $\tan(\delta) = 0.40$, seems not to have reached a threshold at which the extrusion uniformity compromises quality.

The addition of CL to the AB1 recipe (ABCL1) resulted in a large drop in yield stress of the material and an increase in the loss tangent and FTI. The FTI increase would suggest a reduction in the tendency of this recipe to show brittle fracture. The addition of AB to the CL1 recipe (CLAB2) resulted in similar changes, with a decrease in the yield stress and an increase in the loss tangent and FTI.

Lastly, it is worth noting that both AB1 and ABCL1 show bigger relative standard deviations than the CLAB4 samples. In the case of AB1 this, however, does not seem to result in bad results in terms of print quality.

5.2.2.3 THREE INTERVAL THIXOTROPIC TEST (3ITT)

A shear-thinning material's change in viscosity over time is referred to as thixotropy. Thixotropic materials respond to and recover from shear stresses with a delayed change in viscosity. The response and recovery to shear change varies significantly between recipes. Longer response and recovery times can be correlated to bad extrudability and shape retention after extrusion respectively.

Figures 81 and 82 show the 3ITT graphs for all materials tested. The graphs show the apparent viscosity as a function of the step time. Just from looking at the graphs alone, it is clear that, overall, higher second-phase shears result in lower phase 2 viscosities, as well as lower phase 3 recovered viscosities. This is, however, not as evident in ABCL1, where no clear trend can be determined. Other differences in the response and recovery behaviour can not be easily seen just from the graphs, therefore the more detailed data gathered will be further discussed.

Table 20 presents the initial viscosities (η_0) of the recipes tested and their phase 2 response behaviour. Table 21 presents their recovery behaviours. In the case of ABCL1, one sample was not included in the analysis due to a mistake in the test settings of this sample for the 10 s⁻¹ second-phase shear test. To be consistent, the results from this batch were also not included in the 20 s⁻¹ second-phase shear test.

ORIGINAL VISCOSITIES

Evaluating the initial viscosity of the recipes, CLAB4 has the highest with an average of 1.2E5-1.3E5 Pa.s, while ABCL1 (1.4E4 -2.2E4 Pa.s) and CLAB2 (2.1E4 -2.3E4 Pa.s) have the lowest averages. Though the samples tested for both the 10s⁻¹ and the 20 s⁻¹ second-phase shear tests were from the same 5 batches, there is a difference in average viscosity measured. The differences between averages can be attributed to slight non-homogeneity in the batches.

Figure 81: Three Interval Thixotropic tests with 10s^{-1} and 20s^{-1} second shear phase for AB1, CLAB4 and ABCL1

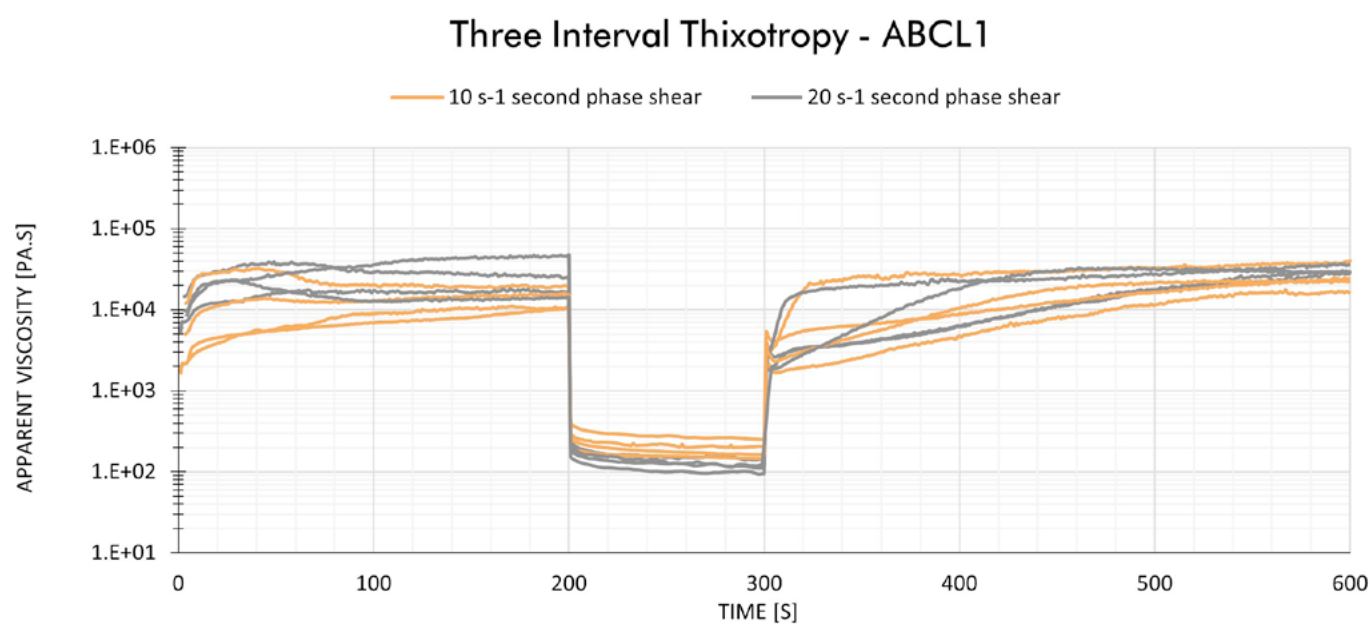
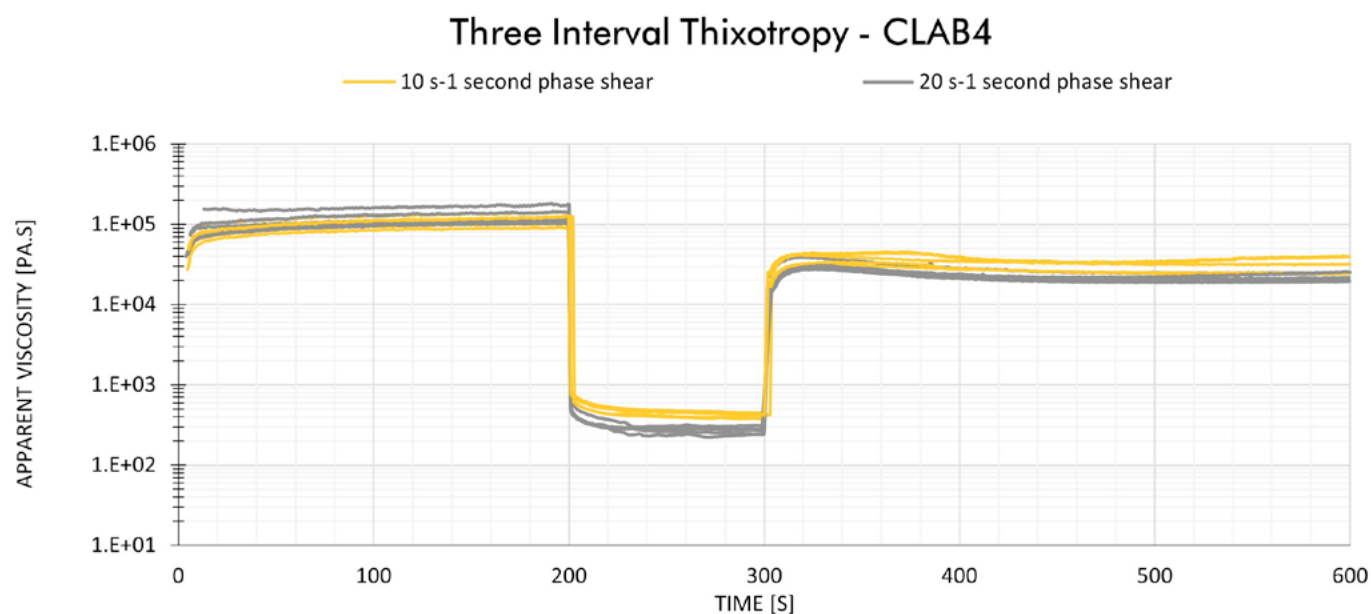
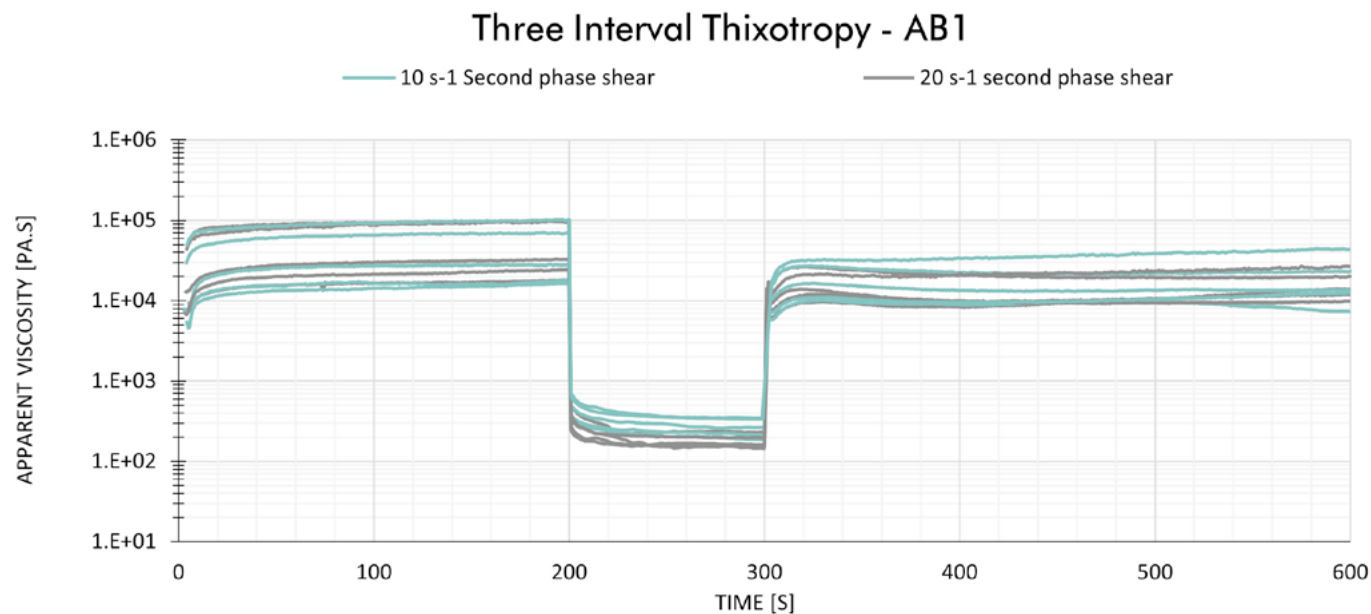


Figure 82: Three Interval Thixotropic tests with 10s^{-1} and 20s^{-1} second shear phase for CL1 and CLAB2

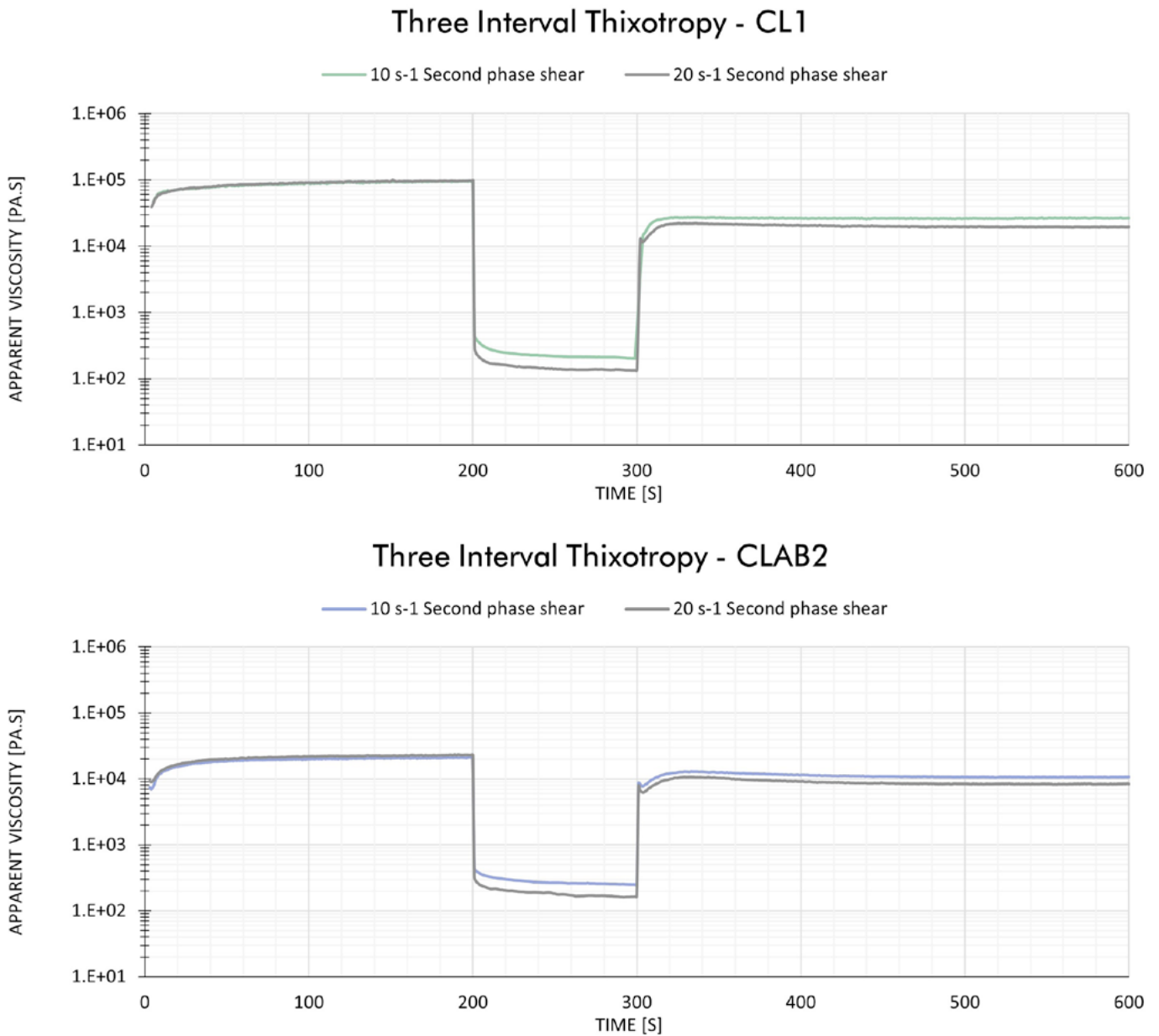


Table 20: determined average initial viscosity (η_0), phase 2 viscosity (η_2), initial responses rate and phase 2 levelling time of recipes based on 3ITT. *Possible inaccuracy in measurements

	Phase 2 shear rate (s^{-1})	n	η_0 (Pa.s)	η_2 after 1 s		η_2 final		Initial Response rate (Pa.s/s)	Phase 2 levelling time (s)
				(Pa.s)	(% of η_0)	(Pa.s)	(% of η_0)		
AB1	10	5	$4.6\text{E}4 \pm 71\%$	$5.2\text{E}2 \pm 28\%$	1.54%	$2.7\text{E}2 \pm 23\%$	0.83%	$-4.52\text{E}4$	$36 \pm 15\%$
	20	5	$5.4\text{E}4 \pm 66\%$	$3.5\text{E}2 \pm 23\%$	0.90%	$1.8\text{E}2 \pm 17\%$	0.48%	$-5.30\text{E}4$	$17 \pm 35\%$
ABCL1	10	4	$1.4\text{E}4 \pm 26\%$	$2.9\text{E}2 \pm 25\%$	2.28%	$1.9\text{E}2 \pm 21\%$	1.47%	$-1.36\text{E}4$	$20 \pm 51\%$
	20	4	$2.2\text{E}4 \pm 33\%$	$2.4\text{E}2 \pm 35\%$	0.98%	$1.5\text{E}2 \pm 44\%$	0.61%	$-2.16\text{E}4$	$13 \pm 24\%$
CLAB4	10	5	$1.2\text{E}5 \pm 16\%$	$7.8\text{E}2 \pm 7.0\%$	0.68%	$4.1\text{E}2 \pm 6.0\%$	0.36%	$-1.15\text{E}5$	$45 \pm 14\%$
	20	5	$1.3\text{E}5 \pm 19\%$	$5.3\text{E}2 \pm 10\%$	0.41%	$2.7\text{E}2 \pm 9.5\%$	0.21%	$-1.29\text{E}5$	$25 \pm 32\%$
CL1	10	1	$9.7\text{E}4$	$4.6\text{E}2$	0.47%	$2.0\text{E}2$	0.21%	$-9.60\text{E}4$ *	29
	20	1	$9.9\text{E}4$	$2.8\text{E}2$	0.29%	$1.3\text{E}2$	0.14%	$-9.41\text{E}4$ *	16
CLAB2	10	1	$2.1\text{E}4$	$4.5\text{E}2$	2.10%	$2.5\text{E}2$	1.17%	$-2.06\text{E}4$	35
	20	1	$2.3\text{E}4$	$3.2\text{E}2$	1.37%	$1.6\text{E}2$	0.70%	$-2.25\text{E}4$	32

Table 21: determined average phase 3 viscosity after 5 seconds (η_3), phase 3 final recovered viscosity ($\eta_{3\text{final}}$), and phase 3 levelling time of recipes based on 3ITT.

	Phase 2 shear rate (s ⁻¹)	n	η_3 after 5 s		$\eta_{3\text{rel}}$ after 5 s (Pa.s)	$\eta_{3\text{final}}$		Phase 3 levelling time (s)
			(Pa.s)	(% of η_0)		(Pa.s)	(% of η_0)	
AB1	10	5	1.23E4 ±45%	32.4%	1.20E4 ±45%	1.99E4 ±64%	49%	24 ±12%
	20	5	1.10E4 ±37%	26.0%	1.08E4 ±37%	1.65E4 ±37%	41%	23 ±15%
ABCL1	10	4	2.89E3 ±32%	21.9%	2.70E3 ±33%	2.55E4 ±34%	182%	-
	20	4	2.96E3 ±46%	13.1%	2.80E3 ±46%	2.72E4 ±11%	127%	-
CLAB4	10	5	2.59E4 ±17%	22.2%	2.55E4 ±17%	3.99E4 ±19%	26%	26 ±26%
	20	5	1.96E4 ±22%	15.0%	1.93E4 ±22%	2.25E4 ±11%	18%	24 ±13%
CL1	10	1	1.59E4	17%	1.58E4	2.65E4	27%	23
	20	1	1.25E4	13%	1.24E4	1.96E4	20%	36
CLAB2	10	1	8.2E3	38%	7.96E3	1.07E4	50%	33
	20	1	6.4E3	28%	6.26E3	8.35E3	36%	31

The better-performing recipes (AB1, CLAB4 and CL1) all have higher original viscosities than the less-performing recipes (ABCL1 and CLAB2). However, AB1 does show a large deviation in original viscosity and AB1 samples were tested that showed values close to the measured viscosities in ABCL1 and CLAB2.

When evaluating the effect of CL and AB addition to a recipe, adding a small amount of CL to an AB-based recipe (ABCL1) decreases the original viscosity. Surprisingly, adding a small amount of AB to a CL1-based recipe has the same effect. Since the weight percentages of added CL and AB are different in both recipes, nothing can be said about the size of this effect for each ingredient.

PHASE 2 RESPONSE BEHAVIOURS

When comparing the better-performing recipes with the less-performing recipes in Table 20, we can also see a clear difference when looking at the response rate. AB1, CLAB4 and CL1 all have a steeper response slope, meaning that they show more pronounced shear thinning. With a response rate of $-1.15E5$ Pa.s/s with $10s^{-1}$ second-phase shear and $-1.29E5$ Pa.s/s with $20s^{-1}$ second-phase shear, CLAB4 shows the strongest shear thinning behaviour.

Interestingly, there is no clear correlation between the performance of the recipes and how quickly they reach a steady-state viscosity in this phase. The worst-performing recipe (ABCL1) surprisingly has the shortest response levelling times ($t=20s$ and $t=13s$) and thus seems to reach a steady state the quickest. The longest response times are found in CLAB4 ($t=45s$ and $t=25s$) and AB1 ($t=36s$ and $t=17s$), which are the best-performing recipes. However, results from the 3ITT test with pre-shear, which will be discussed in Chapter 5.2.2.4, give a more accurate image of the behaviour of the materials in the context of mixing and printing.

The addition of CL to an AB-based recipe (ABCL1) and the addition of AB to a CL-based recipe (CLAB2) both result in a change in second-phase viscosity. CL to AB addition leads to a decrease in second-phase viscosity, whereas AB to CL addition has the opposite effect. Both also affect the response times of the recipes. The addition of CL to AB1 in ABCL1 causes a drop in response times, whereas the addition of AB to CL1 in CLAB2 shows an increase in response time.

EFFECT OF SHEAR RATE ON PHASE 2 RESPONSE BEHAVIOURS

As anticipated for shear-thinning materials, higher shears yielded lower phase 2 viscosities (η_2) across all recipes tested.

The biggest difference in second-phase viscosities for 10s^{-1} shear and 20s^{-1} shear is found in CLAB4 with an average difference of $1.4\text{E}2\text{ Pa}\cdot\text{s}$ ($4.1\text{E}2\text{-}2.7\text{E}2$), followed by AB1 with a difference of $0.9\text{ Pa}\cdot\text{s}$. This corresponds with the earlier finding that CLAB4 and AB1 show stronger shear-thinning behaviour compared to the less-performing ABCL1 recipe.

Differences found in phase 2 viscosities for CL1 and CLAB2 do not fully correspond with the previously found shear thinning behaviour based on the response rate. This is likely caused by the limited amount of samples being tested.

Furthermore, it appears that the degree of shear has a substantial impact on the response time across all recipes. A higher shear rate during the second phase appears to yield a faster initial response rate and levelling time. Only in CL1 do we see a lower initial response rate with higher shears. However, only 1 sample was measured for CL1, so this could be an inaccuracy in the measurements. In addition, the improvement of response in CL1 with higher phase two shears is still evident in the observed drop in levelling time.

Regarding ABCL1, not all tested batches show a clear decrease in response time with higher second-phase shears. Even though there is a clear difference when looking at the measured averages.

Lastly, it is noteworthy that the graphs with higher second-phase shears show more irregular and thus less controlled behaviour.

PHASE 3 RECOVERY BEHAVIOURS

Table 21 summarizes the data evaluating the recovery behaviour in phase 3.

When comparing the better-performing recipes with the less-performing recipes, we see that the less-performing CLAB2 and ABCL1 both show better recovery in terms of percentage recovered at the end of phase 3. However, in the case of CLAB2, the recovered viscosity is still quite a lot lower than those

of the good-performing recipes which can explain the lower quality result ($\eta_{3\text{final}} = 1.07\text{E}4$; $\eta_{3\text{final}} = 8.35\text{E}3$).

ABCL1, on the other hand, does show a high final recovered viscosity ($\eta_{3\text{final}} = 2.26\text{E}4\text{ Pa}\cdot\text{s}$; $\eta_{3\text{final}} = 2.43\text{E}4\text{ Pa}\cdot\text{s}$). Unfortunately, reaching this steady state of recovered viscosity takes a long time and its viscosity after 5 seconds of recovery, is lower than that of all other recipes ($\eta_3 = 2.89\text{E}3\text{ Pa}\cdot\text{s}$; $\eta_3 = 2.96\text{E}3\text{ Pa}\cdot\text{s}$).

Thus it seems that the addition of CL to an AB1 recipe (ABCL1) resulted in a lower recovered viscosity at 5 seconds, but a higher recovered viscosity at 5 min. The addition of CL has improved the final recovery percentage but has significantly slowed down the recovery rate as can be seen in the graph and the differences in viscosity at the 5s and 300s mark.

The addition of AB to a CL-base recipe (CLAB2) resulted in a higher overall recovered percentage, however, the final viscosity and the 5-second viscosity are both lower than in the CL-only recipe (CL1).

EFFECT OF SHEAR RATE ON PHASE 3 RECOVERY BEHAVIOURS

With all recipes, higher shear rates in the second phase result in lower recovered viscosities after 5 min, except for in ABCL1. The biggest difference in recovered viscosities between the different second-phase shears is again found in CLAB4, with a difference of $1.74\text{E}4\text{ Pa}\cdot\text{s}$. This corresponds with its biggest difference in phase 2 viscosities found with the different shears.

Upon analysing the relative recovery for various recipes, it becomes evident that a higher shear in the second phase seems to result in a slower initial recovery rate, though slightly. Thus, in addition to the overall recovered viscosity being lower with higher second-phase shears, the relative amount of viscosity recovered in the evaluated time spans is also lower.

Though the averages from most recipes, apart from CL1, suggest a shorter levelling time when higher second-phase shears are used, the differences are likely not significant. The differences are small, and the trend is not seen in all the individual batches tested. Some batches showed better levelling times when a 20s^{-1} shear was applied, whereas others showed the opposite effect. The levelling times of CL1 do show a clear difference. With CL1, a larger second-phase shear results in a slower levelling of the viscosity in phase 3. If this is always the case in CL1 can not be said for certain, because only 1 sample was tested ($n=1$). In ABCL1, the increase of viscosity in

phase 3 was too high to speak of levelling, thus it was left out of the analysis.

The findings of phase 3 also indicate that while the viscosities of recipes achieve a steady state within the 5-minute recovery period, there is still a marginal increase, suggesting that the viscosity continues to recover albeit at a low rate.

Lastly, it is again noteworthy that the measurements done for AB1 and ABCL1 show a lot more deviation than those of CLAB4.

Figure 83: Three Interval Thixotropic tests with and without 5 min 10s^{-1} pre shear conditioning for AB1 and CLAB4.

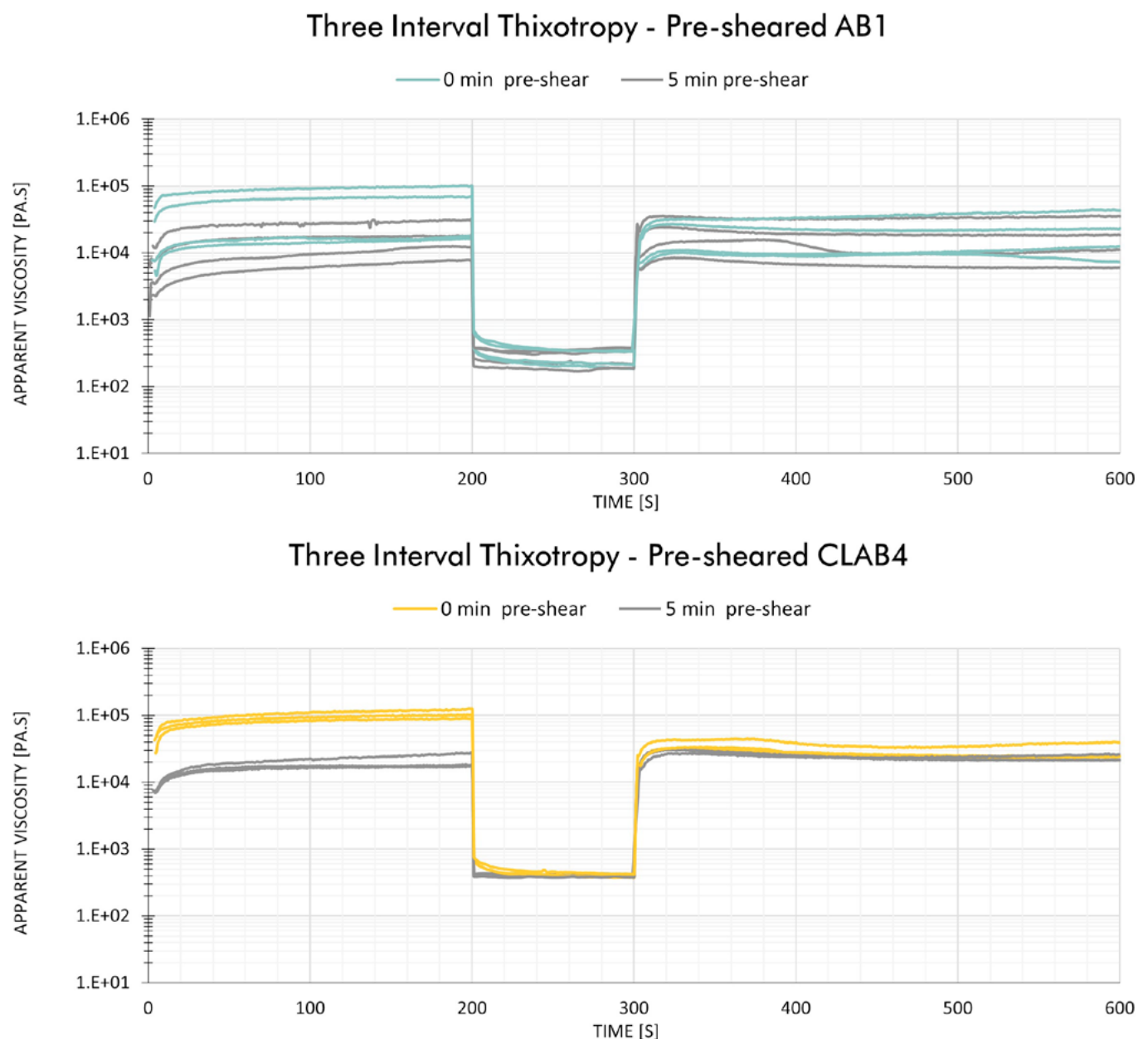
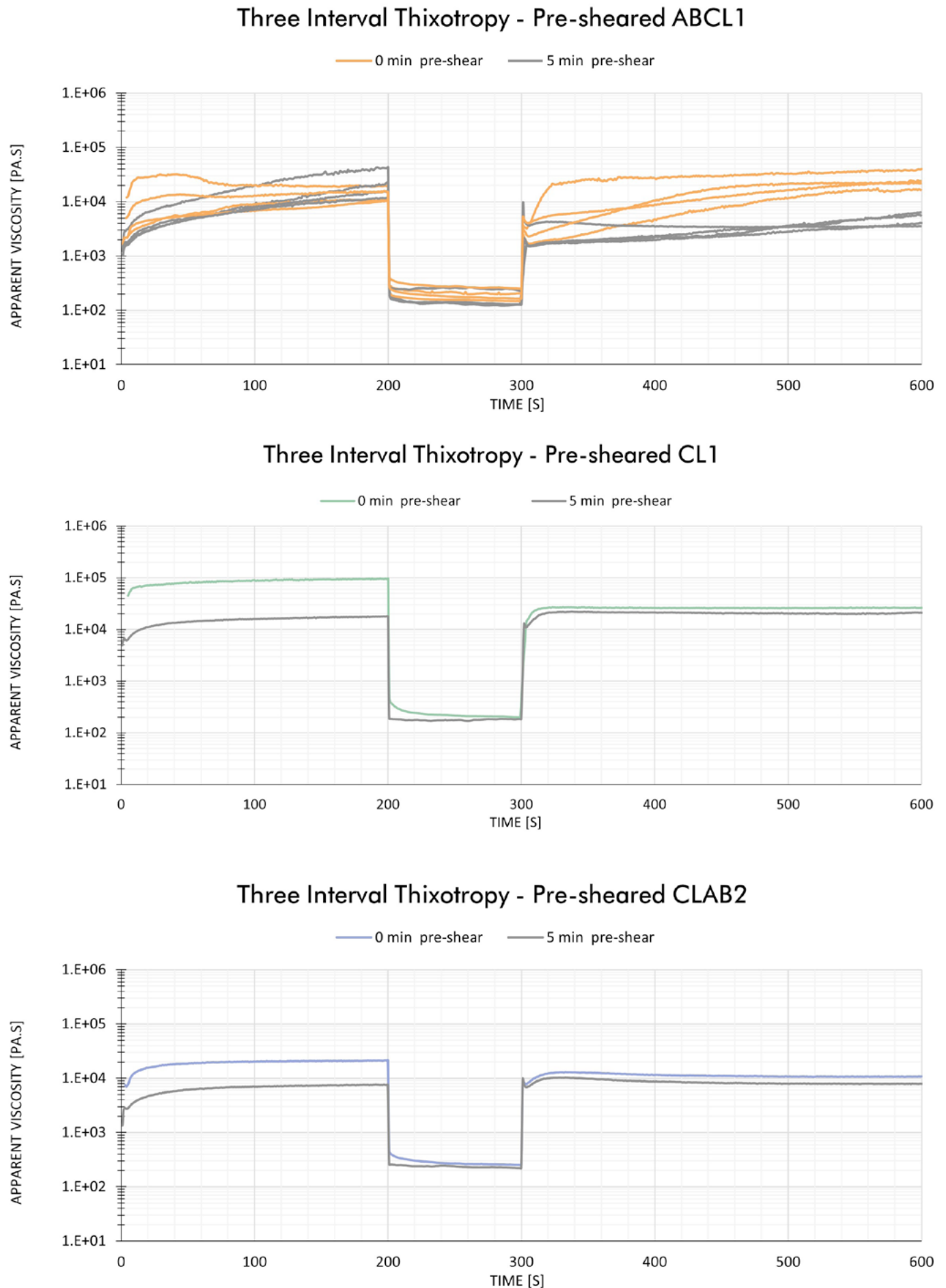


Figure 84: Three Interval Thixotropic tests with and without 5 min $10s^{-1}$ pre shear conditioning for ABCL1, CL1 and CLAB2



5.2.2.4 THREE INTERVAL THIXOTROPIC TEST (3ITT) WITH PRE-SHEARING

Figure 83 and 84 show the 3ITT graphs for all materials tested after being subjected to pre-shearing steps and compares them to the 10 s^{-1} second-phase shear 3ITT graphs of Chapter 5.2.2.3.

All graphs demonstrate a noticeable distinction in behaviour between pre-sheared and non-pre-sheared materials. The most notable change is the accelerated response to shear in phase 2. Extruding the materials immediately after mixing proves to be advantageous, as a faster response time leads to a more controlled flow of material at the onset of extrusion. Overall, this underscores the influence of the mixing process on the rheological behaviour of the materials, thereby affecting the quality of the prints.

ORIGINAL VISCOSITIES

Table 22 presents the initial viscosities (η_0) of the pre-sheared and non-pre-sheared recipes tested and their phase 2 response behaviour. In all recipes, pre-shearing results in lower initial viscosities, consistent with the results from Chapter 5.2.2.3 that neither of the recipes show full recovery after shearing in a short time span (in this case 2 min). With $8.40\text{E}4 \text{ Pa}$, CLAB4 shows the biggest drop

in original viscosity caused by pre-shearing. However, its original viscosity ($2.10\text{E}4 \text{ Pa}$) is still one of the highest among the pre-sheared recipes.

The most noteworthy finding is that ABCL1 seems to have an improved original viscosity at the 200s mark of phase 1 when it is pre-sheared. though it starts off with a lower viscosity in phase 1, it shows a steep increase within the 200 seconds measured.

PHASE 2 RESPONSE BEHAVIOURS

When looking at the changes in response behaviour, the most pronounced effect caused by pre-shearing is the difference in levelling time. For all recipes, except for ABCL1, Pre-shearing shows a clear improvement in the response levelling time and a big drop in phase 2 viscosity at 1 second.

Apart from ABCL1, all pre-sheared samples almost immediately reach a steady state in the second phase. Of the best-performing recipes, CLAB4 has a levelling time of less than 1s. For AB1, the rheometer missed measurements at 1 and 2 seconds, so we can only conclude that the levelling time is under 3 seconds. It could still be as quick as 1 second.

When printing samples in this research, the material has always been mixed right before printing and thus the effects caused by pre-

Table 22: determined average initial viscosity (η_0), phase 2 viscosity (η_2), initial responses rate and phase 2 levelling time of recipes based on 3ITT with 5 min 10s^{-1} and 2 min rest.

	Pre shear (min)	n	η_0 (Pa.s)	η_2 after 1 s		η_2 final		Phase 2 levelling time (s)
				(Pa.s)	(% of η_0)	(Pa.s)	(% of η_0)	
AB1	0	4	$5.09\text{E}4 \pm 70\%$	$5.20\text{E}2 \pm 31\%$	1.47%	$2.71\text{E}2 \pm 26\%$	0.80%	$34 \pm 13\%$
	5	4	$1.75\text{E}4 \pm 52\%$	$3.15\text{E}2 \pm 25\%$	2.05%	$2.80\text{E}2 \pm 28\%$	1.81%	$<3 \pm 70\% *$
ABCL1	0	4	$1.40\text{E}4 \pm 26\%$	$2.94\text{E}2 \pm 25\%$	2.28%	$1.91\text{E}2 \pm 21\%$	1.47%	$20 \pm 51\%$
	5	4	$2.32\text{E}4 \pm 52\%$	$2.27\text{E}2 \pm 15\%$	1.22%	$1.52\text{E}2 \pm 28\%$	0.85%	$5 \pm 51\%$
CLAB4	0	3	$1.05\text{E}5 \pm 14\%$	$7.42\text{E}2 \pm 3.4\%$	0.68%	$3.96\text{E}2 \pm 5.3\%$	0.38%	$42 \pm 11\%$
	5	3	$2.10\text{E}4 \pm 22\%$	$4.07\text{E}2 \pm 2.8\%$	2.03%	$3.95\text{E}2 \pm 2.1\%$	1.97%	$<1 \pm 0\% *$
CL1	0	1	$9.68\text{E}4$	$4.55\text{E}2$	0.47%	$2.0\text{E}2$	0.21%	29
	5	1	$1.78\text{E}4$	$1.90\text{E}2$	1.06%	$1.84\text{E}2$	1.03%	<1
CLAB2	0	1	$2.13\text{E}4$	$4.47\text{E}2$	2.10%	$2.5\text{E}2$	1.17%	35
	5	1	$7.57\text{E}3$	$2.55\text{E}2$	3.37%	$2.19\text{E}2$	2.89%	1

shearing are expected to have been present in all printed samples. With pre-shearing included, ABCL1 does not have the quickest levelling time anymore, but instead the slowest (5s). Its now slower levelling time compared to the other recipes can partially explain its inferior performance in terms of print quality, as a longer levelling time can result in less uniform extrusion.

PHASE 3 RECOVERY BEHAVIOURS

Table 23 summarizes the changes in recovery behaviour caused by pre-shearing.

The most noteworthy change is the increase in the percentage of recovered viscosity in phase 3 in all recipes except for ABCL1. The differences in phase 3 viscosities are small, especially when taking into account the variances between samples tested. Though the pre-shearing causes a significant drop in original viscosity, this effect does not translate as heavily into the final recovered viscosity in phase 3. In printing, this would mean that mixing before printing does not have a huge effect on the viscosity of the material after extrusion. However, In ABCL1, mixing does have a significant effect on the end viscosity, with an average end viscosity measured of 4.8E3 Pa.s compared to the 2.6E4 pa.s with no pre-shearing.

In terms of levelling, it seems likely that pre-shearing reduces the phase 3 levelling time for AB1, CLAB4 and CLAB2. In ABCL1, the increase of viscosity in phase 3 is still too high to speak of levelling, thus it was left out of the analysis. CL1 seems to display the opposite effect of the other recipes with an increase in levelling time due to pre-shearing. This finding correlated with the finding in Chapter 3.2.2.3, where CL1 showed longer phase 3 levelling times when a higher shear was applied in phase 2.

When considering recovery behaviour and its impact on print quality, it is crucial to note that the viscosity immediately after extrusion is more critical than the recovery time. For printed lines to maintain stability, the viscosity right after extrusion must exceed a specific threshold, ensuring it is stiff enough to maintain its shape. The time it takes to reach a steady state thereafter is of secondary importance.

The poor performance of ABCL1 in terms of shape fidelity may suggest that its initial recovered viscosity in phase 3 falls below this threshold. With average viscosities of 2.89E3 Pa.s (no pre-shear) and 2.10E3 Pa.s (pre-shear) at the 5-second mark, its viscosity at this point is lower compared to the other recipes.

Table 23: determined average phase 3 viscosity after 5 seconds (η_3), phase 3 final recovered viscosity ($\eta_{3\text{final}}$), and phase 3 levelling time of recipes based on 3ITT with 5 min 10s^{-1} and 2 min rest.

	Pre shear (min)	n	η_3 after 5 s		η_{3_rel} after 5 s	η_3 final		Phase 3 levelling time (s)
			(Pa.s)	(% of η_0)		(Pa.s)	(% of η_0)	
AB1	0	4	1.26E4 \pm 49%	30.5%	1.23E4 \pm 49%	2.16E4 \pm 64%	48.7%	24 \pm 12%
	5	4	1.49E4 \pm 56%	82.1%	1.46E4 \pm 57%	1.77E4 \pm 62%	95.2%	21 \pm 16%
ABCL1	0	4	2.89E3 \pm 32%	21.9%	2.70E4 \pm 33%	2.6E4 \pm 34%	182.2%	-
	5	4	2.10E3 \pm 45%	11.9%	1.94E3 \pm 23%	4.8E3 \pm 23%	27.6%	-
CLAB4	0	3	2.47E4 \pm 20%	23.4%	2.43E4 \pm 20%	2.95E4 \pm 19%	27.8%	29 \pm 21%
	5	3	2.02E4 \pm 13%	103.0%	1.98E4 \pm 13%	2.28E4 \pm 9%	111.2%	23 \pm 6%
CL1	0	1	1.6E4	17%	1.58E4	2.6E4	27%	23
	5	1	1.2E4	67.1%	1.18E4	2.1E4	117%	37
CLAB2	0	1	8.2E3	38%	7.96E3	1.1E4	50%	33
	5	1	7.1E3	93.9%	6.89E3	8.0E3	105%	26

CLAB2 exhibits the second-lowest viscosities of 8.2E3 Pa.s (no pre-shear) and 7.1E3 Pa.s (pre-shear) at this juncture. Despite some slight sagging, its overall stability is satisfactory. This suggests that the minimum viscosity threshold for prints to be stable enough is likely somewhere between 2.89E3 and 7.1E3 Pa.s.

5.2.3 CONCLUSION & DISCUSSION

The rheology experiments executed can help correlate the print quality of the evaluated recipes to their rheology characteristics and answer the research sub-questions from Chapter 5.2. In this conclusion, each question will be addressed.

1. Which rheology characteristics substantiate the superior performance of AB1 and CLAB2 compared to other developed recipes?

First of all, AB1 and CLAB4 have a higher yield stress than ABCL1, even though this results in higher shears required for the material to flow, it also means the material holds its shape better under the weight of multiple layers. The higher yield stress of both recipes compared to ABCL1 can thus partly explain why ABCL1 shows worse print quality, especially in terms of print sagging.

Secondly, When looking at the response and recovery behaviours of these recipes we can see clear differences between the good and bad performing recipes. Pre-sheared (mixed) AB1 and CLAB4 almost immediately reach a steady state when shear is applied in phase two, whereas with ABCL1 this takes longer. The quick levelling of viscosity in this phase allows for more consistent flow during extrusion and thus less need for adjusting the extrusion pressure used over time.

Additionally, ABCL1's recovery behaviour is a lot slower compared to the other two recipes. Even though the eventually recovered viscosity might be high enough for structural stability, the time it takes to reach this point is limiting the structural stability of this material when printing at a normal speed. For ABCL1 to print

better quality prints that sag less, a waiting time in between printing layers would have to be installed. Though this might help to print a stable print of a few layers, the recipe will still collapse earlier compared to AB1 and CLAB4 due to its lower yield stress.

lastly, ABCL1's exact behaviour is not as predictable which can be seen in the different behaviours found in different samples. This suggests that ABCL1 is a lot more sensitive to changing factors such as environmental conditions and the method of loading.

2. Does the shear rate influence the response and recovery time of the developed recipes? And is this always the same?

In terms of response rates, higher shears overall seem to result in quicker initial responses as well as an earlier reaching of the steady state. This could be explained by the fact that higher shears create more force to break the interactions within the material, causing a steady state to be reached more quickly. If this is actual the case would need to be investigated by a specialist In material chemistry.

This theory would also explain why pre-shearing helps to improve the response behaviour as parts of the interactions within the material that are not recovered yet, would not have to be broken this time round.

When looking at the recovery, a higher second-phase shear only seems to result in a drop in recovered viscosity. It does not significantly improve the levelling time. Only in CL1 does it negatively affect the levelling time. We can, however, not say if this is an accurate result since only one sample was tested for this recipe.

All in all, higher shears predominantly show positive effects on the response behaviour of the recipes, resulting in a more consistent flow during extrusion. However, they do decrease the final recovered viscosity which can be detrimental to the structural stability of the print if this value becomes too low.

To conclude, it is thus important to find a balance between quick response behaviour and sufficient recovered viscosity to allow for both a consistent flow and good structural stability. When printing, the amount of shear can be adapted by using different diameter nozzles or by adjusting the print speed, which would require more or less extrusion pressure.

3. To what extent does shear history as referred to by Tagliaferri et al. (2021) play a role in the rheology characteristics and thus printability of the materials?

Shear history has a high influence on the response and recovery behaviour of the material. It has both “negative” and “positive” effects. On the one hand, shear history caused recipes to have a lower initial viscosity after shearing. On the other hand, it improved the response behaviour of all recipes (though less in ABCL1).

When formulating a recipe, however, the drop in initial viscosity can be taken into account, making the positive effect of pre-shearing on the response behaviour more valuable. The improved response results in more uniform extrusion at set extrusion pressures when printing, eliminating the need to adjust extrusion pressures at the start of a print.

Though pre-shearing lowers the initial viscosity of a material, the effect of it on the eventually recovered viscosity is small. The recovered viscosity of pre-sheared and non-pre-sheared recipes are relatively close to each other. Thus we can argue that the pre-shearing would have nearly no effect on the stability of the material after printing. Additionally, pre-shearing results in slightly quicker recovery levelling in AB1, CLAB4 and CLAB2. In CL1 the effect is opposite.

To conclude, pre-shearing, comparable to mixing, predominantly improves the response behaviour of the recipes and does not have a huge effect on the viscosity of the material after extrusion. Mixing or remixing a material just before printing can therefore be seen as a beneficial step in the production process. Tweaking the mixing procedure can thus play a key factor in optimizing the print quality of materials.

What is the influence of AB and CL on the rheology characteristics of the recipe?

As can be concluded from all results shown, the addition of either AB or CL does not follow a general trend. In terms of initial viscosity, for example. Both adding AB and CL can decrease the viscosity of a recipe. It thus seems that there is no easy way to adjust a specific rheology characteristic of a recipe by adding one or the other.

The resulting rheology seems to be mainly influenced by the ratios between ingredients and therefore their interaction with each other. As already concluded in a lot of papers in this field, there is not really a general guideline to follow when you want to reach a certain behaviour in soft materials.

Additionally, only 1 sample per recipe and two recipe variations were tested. Testing more samples and more variations might help to find trends. This, however, is a time-consuming task and thus does not fit in the scope of this research.

However, through observing the recipes that were tested using multiple samples, a significant distinction between recipes primarily based on AB (ABCL1, AB1) and those mainly based on CL (CLAB4) was made. AB-based recipes exhibited more variation between samples. While this does not directly impact the print quality of AB1 with the current printer and settings, it could pose issues if the production would eventually be commercialised. Currently, slight adjustments in printer settings (like extrusion pressure) can account for the differences between samples. However, if this material were to be produced on a larger scale, constantly adjusting settings would not be cost-effective.

General remarks

Based on all results we can conclude that rheology can play an important part in the printability of formulated materials and that looking into these characteristics can help understand materials better and eventually even help perfect them. However, the time it takes to execute these tests is too long for it to

be used as a tool in the initial formulation of recipes, as a trial-and-error workflow would require less time.

Yet, Rheology tests have the potential to be vital in later stages of the process. They offer a means to refine the behaviour of an established recipe, particularly when these materials need to meet certain quality standards for commercial and large-scale production. Within this domain, rheology testing can help to significantly enhance the precision and repeatability of a material's print quality.

In future research, rheology test results could also serve as valuable input for configuring printer settings, eliminating the necessity for trial-and-error adjustments of printer settings. This approach would effectively mitigate challenges from subtle batch variations, as rheology results could promptly inform the optimal settings for superior print quality.

5.3 REPRINTABILITY: DEGRADATION OF PRINT QUALITY

With the need to reduce the environmental footprint of additive manufacturing, the possibility of reprintability with low-quality degradation can be another significant improvement. This part of the study's objective was threefold:

1. To assess the feasibility of reprinting the developed materials.
2. To evaluate the print quality degradation during the reprinting process.
3. To determine the material efficiency: the percentage of material lost per cycle.

The first two objectives were motivated by the known degradation patterns frequently observed in recycled materials, which are caused by contaminants, structural changes, and thermal history. By not employing heat during printing, the aspect of thermal history in the developed materials is minimized or

maybe even eliminated. It was thus valuable to check if this may lead to enhanced reprintability and reduced quality degradation.

The final objective stemmed from the substantial amount of ink that tends to remain trapped in the printer's syringe without being properly extruded. Moreover, it was anticipated that there would be some material loss during the grinding process of samples for reprinting and the mixing of the material.

5.3.1 MATERIALS & METHODS

5.3.1.1 EXPERIMENTAL SETUP

Both AB1 and CLAB4 were evaluated on their reprintability. The initial recipes for both materials were mixed following the predetermined procedure in Chapter 3.2.2.1, after which they were extruded in lines using the air-pressurised syringe of the Eazio bio.

The reason for extruding lines instead of printing full models was to reduce the time needed for both the extruding and drying of the material. Though these conditions are not 100% similar to printing a model and thus might result in slightly different results, this decision allowed the test to incorporate 3 cycles of reprintability for both materials. In the case of this research, testing multiple reprint cycles was deemed more valuable.

The material was extruded without the use of a nozzle to reduce the extrusion time. This resulted in lines with a diameter of 2 mm.

The preparation of the material for each reprint cycle included the following steps:

1. Grinding of the extruded lines/samples (when dry) into a powder with particle sizes smaller than 500 μ m.
2. Formulation of a paste-like material by the re-addition of solvents. In this case water and ethanol.

Grinding experiments were done using a Victorio VKP1024A grain mill, a coffee grinder, a pestle and mortar and a Waring commercial laboratory blender.

After testing different methods, the decision was made to use the blender in combination with a 500 μ m sieve to ensure small enough particle sizes to prevent clogging. This method proved to be the quickest.

Figure 85 illustrates the process employed for formulating a reprintable paste. The material was ground using high-speed settings in cycles of 1 minute of grinding followed by 1 minute of rest to prevent overheating of the materials. Powder that was not fine enough to pass through the sieve was pulverized further using the pestle and mortar until it was fine enough. The powder was stored in closed containers until it was used for paste formulation.

The recipe for reprinting was created by adding solvents to the powder. For all recipes, the amount of ground powder equivalent to the total mass of dry materials in the virgin recipe was used. Initially this, amount of ground powder was mixed with the original quantity of solvents used in the virgin recipe. However, slight adaptations were made during the process to achieve the desired viscosity.

Table 24 displays the virgin recipes, the original reprint recipes and the final adapted reprint recipes with their corresponding extrusion pressures. The same reprint recipes were used for all reprint cycles.

Table 24: Virgin recipe, initial reprint recipe and final reprint recipe of both AB1 and CLAB4, including the corresponding extrusion pressures.

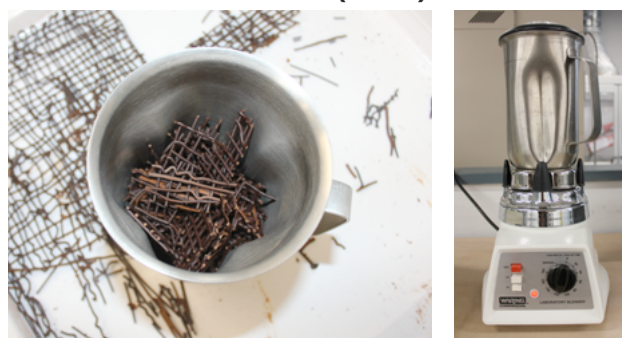
Recipe	Ingredients (g)	Extrusion pressure (Mpa)
AB1 virgin	11 PSF; 27 AB; 11 Water; 7 Ethanol	0.46
AB1 Reprint v1	38 ground print; 11 Water; 7 Ethanol	0.32
AB1 Reprint final	38 ground print; 10.5 water; 6.5 Ethanol	0.55
CLAB4 virgin	18 PSF; 16 CL; 9 AB; 14 Water; 6 Ethanol	0.58
CLAB4 Reprint v1	43 ground print; 14 Water; 6 Ethanol	0.15
CLAB4 Reprint final	4 g ground print; 12.5 Water; 4.5 Ethanol	0.49

Figure 85: Reprinting process

1. DRYING OF THE EXTRUDED (VIRGIN) MATERIAL



2. GRINDING OF THE EXTRUDED (VIRGIN) MATERIAL



3. ENSURING A PARTICLE SIZE OF <500 μ M



3. STORING OF THE GROUND MATERIAL FOR REPRINTABLE PASTE FORMULATION



3. PREPARING THE PASTE BY ADDING POWDER TO SOLVENTS & MIXING



For each cycle of reprints, two quality assessment samples and two organically shaped vases were printed. Only two samples for each cycle and test were printed due to time constraints and limited ingredient availability. For comparison, all samples were printed using the same fan setup and printer settings used in Chapter 5.1 (Table 14). The material left over after each reprint cycle was extruded again for use in the next cycle.

5.3.1.2 QUALITY METRICS AND DATA COLLECTION

All quality assessment samples were rated by evaluating the same quality aspects used in Chapter 5.1 Table 15. These include dimensional accuracy, bridging and overhang capabilities, warpage, corner sharpness and surface finish. The vase print served as a visual demonstrator of the reprintability.

To measure the efficiency of the reprinting process, the weights of the dry-reprinted materials were measured in all steps of the process; pre-grinding, post-grinding and post-printing. Furthermore, an evaluation of the residual material, both within the mixing beaker and the extrusion syringe, was conducted. These residues were left to dry, after which their weights were determined.

The objective was to pinpoint the particular stages in which material loss predominantly occurred; be it during the grinding, mixing, or the printing process itself. This approach allowed for an evaluation of the overall efficiency of the process and lays the groundwork for targeted improvements in areas with higher material loss rates.

5.3.2 RESULTS

Figure 86 shows some quality samples printed for each reprint cycle. Figures 87 and 88 show the boxplots of the measured quality metrics over 3 reprint cycles. The quality metrics of the prints over three reprint cycles are compared to the original quality metrics measured in Chapter 5.1. It is important to note that the data available for each cycle varies, with the virgin material having

a sample size of 8 or 9, while subsequent reprint cycles have smaller sample sizes, ranging from 2 to 3 samples. The discrepancy in sample sizes may impact the interpretability of the boxplots and should be taken into consideration when drawing conclusions. Additionally, with only 2 samples in some reprint cycles, constructing a robust box plot is inherently limited. This may result in potentially misleading visualizations.

Despite these limitations, the boxplots serve as a valuable visual tool for initial insights into the quality metrics of the printed samples across different reprint cycles. Since only a limited amount of quality samples were printed for each reprint cycle, no significant effects are proven in this section. Yet, the results can give a good indication of the possibility of reprinting the materials for multiple cycles. Future studies with larger and more consistent sample sizes are recommended to validate these findings.

5.3.2.1 REPRINT RECIPE ADAPTATIONS

As shown in Table 24, different reprint recipes were experimented with. Assuming complete solvent evaporation during drying, the initial reprint recipe incorporated the original quantity of solvents used in the virgin recipe. Surprisingly, with this recipe, both the AB1 and CLAB4 reprint recipes seemed to yield lower viscosities compared to the virgin recipes. This outcome was further supported by the observed reduction in necessary extrusion pressure during printing.

The lower viscosity observed in the reprint recipes could be attributed to the interactions between solvent molecules with other ingredients of the virgin materials, impeding their evaporation (e.g. hydrogen bonds). In the virgin material, the presence of solvent molecules in a bonded state would hinder their escape during the drying process. Consequently, the presence of pre-established bonds reduces the number of available bonding sites for newly introduced water and ethanol molecules in the reprint recipes. This scarcity of available bonding sites could be the cause of the lower quantity of solvents needed to achieve the original viscosity.

Figure 86: Quality assesment samples of AB1 (a) and CLAB4 (b) over 3 reprint cycles

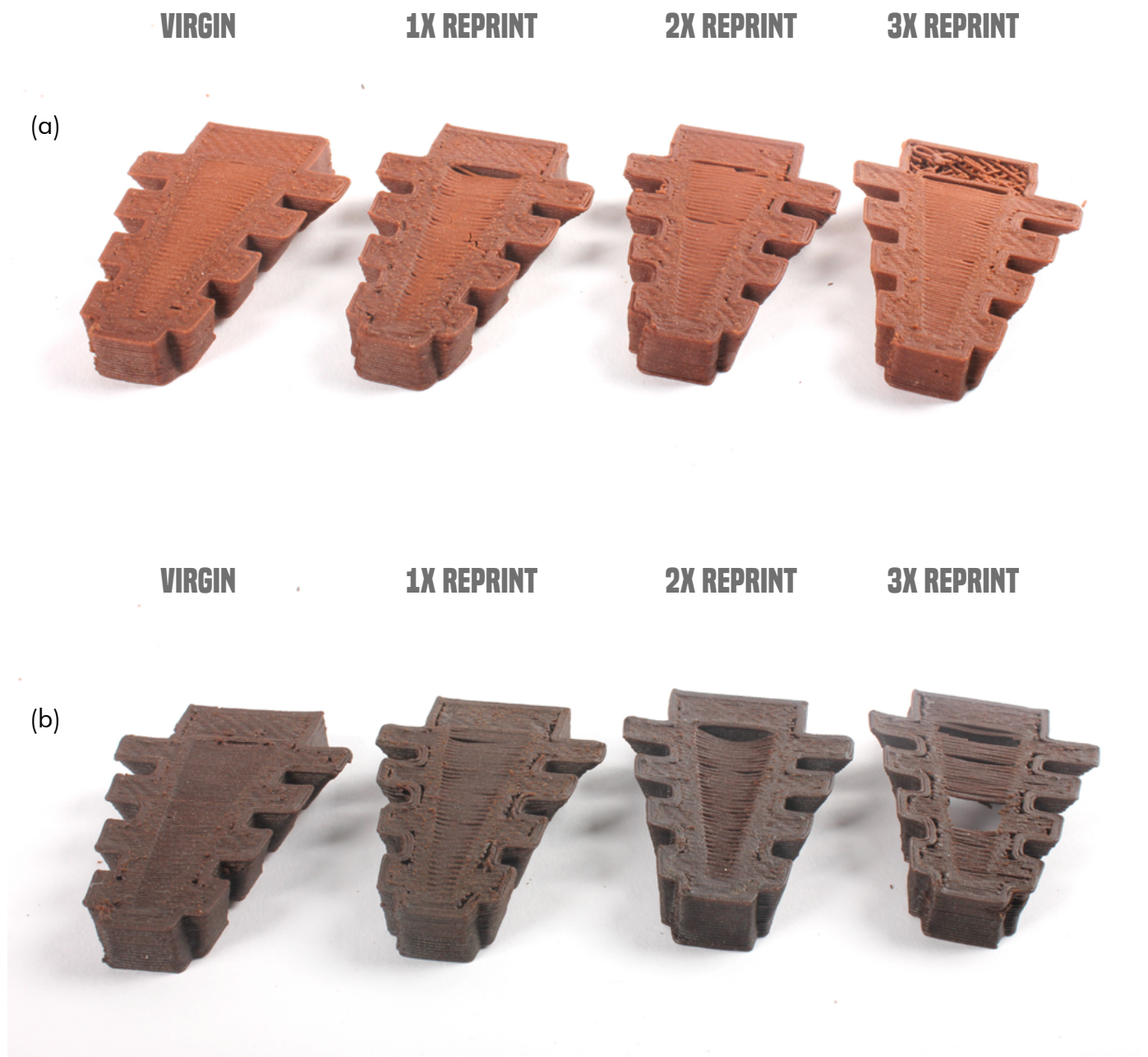
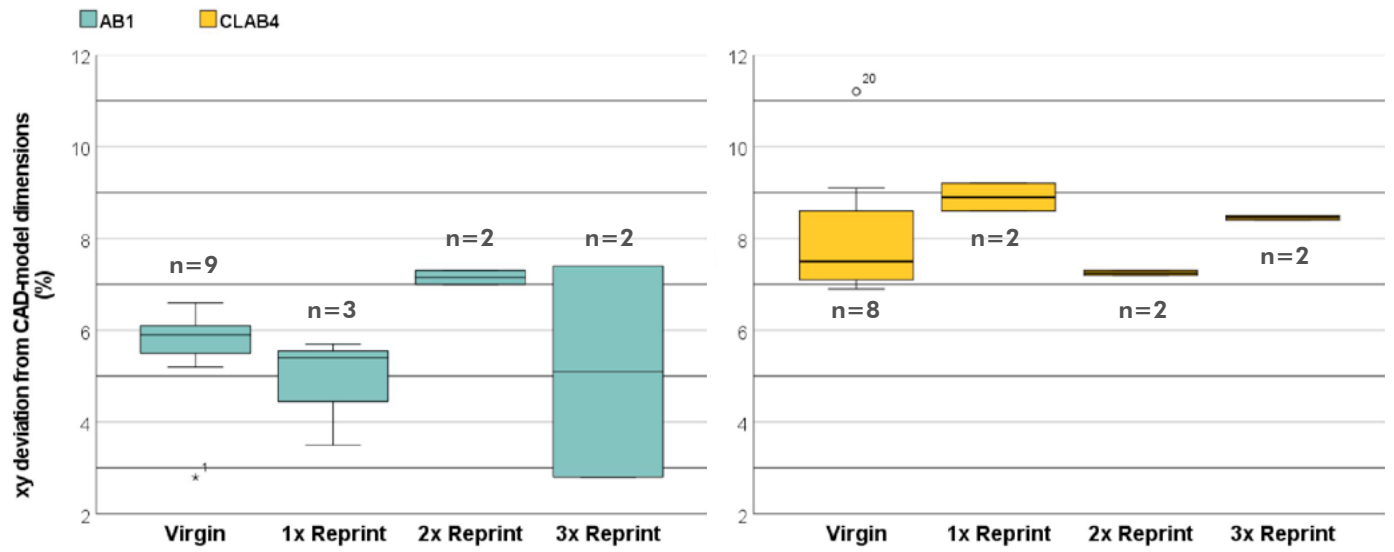
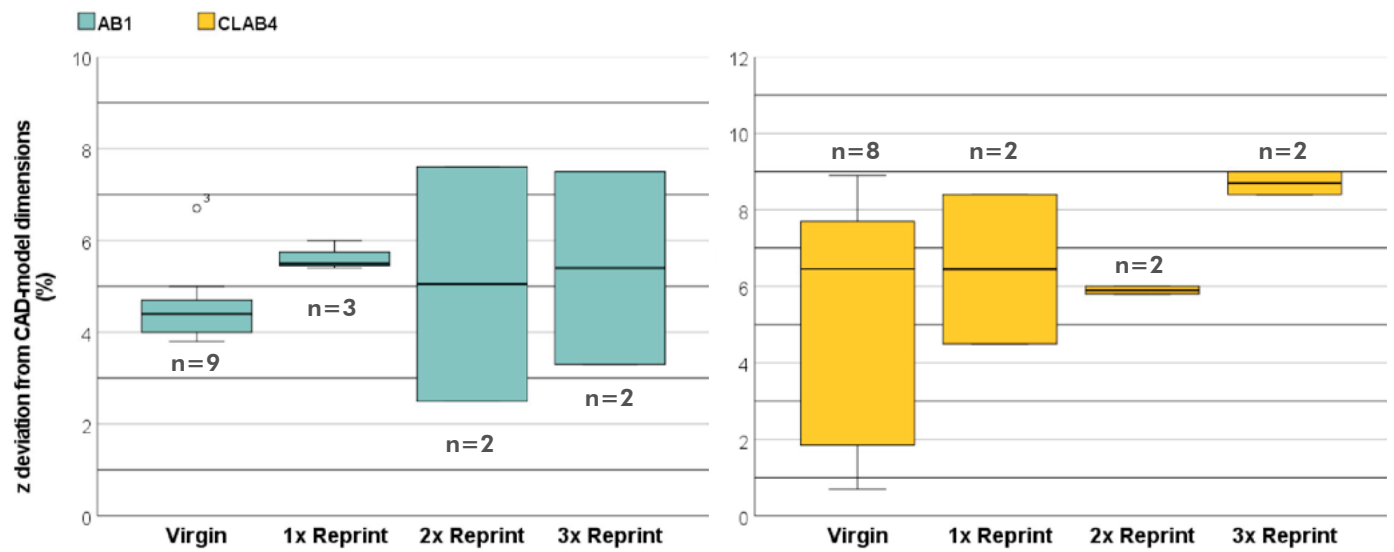


Figure 87: Box plots displaying the distribution of virgin material and 3 cycles of reprinting for (a) dimensional accuracy in the xy plane, (b) in the z-plane, and (c) bridging of AB1 (blue) and CLAB4 (yellow). The plot includes: the median (solid line within the box), lower and upper quartiles (bottom and top boundaries of the box, respectively), and minimum and maximum values (whiskers)

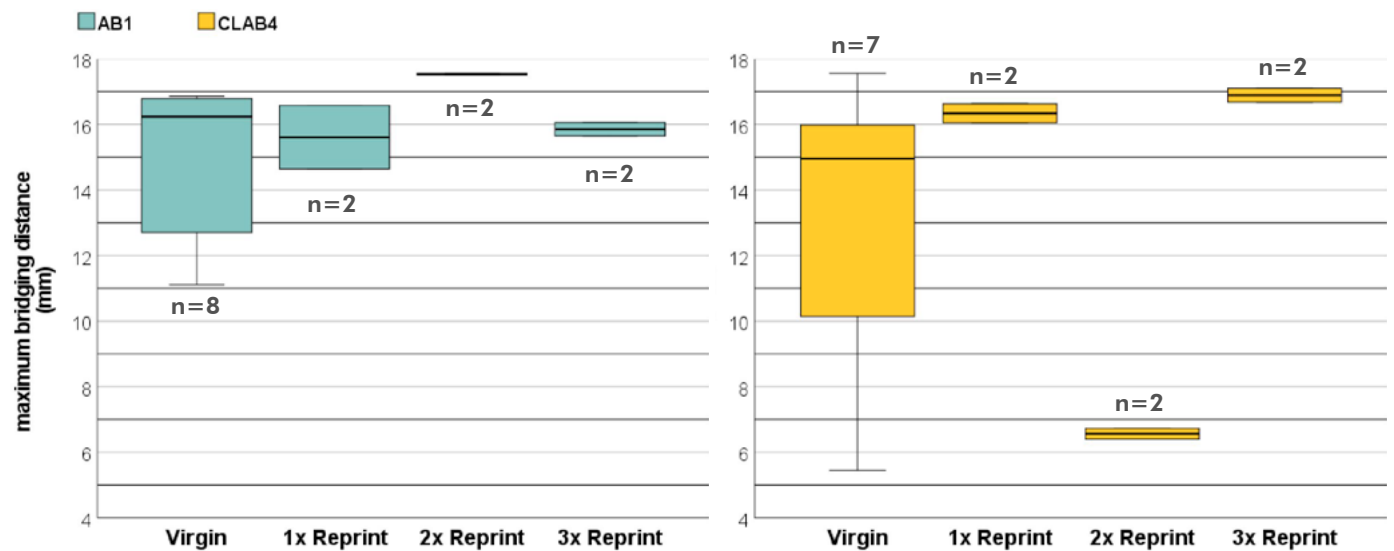
(a) DIMENSIONAL ACCURACY IN THE XY-PLANE OF AB1 & CLAB4



(b) DIMENSIONAL ACCURACY IN THE Z-PLANE OF AB1 & CLAB4



(c) MAXIMUM BRIDGING IN AB1 & CLAB4



5.3.2.1 DIMENSIONAL ACCURACY

The boxplots in Figure 87a&b visualise the dimensional accuracy of samples across multiple reprint cycles.

In both AB1 and CLAB4, no clear trend in degradation of quality over three reprint cycles is visible. This suggests that a trend in degradation, if present, is too small to be proven with the limited amount of samples printed. Yet some interesting observations can be made.

In CLAB4, the average dimensional deviations both in the xy-plane and z-plane are higher in reprint cycles 1 and 3 than in the virgin material. Despite this, these values still fall within the deviation range of the virgin material. This complicates the determination of whether signs of degradation are present, particularly since the average dimensional deviation is lower in the second reprint cycle.

In AB1, the average deviation in the xy-plane does exceed the deviation range of the virgin material in the second and third reprint cycles. However, in the 2x reprint, the average is higher, whereas in the 3x reprint, the average is lower. Thus, no trend can be spotted. The average deviations from the CAD model in the z-direction do hint at a possible trend in degradation, as the averages of the reprinted samples are all higher than the upper limit of the Virgin sample boxplot. However, these results could be skewed due to the limited amount of samples tested with the reprints.

5.3.2.2 BRIDGING

The boxplots in Figure 87c illustrate the maximum bridging distances of AB1 and CLAB4 over multiple reprint cycles.

In both AB1 and CLAB4, there is no apparent decrease in maximum bridging distance as reprint cycles increase. In all cases, except for the second reprint cycle of AB1, the average bridging distances measured fall within the deviation range of the virgin material averages.

Notably, the average bridging distance of 17.54 mm for AB1 in the second reprint cycle surpasses the average of 14.93 for the virgin material, suggesting potential improvement due to reprinting. However, given the limited sample size, it is probable that this enhanced average is influenced by other factors. This is especially pertinent since the averages of reprint cycles 1 and 3 do not support this observation.

CLAB4 shows a big drop in maximum printing distance at the 2x reprint. Since the 3x reprint shows sufficiently better results again, it is expected that this drop was caused due to other factors than the reprinting.

5.3.2.3 OVERHANG

The boxplots in Figure 88a show the maximum acceptable overhang angle of AB1 and CLAB4 over multiple reprint cycles. No overhangs higher than 40° were printed, therefore this is the maximum in all recipes. Again, for both recipes, no clear degradation of quality with each reprint cycle is visible.

In AB1, there appears to be a potential improvement in the maximum overhang observed in the reprinted samples. All AB1 samples in reprint cycle 3 exhibit a maximum overhang angle of 40°, whereas the virgin samples and the first and second reprint cycles of AB1 also include samples with a maximum overhang of 35°.

However, definitive confirmation is not possible due to the limited number of reprinted samples evaluated in the reprint cycles (n=2). The improved overhang may equally be attributed to enhanced environmental conditions during printing.

Yet, there is a possibility of an actual increase in overhang quality over multiple reprint cycles. However, given that 40° represents the maximum overhang that was measurable in the assessment model, this increase might not be as visible in the results. Future research is recommended to include more samples and larger overhangs for comprehensive testing.

5.3.2.4 WARPAGE

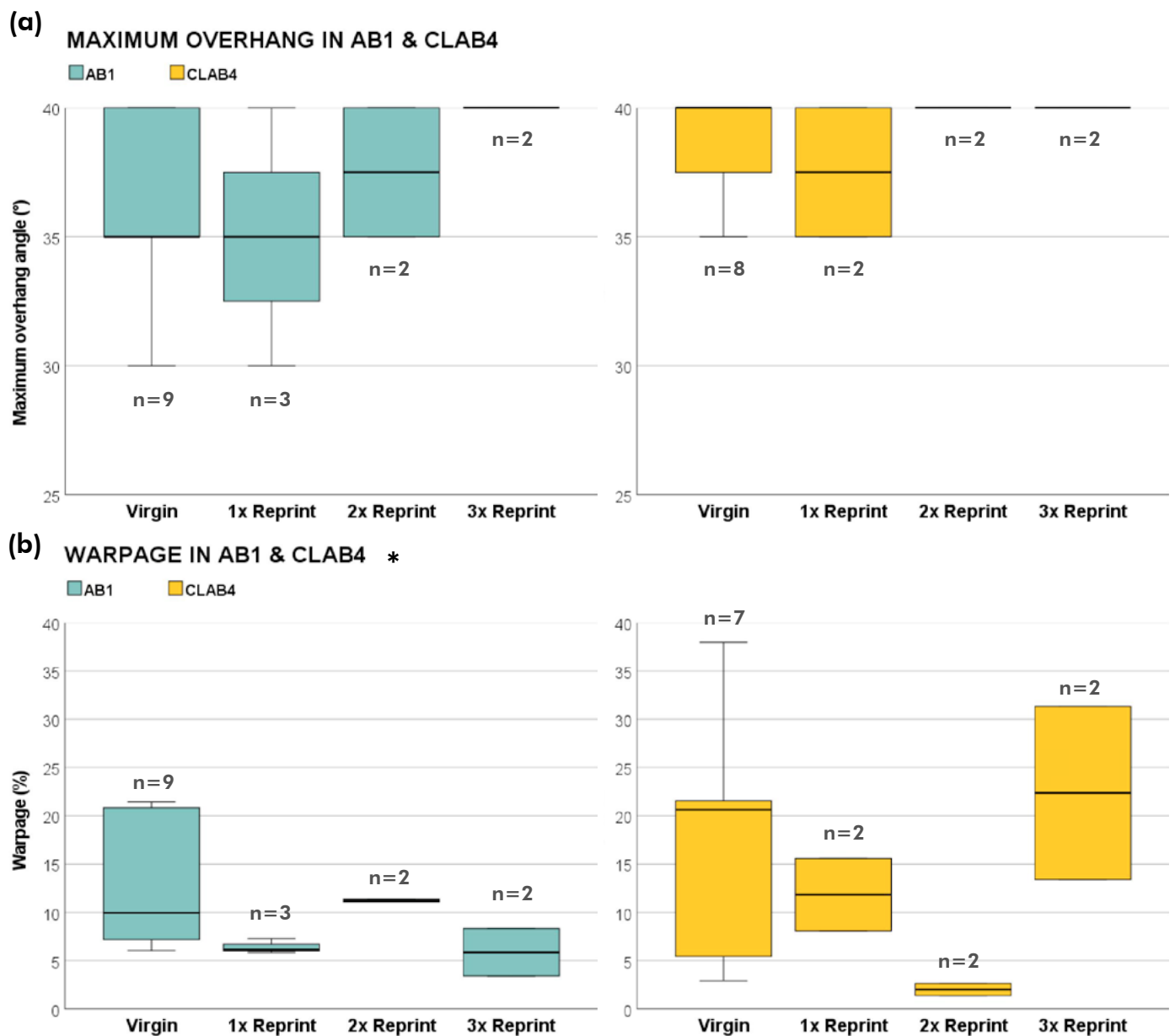
The boxplots in Figure F88b display the warpage in AB1 and CLAB4 over multiple reprint cycles. Again, no significant trend in changes of quality with each reprint cycle is visible. As discussed in Chapter 5.1 the main driver in warpage is assumed to be the way the sample is dried and since this was not controlled within this research, no good conclusions can be drawn based on this data.

5.3.2.5 SURFACE FINISH & CORNER SHARPNESS

Due to the unavailability of proper measuring equipment, this assessment relied on subjective ratings to evaluate the surface finish and corner sharpness of the two recipes as explained previously.

No noteworthy changes in surface finish or corner sharpness were observed in the reprinted samples.

Figure 88: Box plots displaying the distribution of virgin material and 3 cycles of reprinting for (a) overhang and (b) warpage of AB1 (blue) and CLAB4 (yellow). The plot includes: the median (solid line within the box), lower and upper quartiles (bottom and top boundaries of the box, respectively), and minimum and maximum values (whiskers).



* measurements were done on an ordinal scale for the maximum overhang angle, but are displayed here as a scale variable for better comparison between quality metrics.

5.3.2.6 VISUAL DEMONSTRATORS

Figure 89 & Figure 90 show visual demonstrators printed for each reprint cycle of AB1 and CLAB4 respectively. In these demonstrators, no clear differences can be detected between the different reprint cycles.

These demonstrators prove that these types of geometries can be printed with good quality even after 3 cycles of reprinting. Though still some print defects can be spotted within these prints, they do not seem to be caused by the reprinting as no trend can be detected.

Figure 89: Reprint quality demonstrators AB1 for (a) virgin (b) 1x reprint (c) 2x reprint and (d) 3x Reprint

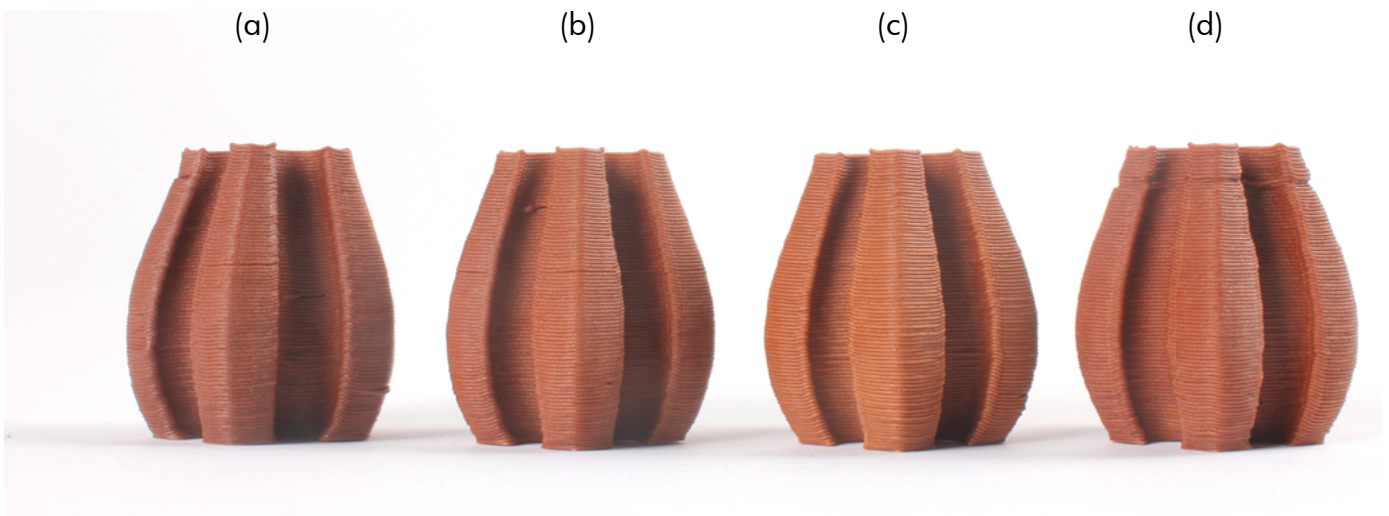
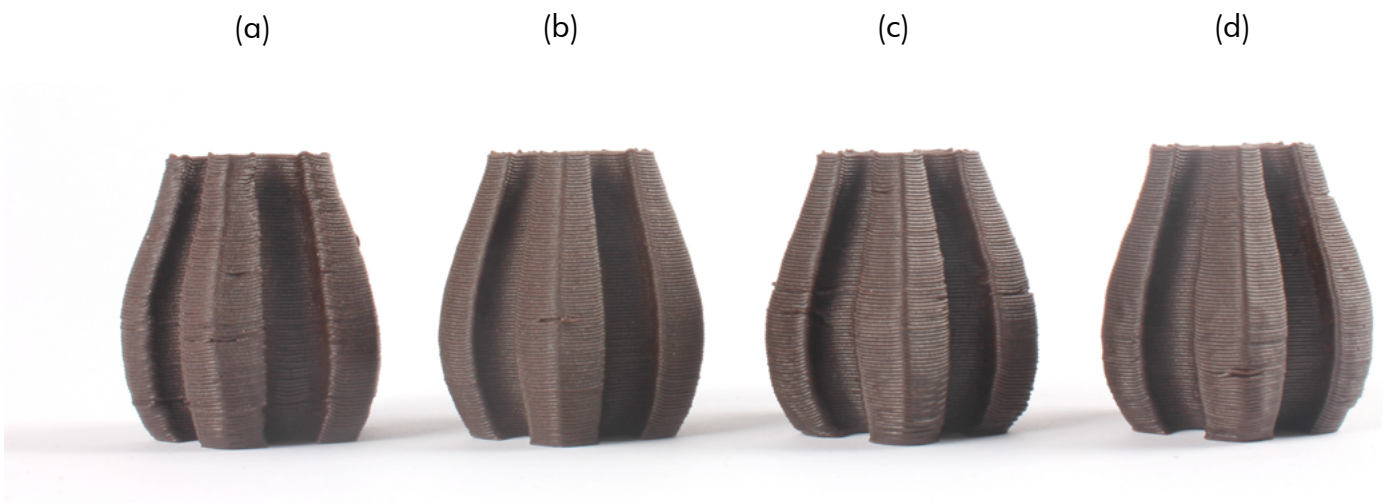


Figure 90: Reprint quality demonstrators CLAB4 for (a) virgin (b) 1x reprint (c) 2x reprint and (d) 3x Reprint



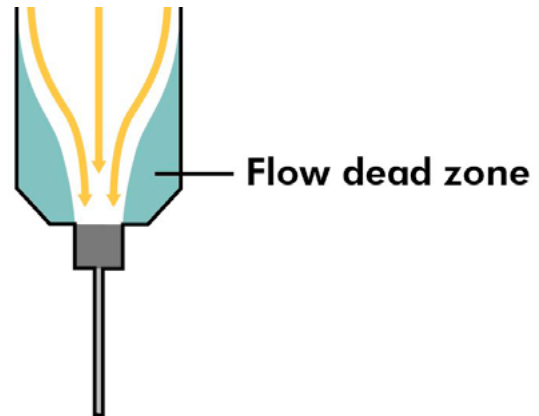
5.3.2.7 PROCESS EFFICIENCY

Figure 91 shows pie charts displaying the areas of material loss in the reprint process of AB1 and CLAB4. The results are based on measurements done while performing the reprintability test. These measurements were not able to be done with high precision and the graph therefore only indicates where the most material loss occurs. To gather the actual precise amount of materials lost in the process, more elaborate research would have to be done.

No significant differences are found between the reprinting efficiency of AB1 and CLAB4. Both recipes experience significant material loss during the printing process. 19.0% in AB1 and 20.4% in CLAB4 per cycle. When utilizing a 30 ml syringe, as employed in this study, a notable portion of material tends to accumulate in flow dead zones (Figure 92).

In this investigation, approximately 19.9% of the initial AB1 material remained in the syringe after extrusion, whereas for CLAB4, this figure was 21.5%. Thus, the flow dead zones in syringes filled with CLAB4 appear to be slightly larger compared to those filled with AB1.

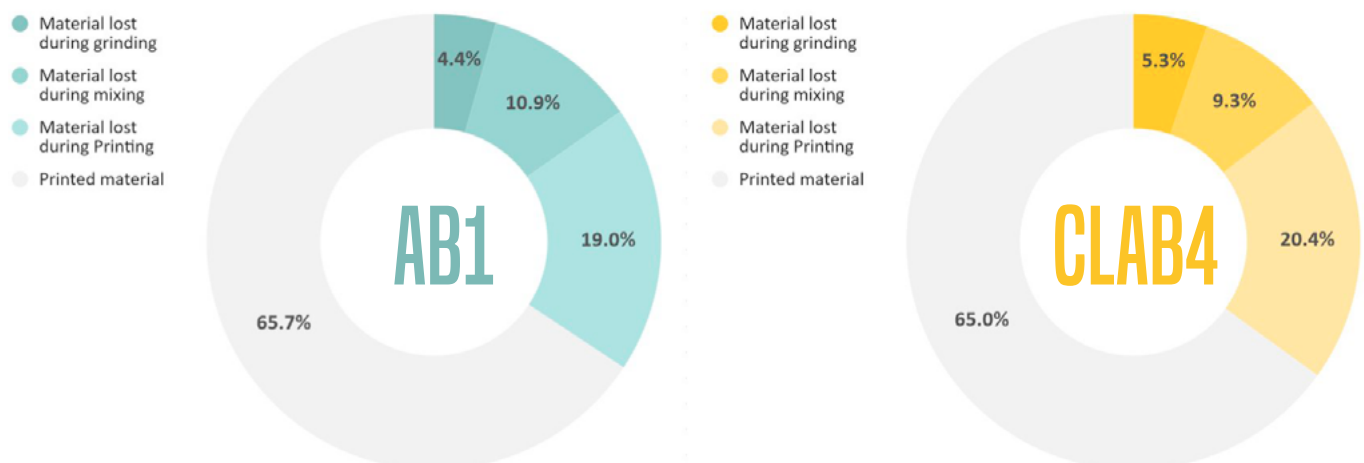
Figure 92: Flow dead zone in extrusion syringe



The second most substantial material loss for both recipes occurs during the mixing phase. 10.9% in AB1 and 9.3% in CLAB4. Approximately 11.4% of each batch made adhered to the beaker or mixer for AB1, and 9.8% for CLAB4. It is anticipated that these values will be lower when larger batches are mixed.

Grinding, results in the least material loss. When using a blender, only a small amount of powder adheres to the walls and is not utilized in the paste-making process for printing.

Figure 91: Pie charts of the materials loss in the reprint process of AB1 (blue) and CLAB4 (yellow) per reprint cycle





5.4 REPRINTABILITY: DEGRADATION OF MECHANICAL PROPERTIES

In addition to the print quality degradation, a second test was conducted to check the degradation of the material's mechanical properties when reprinted. Though the mechanical properties and improvement of them initially were not in the scope of this research, the decision was made to still conduct a small test evaluating these properties. Since there was no clear degradation of print quality visible even after 3 reprint cycles in both AB1 and CLAB4, the question arose if this would also translate to a minimal degradation of mechanical properties.

All tests were performed by Christophe Raynaud as a part of his internship at the TU Delft.

5.4.1 MATERIALS & METHODS

5.4.1.1 EXPERIMENTAL SETUP

To evaluate the decline in mechanical strength across multiple reprint cycles, this part of the research involved the printing of six 3-point-bend-test samples for 2 reprint cycles, including samples of the virgin recipe. The virgin and adapted reprint recipes of AB1 and CLAB4, as displayed in Table 24 of Chapter 5.3.1.1, were employed to print the samples.

The test samples were fabricated according to the "ASTM C1161-18 Test Method for Flexural Strength of Advanced Ceramics at Ambient Temperature". The choice was made to use the ceramics' standard due to the perceived brittleness of the developed materials. The standard led to the printing of samples with the dimensions of 8x6x95 mm (depth x height x length). The same print settings as in Chapter 5.1 were used.

Samples were left to dry completely before the tests were conducted (8 days). To reduce internal stress which can result in structural weaknesses and defects, prints were removed from the print bed after 1 day and placed on a mesh. This facilitated uniform airflow on all sides during the drying process, resulting in more even solidification and a consequent reduction in internal stresses.

Tables 25 & 26 present an overview of the printed samples, along with their final dimensions post-drying. Samples without measurements failed before measuring.

The sample's dimensions were not adjusted based on the known dimensional inaccuracy data for each recipe, causing them to deviate from the intended specifications. It is recommended to incorporate this adjustment in future research.

3-point-bend tests were performed using a Zwick/Roell with 80-mm outer span three-point fixtures. Figure 93 shows a visualisation of the test setup.

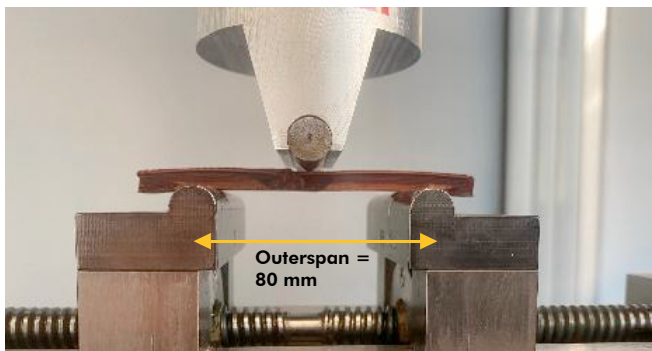
Table 25: Actual dimensions of 3-point-bend test samples of AB1

	#	x (mm)	y (mm)	z (mm)
AB1 Virgin	1	90.04	7.72	5.82
	2	89.7	7.51	5.86
	3	90.64	7.89	5.61
	4	90.61	7.89	5.65
	5	91.32	9.51	6.09
	6	90.76	9.42	6.01
AB1 1x reprint	1	90.75	7.77	5,67
	2	90.26	7.63	5,79
	3	90.39	8.43	5.68
	4	90.36	8.95	5.65
	5	90.08	8.55	5.8
	6	89.83	8.04	5.97
AB1 2x reprint	1	90.8	7.73	5.47
	2	90.39	7.75	5.35
	3	91.11	8.24	5.53
	4	91.23	8.41	5.79
	5	90.02	7.99	5.73
	6	-	-	-

Table 26: Actual dimensions of 3-point-bend test samples of CLAB4

	#	x (mm)	y (mm)	z (mm)
CLAB4 Virgin	1	-	-	-
	2	89.81	7.67	5.84
	3	89.55	7.89	5.72
	4	-	-	-
	5	-	-	-
	6	-	-	-
CLAB4 1x reprint	1	89.66	7.74	5.57
	2	89.14	7.46	5.62
	3	89.28	8.22	5.62
	4	89.03	8.75	5.53
	5	88.43	7.53	5.66
	6	88.89	7.9	5.78
CLAB4 2x reprint	1	91.94	8.35	5.31
	2	92.75	7.8	5.59
	3	90.42	8.08	5.41
	4	90.05	9.16	5.02
	5	92.05	7.75	5.1
	6	91.32	8.47	5.23

Figure 93: 3-point-bend test setup, 80 mm outerspan



5.4.1.2 QUALITY METRICS AND DATA COLLECTION

Utilizing the Zwick/Roell testXpert testing software, load-displacement curves were generated for each set of samples. From these results, the average maximum force and displacement prior to failure were computed for every recipe and reprint cycle.

5.4.2 RESULTS

In this section, we present the outcomes of the 3-point-bend tests conducted on both the virgin and reprinted AB1 and CLAB4 specimens.

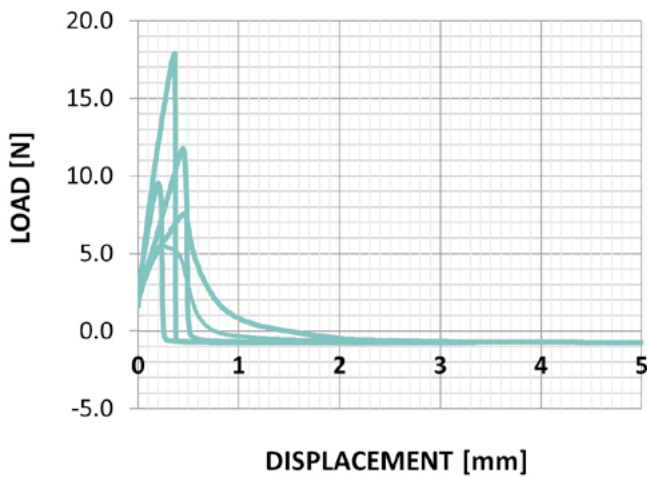
Figure 94 showcases the load-displacement curves for these samples, included are the average load at failure (F_{max}) and its corresponding average displacement (d_L), along with the relative deviation of the tested specimens.

Unfortunately, due to errors in the formulation of the AB1 2x reprint, data from these samples has been excluded from the analysis.

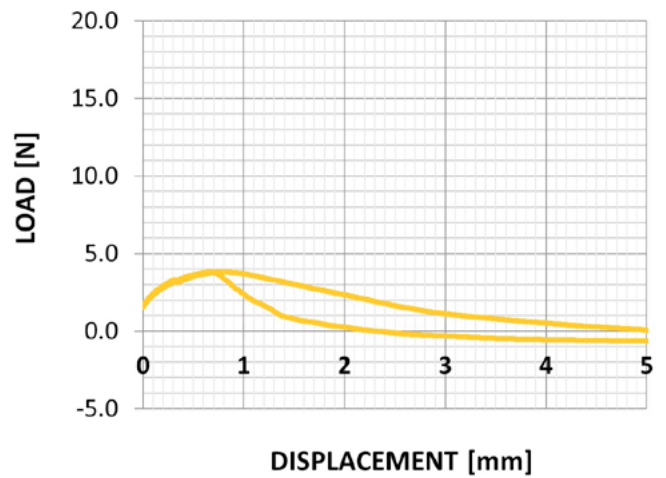
Furthermore, some samples encountered issues such as warping or breakage, rendering them unsuitable for testing. All untested samples are denoted in grey in Tables 25 & 26.

Figure 94: Pie charts of the materials loss in the reprint process of AB1 (blue) and CLAB4 (yellow)

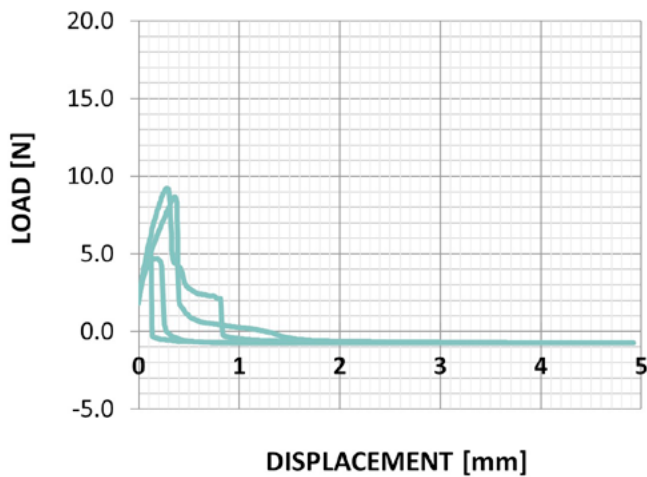
Load Displacement Curves of Virgin AB1



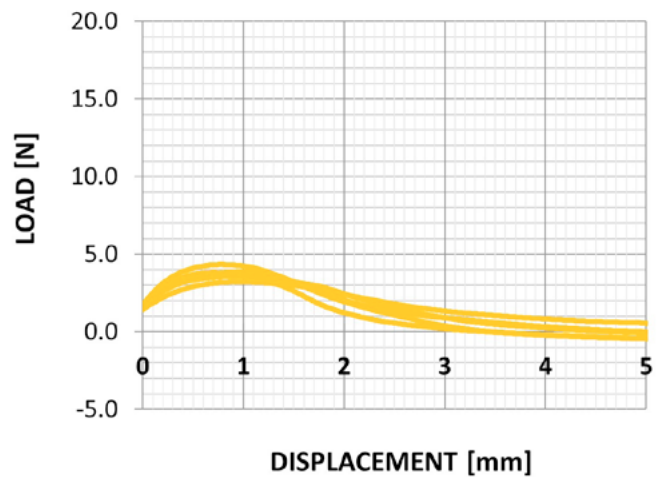
Load Displacement Curves of Virgin CLAB4



Load Displacement Curves of 1x Reprinted AB1



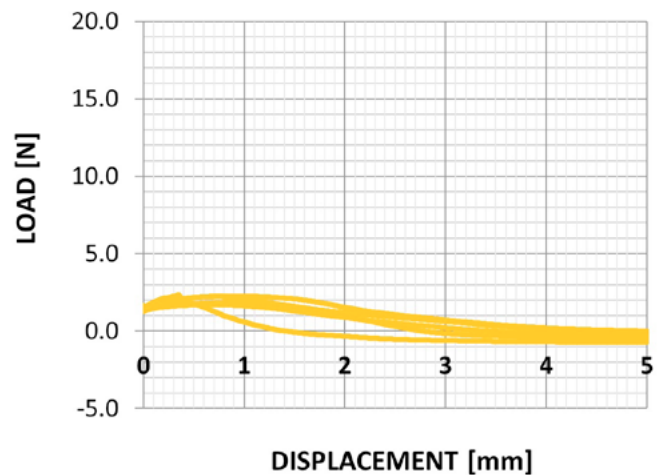
Load Displacement Curves of 1x Reprinted CLAB4



AB1	n	Fmax (N)	dL at Fmax (mm)
Virgin	5	10.46 ± 40.76%	0.34 ± 31.54%
1x reprint	4	6.89 ± 30.23%	0.22 ± 47.92%

CLAB4	n	Fmax (N)	dL at Fmax (mm)
Virgin	2	3.79 ± 0.83%	0.70 ± 0.12%
1x reprint	5	3.76 ± 9.73%	0.86 ± 12.33%
2x reprint	5	2.01 ± 11.96%	0.62 ± 40.96%

Load Displacement Curves of 2x Reprinted CLAB4



5.4.2.1 DEGRADATION OF MECHANICAL PROPERTIES

In the evaluation of virgin materials, AB1 demonstrated an average load at failure (F_{max}) of 10.46 N, with a corresponding average displacement (dL) of 0.34 mm. In contrast, CLAB4 exhibited an F_{max} of 3.79 N and a dL of 0.7 mm.

Upon a single reprinting, AB1 experienced a noticeable decrease in average F_{max} , dropping to 6.89 N, accompanied by a reduced dL of 0.2 mm. In the case of CLAB4, there is no distinct reduction in F_{max} between the virgin and once-reprinted material. The average load at failure for the once-reprinted CLAB4 was 3.76 N, merely 0.03 N lower than the virgin average. The corresponding average displacement measured was 0.86 mm.

CLAB4 did show signs of undergoing degradation after two reprints. Its average load at failure was reduced to 2.01 N, and the corresponding average displacement was 0.62 mm.

5.4.2.2 DIFFERENCES IN THE MECHANICAL BEHAVIOUR OF AB1 AND CLAB4

The load-displacement curves for all AB1 samples show a steep incline followed by a rapid drop, indicating a material with low ductility. This suggests that AB1 is more prone to brittle failure under applied stress. On the other hand, the load-displacement curves for CLAB4 samples display a gradual rise followed by a gentler decline. This indicates a material with greater ductility, capable of undergoing more deformation before ultimate failure.

Out of the tested recipes, AB1 withstands the most amount of force before failure but is more brittle compared to CLAB4. Interestingly, this does not correspond to the lower FTI of AB1 compared to CLAB4 in rheology measurements, which would indicate that CLAB4 is more prone to brittle fracture.

When looking at the variance between the tested samples, AB1 shows bigger differences compared to CLAB4. This does correlate with the large variances found in rheology measurements of AB1. Although the variance in rheology characteristics did not affect the print quality, it seems to have impacted the variance in mechanical properties.

5.4.3 CONCLUSION & DISCUSSION

The observed degradation in mechanical properties upon reprinting provides insights into the behaviour of AB1 and CLAB4. AB1 experiences a substantial 34% reduction in load at failure (F_{max}) after the first reprint, indicating a higher susceptibility to mechanical deterioration. In contrast, CLAB4 shows remarkable resilience, with only a marginal 1% reduction in F_{max} after the first reprint. However, a significant 47% reduction in F_{max} occurs in CLAB4 after a second reprint.

Load-displacement curves reveal that AB1 is more brittle, while CLAB4 demonstrates higher ductility. This contradicts rheological measurements, indicating the complexity of material behaviour. These contradicting values could be attributed to the high variances between samples of AB1, both in the rheology measurements and in the load-displacement graphs.

Variance analysis also highlights greater differences in AB1 samples compared to CLAB4, correlating with variances found in the rheology measurements in Chapter 5.2. As already addressed, these variances could be caused by lower material uniformity in AB1.

All in All, though little degradation is visible in terms of print quality over multiple reprint cycles, the mechanical properties do seem to degrade, though more pronounced in AB1 than in CLAB4. Additionally, the mechanical properties of these materials are not very high and for these materials to be more durable, it is necessary to improve these properties. More research on mechanical properties and how to improve them in DIW materials is thus a valuable topic for further research.

5.5 PRINTING LARGER STRUCTURES

In the final phase of the process, several additional structures were printed, some of which would have been challenging to produce using conventional methods like injection moulding.

Upon examining Figures 95 and 96, it becomes evident that both materials encounter difficulties with thin-walled features, especially when transitioning from a smaller to a larger diameter. This issue stems from incomplete solidification of the material during the printing process. Consequently, these walls become sensitive to movement, particularly when smaller features within the print are followed by outward overhangs. The amplified gravitational force on the material, caused

by the added weight from multiple layers and further amplified by the extended leverage caused by overhangs, contributes to yielding at weaker (thinner) points.

Addressing this problem is anticipated by increasing wall thickness or adjusting infill. However, due to significant environmental changes in the lab during the final week of printing, it wasn't possible to verify this solution. The temperature dropped from 25 to 20 degrees Celsius and the humidity from 60% to 41%. As a result, the nozzle repeatedly clogged before reaching critical features within the prints.

Figures 97, 98, 99 and 100 show other models printed. Due to clogging, not all were able to finish printing.

Figure 95: Twisting vase shape with converging and diverging overhangs printed with AB1(a) and CLAB4(b), Collapse due to weak spot in the model.



Figure 96: Vase shape with converging and diverging overhangs printed with AB, Collapse due to weak spot in the model.



Figure 97: Vase shapes printed with AB1 (a) and CLAB4 (b)



Figure 98: Vase shaspe printed with CLAB4



Figure 99: Completely finished prints of vase model with AB1 (a) and CLAB4 (b)



Figure 100: Overview of all samples printed



6. THESIS CONCLUSION & DISCUSSION

Throughout this thesis, the core emphasis has revolved around the need for sustainable advancements in 3D printing methodologies and materials. Reducing the environmental impact by printing with cellulose waste (Pecan shells) at ambient temperature is a great step forward. However, central to this pursuit is the imperative need for print quality enhancements. The research undertaken underscores the vital significance of not just eco-friendly approaches but also the demand for their improved print quality standards to render these methods and materials viable as alternatives to the commonly used 3D-print plastics in the future.

With the print quality optimisation of two different recipes (AB1 and CLAB4) for ambient printing, this research lays the groundwork for advancing the quality of sustainable materials for ambient printing, creating opportunities for further evolution in this field.

While the study falls short of achieving the print quality standards of commonly used plastics in FDM, it provides invaluable insights into the factors influencing print quality. Given the extensive scope of research covered, this chapter integrates both the conclusion and discussion into a unified narrative. The Chapter aims to address the research questions. For an extensive print quality comparison of the two final materials and their precise quality measurements, please see the conclusion in Chapter 5.1.

6.1. INK FORMULATION, PRINT PARAMETERS & ENVIRONMENTAL CONDITIONS

RQ1. *What is the effect of ink formulation, print parameters and environmental factors on the resulting print quality of biowaste-derived materials fabricated under ambient conditions?*

6.1.1 INK COMPOSITION

Various compositions were explored both in the initial tinkering (Chapter 3) and the subsequent recipe optimization phase (Chapter 4), shedding light on the impact of ink composition on print quality. Not all ingredients proved compatible, resulting in mixtures lacking sufficient binding or uniformity. Out of the 10 tested binders, four yielded printable inks: All binder, All-purpose glue, Sodium Alginate, and Calcium Lignosulphonate.

Each ink formulation had distinct strengths and weaknesses in terms of print quality and durability. All-binder recipes presented overall good print quality and excelled in bridging capabilities. However, they exhibited material buildup at the nozzle hindering the surface finish. On the other hand, Calcium lignosulfonate-based inks showcased superior surface finish and the most efficient mixing properties. Despite these advantages, they displayed less quality in terms of dimensional accuracy and bridging. The All-purpose glue formulations demonstrated superior dimensional accuracy and were water-resistant, yet they suffered from non-uniform extrusion, clogging susceptibility, and poor bridging. Conversely, Sodium alginate-based inks, initially explored for their combined water insolubility and reprint ability, exhibited poor quality due to significant shrinkage, material cracking, bad bridging and long mixing times (> 30 min).

Combining different binders to potentially combine their advantages and eliminate limitations proved difficult. In most cases, incompatibility between binders resulted in bad printability. Only combinations of All binder and Calcium lignosulfonate and all binder and sodium alginate generated printable results.

Although incorporating all binder into the Sodium alginate recipe addressed issues like

shrinkage and cracking, it hindered achieving water insolubility through crosslinking, nullifying the ink's potential advantages over other formulations and halting its further development.

The recipe combining All binder and Calcium Lignosulphonate, however, was successful resulting in the final CLAB4 recipe that shows an improved surface finish compared to the all binder only based recipe (AB1) and slightly better maximum overhang, yet scores less on Dimensional accuracy, maximum bridging distance, and susceptibility to warpage.

Of all the tested recipes CLAB4 and AB1 resulted in the best print quality and were used for more detailed print quality and rheology evaluation.

6.1.1.1 INK COMPOSITION GUIDELINES

Tinkering proved that there is no clear-cut path to achieving an ink that results in good print quality. When looking at the composition, the optimal ratios between ingredients strongly differentiate based on the ingredients used. The behaviour of the ink is a result of the individual qualities of the ingredients but more importantly, the interactions among its components. This creates a complex interplay of properties which are not easily explained by a common trend. It can thus be concluded that with the current knowledge, a process of trial-and-error is the only option in the initial phase of material development, though previous results with ingredients can be used as a valuable starting point. Yet, there are some general guidelines to help the initial development of a printable paste.

1. Adjusting the solid-to-liquid content of a mixture can help to achieve the desired viscosity of the ink
2. Filler content and binder content can be adjusted to further improve the shape fidelity and dimensional accuracy. Adding extra filler and binder can help to reduce shrinkage and improve stability, however, too much can increase the occurrence of clogging.

3. The ethanol and water ratio can be adjusted to change the solidification rate and shape fidelity. Higher ethanol ratios can improve the drying rate and thus the shape stability after printing, however, too high ethanol contents can cause preliminary solidification, causing material to dry out before being extruded.

Though following these guidelines helps to have a more systematic approach when developing printable ink, they have some limitations. First of all, the interactions explored by these guidelines are limited. While they offer an easy way to get to the right consistency and drying behaviour of the ink, they do not fully take into account the effect the ratio between binder and filler might have on rheology behaviour and the differences in the viscosity of ethanol and water. When a material is further developed, more attention should be paid to the potential effect of binder-to-filler ratios.

6.1.1.2 COMPOSITIONS EFFECT ON PRECISION

The comprehensive evaluation of the two final developed recipes in Chapter 5 sheds light on how the composition of an ink can also affect precision. While AB1 exhibits greater variability in rheology tests compared to CLAB4, it surprisingly demonstrates significantly less variability in achieved print quality across samples.

The variance observed in rheology measurements could be attributed to the potentially larger variation within the all-binder component, sourced from a supermarket, contrasting with the standardized industrial quality of CL. However, this does not seem to significantly influence the variability in print quality. This discrepancy can be explained by the varied extrusion pressure used to achieve the desired extrusion rate, which displayed greater variation in AB1 than in CLAB4. By determining the best extrusion pressure per print, negative effects caused by differences in rheology characteristics seem to have been largely prevented in AB1.

As CLAB4 showcases more precise rheology, its increased variability in print quality is not

explained by ingredient variability. Rather, the difference in quality in CLAB4 samples could be caused by heightened sensitivity to drying conditions.

6.1.1.3. COMPOSITIONS EFFECT ON PRINT SPEED AND LAYER HEIGHT

The printability mapping of different recipe compositions revealed significant differences in print speeds. AB1 exhibited a wider range, printing effectively from 6mm/s to 12 mm/s, compared to CLAB4, which printed within 6 mm/s and 9 mm/s. The maximum print speed is limited by the available extrusion pressure. Rheology behaviour, influenced by composition, directly impacts 3D print speeds. Compositions with lower yield and flow stresses, like AB1, flow more easily under lower pressures, increasing the achievable print speeds within the printer's pressure constraints. However, a lower yield stress can compromise stability if the yield threshold is reached due to the weight of multiple printed layers or due to printer movement. Yet, the differences in sagging between AB1 and CLAB4 were inconclusive, suggesting the yield threshold likely was not reached or the material had solidified enough for added stability within the printed height of AB1.

When examining the printer's force impact, AB1 does display indications of nearing the yield threshold. This is evident in a comparison between AB1 and CLAB4 print quality at high speeds and reduced layer heights. AB1 performs well at higher speeds (12mm/s) compared to CLAB4 when the layer height is 0.6 mm. However, at a reduced layer height of 0.55 mm, the force exerted by the nozzle movement on AB1 seems to diminish the print quality at speeds over 9mm/s. This decline likely occurs as the force on the structure increases with the combination of reduced layer height and higher speed and in doing so enters a force range in which yielding can become critical.

6.1.2 INK PREPARATION

In addition to composition, achieving high-quality 3D prints depends on the proper

preparation of the materials, which includes the order, time, and speed of ingredient mixing. Research has shown that the mixing method should be adapted to the specific materials used. However, in all materials tested, some trends occurred regarding the best practice for mixing:

1. Solvents should precede the gradual addition of the binder, allowing gradual dissolution for better uniformity.
2. Adding solid particles after complete dissolution, instead of mixing them with dry ingredients initially, consistently yielded the most uniform mixture.

However, no clear trends were found in the mixing sequence of binder addition when multiple binders were employed. While some materials, like CLAB4, showed no discernible difference in results when binders were simultaneously added instead of separately, others, like those combining sodium alginate and all binder, exhibited distinct differences in outcome based on the sequence of addition

6.1.2.1. THE SHEAR HISTORY OF MIXING

The conducted rheology tests (Chapter 5.2) offered profound insights into the influence of mixing on ink rheological behaviour. Shear history was observed to significantly impact all tested materials. Pre-shearing, akin to the mixing process, exhibited a positive effect on the response behaviour of the final recipes (AB1 and CLAB4). Notably, pre-shearing drastically reduced the time required for these recipes to attain consistent viscosity under shear, resulting in more uniform extrusion at predetermined pressures during printing, consequently enhancing the print quality. Furthermore, pre-shearing slightly accelerated viscosity recovery after extrusion in AB1 and CLAB4, albeit to a lesser degree.

Although pre-shearing reduced initial viscosity, its effect on the recovered viscosity after extrusion was limited and manageable within the material formulation process.

To conclude, implementing a mixing or remixing step before printing proves

beneficial, highlighting the importance of fine-tuning mixing duration and speed to further optimize material print quality.

6.1.3 PRINTER SETTINGS

Apart from ink composition and preparation, printer parameters have also been shown to significantly influence the quality of prints. Throughout the optimization phase (Chapter 4), various print parameters were explored to assess their impact on the print quality of ingredients. These parameters encompassed print speed, layer height, nozzle size, layer width, and jerk settings. While the material's composition determines the feasible maximum and minimum values of these settings resulting in printability, there are consistent trends observed across all compositions concerning quality metrics and print settings.

Print speed - The print speed significantly impacts print quality. When not constrained by maximum extrusion pressure, a material's maximum print speed with acceptable print quality is constrained by its sensitivity to printer movement and solidification rate (which varies based on composition). At higher print speeds, increased nozzle movement force can deform or collapse prints. Moreover, higher speeds limit the drying time of the material during printing, resulting in less print stability. Thin-walled high features with overhangs are particularly sensitive to rapid head movements and reduced solidification between layers.

To conclude, while higher print speeds might enhance efficiency, there is a threshold beyond which print quality becomes compromised. Optimizing print speeds should align with material rheology and the specific features of the model being printed. For high, thin-walled samples with overhangs, reducing print speeds is advisable, whereas for low samples with thicker walls or infill increasing speed can enhance efficiency. Lower quality due to insufficient drying can partially be solved by using fans during printing.

Noteworthy, Printing at the lowest possible speed does not always guarantee the best print quality with these materials. Interestingly, in nearly all tested samples, the lowest speeds

and corresponding extrusion pressures led to slightly non-uniform extrusion and less controlled quality. This could be due to fibres taking longer to align at lower extrusion pressures, resulting in a slower viscosity drop due to shear. This aligns with the findings of the 3ITT test in Chapter 5.1, where higher shears led to quicker material responses.

Nozzle size and layer height and width - Nozzle size, layer height and layer width are print parameters that influence the maximum resolution and details that can be reached and in doing so the surface finish of the printed samples.

Smaller nozzles create finer details but extend printing times due to their higher requirement for extrusion pressure. In addition, smaller nozzles increase the likelihood of clogging to occur. With the developed material AB1 and CLAB4 a nozzle diameter of 0.81 mm was the smallest nozzle to show good detail resolution without excessive clogging.

Layer height defines the thickness of each printed layer, impacting vertical resolution. Smaller layer heights offer better detail but do prolong printing times and as explained earlier, can cause prints to deform or collapse. Additionally, too small layer heights can result in material sticking to the nozzle, causing gaps in the print. Too big layer heights, on the other hand, cause inaccuracy in the placement of printed lines.

The layer width setting in slicing software, such as Cura, directly impacts the adhesion between printed lines and the dimensional accuracy of objects. Setting the layer width too small can lead to excessive overlap between lines, causing the print to expand and create spots with excess material. Conversely, overly wide layer width settings can cause inadequate overlap between lines, resulting in poor adhesion and gaps in the print. Thus, achieving the optimal layer width is crucial to ensure proper adhesion and accurate dimensions in the printed object.

Jerk settings - The impact of jerk settings (the maximum instantaneous velocity change of the print head) on print quality was evident in

this study. Optimal performance was achieved when jerk settings matched the printing speeds. Lower jerk settings resulted in over-extrusion and material overlap during corner printing.

However, the setup used in this research placed constraints on achieving maximum print quality. The Eazao Bio printer requires manual regulation of extrusion pressure, thus a constant pressure was maintained throughout the printing. This led to lower jerk settings (slower deceleration) in corners leading to over-extrusion. To prevent over-extrusion, quick deceleration was necessary which translated into the jerk settings being the same value as the speed. However, quick deceleration increased the likelihood of printed walls to warp due to the additional force exerted on them, especially when the print speed was high.

Future research should focus on regulating extrusion pressure to enable slower deceleration (lower jerk settings) without causing over-extrusion, offering potential improvements in corner detailing and higher-speed printing.

6.1.4 ENVIRONMENTAL CONDITIONS

Evaluation of print quality in AB1 and CLAB4 at varying temperatures and air humidities highlighted the impact of environmental conditions on the achieved print quality (Chapter 5.1). However, due to uncontrolled temperature and humidity, conclusive evidence remains elusive, evident in relatively low R^2 values across all data. This suggests additional unexplored factors driving data variance, potentially including drying conditions, ingredient variability, and print environment airflow.

The effect found to be most likely true in both recipes is the improved maximum bridging distance with decreased humidity, attributed to accelerated solidification rates due to moisture content differences between print and ambient air. Other correlations found are detailed in Chapter 5.1.3's conclusion. Because of the lower certainty of these correlations, they are not included here.

Overall, while precise effects are not confirmed, the findings collectively indicated the likelihood of substantial environmental influence on print quality. A comprehensive understanding requires further investigation, emphasising the need to control environmental parameters during printing to enhance precision and consistency, crucial for large-scale production optimisation.

6.2. IMPORTANCE OF RHEOLOGY CHARACTERISTICS

RQ2 *What are the specific rheology characteristics that need to be considered when formulating inks for optimized print quality? and how are they influenced?*

The rheology characteristics crucial for optimised print quality in ink formulation were determined by various correlations found between print quality and rheology characteristics in Chapter 5.2. For precise values and measurements of the rheology refer to this Chapter. The most important rheology characteristics and their influence on rheology are presented here.

Shear thinning and viscoelastic behaviour– The most important in developing a material for ambient printing is that it is shear-thinning and viscoelastic. It needs to show a sufficient drop in viscosity when shear is applied and return to a higher viscosity when shear is removed.

Yield stress– The yield stress, determined by the yield onset point and the flow stress, dictates the required extrusion pressure and the maximum achievable print speed. It also determines the tolerance for printing consecutive layers without sagging and the sensitivity to nozzle movement, as previously noted.

Notably, well-performing recipes such as AB1 and CLAB4 exhibited yield stresses of 4.3×10^3 Pa and 9.7×10^3 Pa, respectively, while the bad-performing recipe showed a yield stress of 33 Pa. Yield stresses within the range of AB1 and CLAB4 are thus recommended and

should be adjusted based on specific material requirements concerning printing height and speed.

Loss tangent ($\tan(\delta)$), loss modulus (G'') and storage modulus (G')- The difference between loss modulus and storage modulus in the LVR addressed by the loss tangent, significantly impacts ink stability. A loss tangent within the range of 0.54 and 0.40, evident in AB1 and CLAB4 respectively, demonstrates improved stability while maintaining extrusion uniformity. In contrast, a 0.68 loss tangent (a smaller difference in G' and G''), observed in the poorly performing recipe, resulted in instability and heightened sensitivity to force variations.

Smaller loss tangents than those found in CLAB4 could lead to problems with non-uniform extrusion according to the literature, but at which value this threshold lays could not be determined with the gathered results.

In addition to the loss tangent, the height of the storage modulus also plays a role in the stability of prints. The statement made by Li et al. (2019) that a storage modulus that exceeds 10^3 Pa is advised for good stability of multiple-layer prints, is substantiated by the results found in this research. AB1 and CLAB4 showed values above this order of magnitude, 2.2×10^4 and 5.9×10^4 respectively, while the lesser-performing recipe showed a value within this order of magnitude; 2.7×10^3 .

Response time and shear history – The response time, or time it takes to reach a levelled viscosity when shear is applied, determines the uniformity of extrusion at the start of printing or after a travel move.

A quick response time is preferred as it affects the uniformity of a printed line and thus the accuracy of the print. As already pointed out, applying a pre-shear to the material by mixing it just before printing results in a significantly improved response time in AB1 in CLAB4 due to shear history. Pre-shearing or (re)mixing the material just before printing can thus be incorporated into the printing process for improved print quality.

Recovery time and recovered viscosity-

The recovery time and recovered viscosity, influence the shape fidelity of the printed lines immediately after they are extruded. With insufficient recovery of viscosity immediately after the shear is removed, printed lines would sag.

The immediate post-extrusion viscosity proved more critical than the time it takes for the viscosity to show levelling (the recovery time). For printed lines to maintain stability, the viscosity right after extrusion must exceed a specific threshold, ensuring it is stiff enough to maintain its shape. The time it takes to reach a steady-state viscosity thereafter is of secondary importance.

The threshold for sufficient recovered viscosity seems to be reached by AB1 and CLAB4 with a recovered viscosity of 1.77×10^4 Pa.s and 2.28×10^4 Pa.s respectively, five seconds after shear. Conversely, the poor-performing recipe, with 4.8×10^3 Pa.s viscosity at the five-second mark, shows sagging, suggesting inadequate stability. Moreover, this recipe also exhibited notably slower levelling compared to AB1 and CLAB4, taking several seconds to minutes to reach higher viscosities. The values presented here are those of the materials pre-sheared before testing, mirroring the effect mixing just before printing had on the printed samples.

6.3. REPRITNABILITY

RQ3 *To what extent does reprinting biobased materials at ambient temperatures affect the print quality across successive printing cycles and what factors contribute to maintaining or degrading print quality over these multiple cycles?*

Chapter 5.3 delved into assessing the degradation of print quality in both AB1 and CLAB4 over three reprint cycles. Surprisingly, there was not a clear trend observed in the degradation or enhancement of print quality across the various measured metrics—dimensional accuracy, maximum bridging, overhang, warpage, and surface finish. The materials demonstrated a reprinting process with notably good results, as even the higher, vase-like structures printed across reprint

cycles exhibited no discernible degradation.

Their exceptional ease of reprinting likely stems from their water solubility and the ability to be printed at room temperature. Plastics in FDM, especially thermoplastics, can undergo more irreversible changes and thermal stresses upon heating and cooling cycles, leading to degradation and a loss of print quality upon reprinting. This is less the case with the water-based materials developed in this research. It is noteworthy that both recipes needed fewer solvents during the reprint cycles compared to the virgin recipe, suggesting that some of the previously added solvents have bonded to the material without evaporating. The required recipe for good quality did not change in between reprint cycles.

Surprisingly, in some cases, reprinting seemed to yield better results than the initial prints. This could be attributed to better environmental conditions during reprinting or the remixing process potentially improving material uniformity.

The print quality assessment showing no distinct trend in quality degradation prompted a closer look at possible mechanical property degradation. Initial findings suggest both materials experience degradation, although at varying rates. AB1 displayed a significant 34% reduction in load at failure (F_{max}) after the first reprint, indicating greater susceptibility to mechanical deterioration. In contrast, CLAB4 exhibited remarkable resilience, showcasing only a marginal 1% reduction in F_{max} after the first reprint. However, a substantial 47% reduction in F_{max} was noticed in CLAB4 after a second reprint. Given the limited samples used, further extensive testing is warranted for a definitive evaluation.

6.4. SODIUM ALGINATE-BASED INK IMPROVEMENTS

RQ4 *How can the print quality of alginate-based recipes be improved to create a material with good print quality, reprintability, and water resistance?*

During the refinement phase, various approaches were explored to enhance the print quality of alginate-based formulations. The objective was to create a final recipe that balanced water insolubility and reprintability through reversible crosslinking of sodium alginate while maintaining satisfactory print quality.

Initially, using sodium alginate as the sole binder resulted in frequent shrinking and cracking during the refinement process. To address this, an alternative recipe was formulated, incorporating additional All Binder. Although this improved print quality across all measured metrics, it could not achieve water insolubility through alginate crosslinking, likely due to the dissolution of the added binder during the crosslinking process.

Other attempts to enhance sodium alginate-based recipes without introducing an additional binder were ineffective. Pre-crosslinking alginate before printing caused rapid solidification and ink inconsistency. Similarly, in-situ crosslinking during printing with a CaCL mist resulted in inadequate bonding between layers.

Of the methods explored, further investigation into in-situ crosslinking might be valuable. Refined control over the delivery and dispersion of the CaCL mist, could potentially prevent the excessive crosslinking that hindered the layer adhesion.

Building on the insights gained, this conclusion and discussion set the stage for addressing the identified limitations and challenges that are pivotal for advancing sustainable printing practices. The next Chapter delves into actionable recommendations aimed at refining material formulations, optimizing printing methodologies, and exploring innovative approaches. By bridging the gaps revealed in this study, the recommendations aim to guide future research into sustainable materials for ambient 3D printing.

7. RECOMMENDATIONS

The avenues explored in this research lay a foundational pathway for future research. Yet, there are still some challenges in the print quality and durability of biowaste-derived materials necessitating further attention. Addressing these gaps will further enhance the viability of the developed materials as sustainable alternatives. This Chapter presents some recommendations for further areas of research and improvement.

8.1 CONTROLLING THE ENVIRONMENTAL CONDITIONS

Throughout this thesis, it has become evident that Direct Ink Writing (DIW) with biowaste-derived materials is highly susceptible to environmental conditions. Changes in room temperature and humidity can significantly affect the quality of the print, causing a material formulation to be printable in one type of environment, while not in another. For instance, the materials developed were easily printable with high quality in the summer (25 degrees, 60% humidity); however, in the autumn (20 degrees, 41 % humidity), the material was shown to be extremely susceptible to clogging. Even small changes in temperature and humidity seem to influence quality metrics such as the maximum bridging distance, for better or for worse.

To achieve higher precision and repeatability of quality when using this print method, controlling the environmental conditions is necessary. Future research should, therefore, focus on gaining a better understanding of the effect of environmental conditions on each of the print quality metrics. This will help determine the ideal environmental conditions for a specific material and maintain them constant, which in turn results in better print quality and precision.

8.2 APPLYING IN-SITU SOLIDIFICATION METHODS

Considering the persisting challenges in achieving shape fidelity, particularly with larger structures, exploring in-situ solidification methods emerges as a promising direction for further exploration. This approach not only addresses shape fidelity issues but also mitigates the impact of environmental conditions and printer movements that often disrupt the stability and accuracy of the prints.

While the method used in this research relies on the thixotropic effect of the material to maintain its shape before slowly solidifying due to solvent evaporation, in situ solidification, like UV curing, accelerates this solidification process. As a result, the material's susceptibility to environmental factors and printer movements is reduced, enhancing stability, accuracy and precision during printing. This would also allow for higher print speeds. Additionally, in-situ solidification could minimise the need for extremely precise rheology characteristics essential for shape fidelity when no solidification occurs within the printing time, potentially reducing the time that has to be spent on material formulation development.

Literature does highlight the need to carefully optimize in-situ solidification, as rapid solidification may compromise layer adhesion or lead to nozzle clogging if incorrectly applied. Future research should focus on balancing the advantages of quicker solidification against potential issues like layer adhesion or nozzle clogging to optimize these techniques. Exploring hybrid approaches that combine thixotropy-based shape fidelity with in-situ solidification might offer promising solutions.

For instance, strategically employing in-situ solidification to stabilize the structure after

printing a certain number of layers could prevent shape fidelity issues arising from the weight of multiple layers and the nozzle movement.

Despite potential possible concerns about higher energy usage and environmental impact compared to the method used in the research, the significant print quality improvement offered by quicker solidification might outweigh these drawbacks. Notably, the overall energy consumption still remains considerably lower compared to thermoplastic printing, especially if a hybrid method is applied.

Overall, incorporating in-situ methods might lead to superior print quality, precision and efficiency, while still maintaining a minimal environmental impact compared to FDM.

8.3 RHEOLOGY OPTIMISATION & RHEOLOGY BASED PROCESS CONTROL

This research has proven the importance of rheology characteristics in achieving good print quality and in doing so, shows the potential of rheometer tests being used as a method for further optimisation of inks.

In the early stages of material development, a trial-and-error approach is likely the quickest method for reaching an ink with the right viscosity and shape fidelity to print simple structures. However, in a later stage of development, the pursuit of precise adjustments to enhance print quality warrants a more nuanced method. Utilizing a rheometer at this stage offers a deeper understanding of which characteristics of the material show potential for improvement. In this stage, analysing how different ingredient ratios and potential additives impact the shear-thinning, response and recovery times, and viscosities before and after extrusion can be the key to further quality improvements.

Moreover, employing a rheometer allows for a methodical approach to fine-tuning established recipes. Integrating rheometer tests within the iterative trial-and-error

process, can streamline the optimization of material formulations and tweak rheology characteristics that can not be easily adjusted by eye.

Additionally, it would be worth looking into process control of the print parameters based on the rheology characteristics of an ink. Process control utilizing rheology as an immediate input for printing parameters offers a responsive approach to optimising the print parameters for each batch being printed. The inherent variability in natural materials sourced from biomass or waste streams can lead to unpredictable fluctuations in rheological properties, directly influencing the required print parameters required for printing at good quality. Using rheology as a monitoring tool allows for the assessment of the material behaviour of different batches under different environmental conditions, enabling substantiated and targeted adjustments to printing parameters for better print quality.

Using a rheometer to test material rheology has certain limitations that warrant consideration. The rheometer applies a rotary shear to assess rheological properties, which isn't directly analogous to the shear experienced during the printing process. Extruding material through a printer's nozzle involves a more intricate form of shear that the rheometer might not perfectly simulate. Therefore, the efficacy of utilizing the rheometer for fine-tuning existing recipes or controlling print parameters needs empirical validation.

Ideally, a method for real-time rheological measurements during the actual printing process would be advantageous to address these discrepancies and optimize print quality more effectively. Developing such a method would be a valuable topic for researchers to explore.

8.4 DURABILITY IMPROVEMENTS

Another recommendation for future research would be to improve the durability of these materials. Even when the print quality is further developed to meet quality standards close to current-day FDM materials such as PLA and ABS, these materials can not be commercially adopted for long-term use applications without improvements in their durability.

Though the impact of the developed materials and the printing process might be lower in terms of environmental consequences, the recurring need for reproducing parts due to their lower durability can accumulate impacts over time. While low-impact materials and methods present a promising avenue towards sustainability, their continuous reproduction to compensate for their lack of durability might potentially counteract their overall ecological benefits. Therefore, it becomes imperative to not only focus on reducing immediate environmental impacts but also to enhance the long-term durability and lifecycle of these materials.

The developed materials in this research have low mechanical properties compared to ABS and PLA and in addition, quickly dissolve when they come in contact with water. Future research could prioritize enhancing the mechanical properties of the developed materials. This could involve exploring various reinforcement techniques such as incorporating fibres or nano-additives to improve tensile strength, impact resistance, and overall structural integrity or pre and post-treatments. In the case of the materials developed in this research, a possible first step in improving the mechanical properties is the pretreatment of the Pecan shell to remove extractives within the material obstructing the bonding between filler and binder materials.

Additionally, focusing on enhancing water resistance through the integration of coatings, surface modifications, or altering the material composition can prevent quick dissolution when exposed to water, expanding the range of applications and improving the overall durability of these materials. However, It

needs to be kept in mind that using these methods might limit the reprintability and biodegradability of these materials. The decreased solubility can affect materials' ability to be easily dissolved and returned to a reprintable ink. Balancing these attributes is crucial for sustainability. Ideally, devising a method that offers reversible water insolubility, enabling the material to resist water when necessary but dissolve or revert to a printable state under controlled conditions, would be an ideal solution. Although Sauerwein et al. (2020) achieved this through reversible crosslinking of sodium alginate, it compromised the print quality. In this study, efforts to enhance the print quality of sodium alginate-based inks while retaining reversible water insolubility were unsuccessful. However, limited time was allocated to this aspect of the research. Further exploration into improving the quality of alginate-based inks or other sustainable methods for achieving water insolubility—ideally maintaining reprintability—could be a valuable area for future investigation.

8.5 PREVENTION OF NOZZLE CLOGGING

The susceptibility to nozzle clogging in DIW also poses a notable gap in both print quality as well as efficiency of the process as prints have to be restarted when the nozzle clogs. Understanding the mechanisms causing clogging and developing effective strategies to control material flow, including nozzle design and processing optimization, is crucial to mitigate this issue and improve overall print quality and efficiency.

8. PERSONAL REFLECTION

All in all, I'm satisfied with the results I achieved within the span of half a year. Though I might have not met the high expectations I set for myself, I think I can still be very proud of all the work that I did and the many things I have learned. While I learned a lot about the subject of room-temperature 3D printing and material development, I think I have learned the most about my preferred way of working. I have learned that I enjoy research a lot, however, I also need time to be hands-on and just produce things. Moreover, I've realized that I thrive when working in a team. Though it was a great learning experience to largely work by myself, I need interactions with others to boost my creativity and my productivity. When working independently, I tend to become overly fixated on perfection. While I regard perfectionism as a valuable trait, I've observed that it can hinder progress when I'm working solo.

Looking back on my process, I have some things I would change.

In the rush to accomplish more and get the results I desired, I often let pressure guide my choices. Driven by my motivation to always achieve more, I sometimes hurried through decisions which would have benefited from some more consideration. This impulsive haste led to some lower-quality outcomes and missed opportunities. Especially in the initial tinkering phase of my research in which I tried a lot without documenting properly.

Yet, in other cases, my perfectionism caused me to overthink decisions too much. This was especially the case in the later stages of the research when I was able to critically look back at my results. In this phase, I lost a lot of time thinking about how I would have done things differently and felt the need to do a lot better and a lot more in the remainder of my project. Looking back, I had nothing to worry about.

The motivation to achieve more eventually resulted in difficulties with my time management. I was so focused on doing more that I often forgot to factor in the necessary time for evaluation and documentation. While my extra efforts were driven by ambition, I didn't realize the toll it took on my overall productivity. I definitely overworked myself multiple times during this project, which negatively affected my productivity and my mental health.

Moving forward, I will take with me that sometimes less is more and that it's good to sometimes slow down to get a better overview of a project. Finding the right balance between quantity, quality and personal health means adjusting my approach. I now understand that the time spent on reflection and careful documentation isn't a hindrance, but rather the basis on which solid results are built. Leaving reflection and documentation to the last minute will only cost you more time. In addition, efficiency, creativity and clarity of mind are strongly affected by stress levels, so giving myself more room to relax, would have most likely resulted in improved decision-making and efficiency.

As I move forward, I'm committed to being more mindful of pressure's influence and the value of taking a step back. I also want to allow myself more time for reflection and room for failure.

REFERENCES

- Achayuthakan, P., & Supphantharika, M. (2015). Effects of guar gum or xanthan gum addition on rheological properties of waxy corn starch.
- Alexeev, I., De Blanken, S., Hagspiel, J., Leeuwerik, J., & Van Limborgh, M. (2021). *PSFE, Sovel Sustainable 3D Printing Materials - Advanced Prototyping Minor* [Unpublished report]. TU Delft.
- Amorim, P. A., D'ávila, M. A., Anand, R., Moldenaers, P., Van Puyvelde, P., & Bloemen, V. (2021). Insights on shear rheology of inks for extrusion-based 3D bioprinting. *Bioprinting*, *22*, e00129. <https://doi.org/10.1016/j.bprint.2021.e00129>
- Amplitude sweeps | Anton Paar Wiki. (n.d.). Anton Paar. Retrieved August 8, 2023, from <https://wiki.anton-paar.com/en/amplitude-sweeps/>
- Andrew, J. J., & Dhakal, H. N. (2022). Sustainable biobased composites for advanced applications: recent trends and future opportunities – A critical review. *Composites Part C: Open Access*, *7*, 100220. <https://doi.org/10.1016/j.jcomc.2021.100220>
- Badr, S., MacCallum, B., Madadian, E., Kerr, G., Naseri, E., MacDonald, D. S., Bodaghkhani, A., Tasker, R. A., & Ahmadi, A. (2022). Development of a mist-based printhead for droplet-based bioprinting of ionically crosslinking hydrogel bioinks. *Bioprinting*, *27*, e00207. <https://doi.org/10.1016/j.bprint.2022.e00207>
- Barrow, E., Lakke, J., Sargentini, J., Vink, L., & Zonneveld, Y. (2022). *Paste is the Future - Advanced Prototyping Minor* [Unpublished report]. TU Delft.
- Balani, S. B., Ghaffar, S. H., Chougan, M., Pei, E., & Şahin, E. (2021). Processes and materials used for direct writing technologies: A review. *Results in Engineering*, *11*, 100257. <https://doi.org/10.1016/j.rineng.2021.100257>
- Bean, R. H., Rau, D. A., Williams, C., & Long, T. E. (2023). Rheology guiding the design and printability of aqueous colloidal composites for additive manufacturing. *Journal of Vinyl & Additive Technology*, *29*(4), 607–616. <https://doi.org/10.1002/vnl.22010>
- Bom, S., Ribeiro, R., Ribeiro, H. M., Santos, C., & Marto, J. (2022). On the progress of hydrogel-based 3D printing: Correlating rheological properties with printing behaviour. *International Journal of Pharmaceutics*, *615*, 121506. <https://doi.org/10.1016/j.ijpharm.2022.121506>
- Bonnaillie, L. M., Zhang, H., Akkurt, S., Yam, K. L., & Tomasula, P. M. (2014). Casein Films: The effects of formulation, environmental conditions and the addition of citric pectin on the structure and mechanical properties. *Polymers*, *6*(7), 2018–2036. <https://doi.org/10.3390/polym6072018>
- Buj-Corral, I., Domínguez-Fernández, A., & Gómez-Gejo, A. (2020). Effect of printing parameters on dimensional error and surface roughness obtained in direct ink writing (DIW) processes. *Materials*, *13*(9), 2157. <https://doi.org/10.3390/ma13092157>
- Cooke, M. E., & Rosenzweig, D. H. (2021). The rheology of direct and suspended extrusion bioprinting. *APL Bioengineering*, *5*(1). <https://doi.org/10.1063/5.0031475>

- Corker, A., Ng, H. C., Poole, R. J., & Garcia-Tuñón, E. (2019). 3D printing with 2D colloids: designing rheology protocols to predict 'printability' of soft-materials. *Soft Matter*, *15*(6), 1444–1456. <https://doi.org/10.1039/c8sm01936c>
- Croom, B. P., Abbott, A., Kemp, J. W., Rueschhoff, L. M., Smieska, L., Woll, A., Stoupin, S., & Koerner, H. (2021). Mechanics of nozzle clogging during direct ink writing of fiber-reinforced composites. *Additive Manufacturing*, *37*, 101701. <https://doi.org/10.1016/j.addma.2020.101701>
- De Leeuw, T., Eimhear, M., Kuijper, C., Lemlij, N., & Van Brummelen, J. (2022). *Never ending printing- Advanced Prototyping Minor* [Unpublished Presentation]. TU Delft.
- Del-Mazo-Barbara, L., & Ginebra, M. (2021). Rheological characterisation of ceramic inks for 3D direct ink writing: A review. *Journal of the European Ceramic Society*, *41*(16), 18–33. <https://doi.org/10.1016/j.jeurceramsoc.2021.08.031>
- De Prá Andrade, M., Piazza, D., & Poletto, M. (2021). Pecan nutshell: morphological, chemical and thermal characterization. *Journal of Materials Research and Technology*, *13*, 2229–2238. <https://doi.org/10.1016/j.jmrt.2021.05.106>
- Despeisse, M., & Ford, S. (2015). The role of additive manufacturing in improving resource efficiency and sustainability. In *IFIP advances in information and communication technology* (pp. 129–136). https://doi.org/10.1007/978-3-319-22759-7_15
- Donders, E. (2022). Sustainable 3D printing using eggshells. TU Delft Repositories. <http://resolver.tudelft.nl/uuid:5d7b743a-58f6-4445-94ca-aa680b854eff>
- Ebers, L., & Laborie, M. (2020). Direct ink writing of Fully Bio-Based Liquid Crystalline Lignin/Hydroxypropyl Cellulose aqueous inks: Optimization of formulations and printing parameters. *ACS Applied Bio Materials*, *3*(10), 6897–6907. <https://doi.org/10.1021/acsabm.0c00800>
- Faludi, J., Hu, Z., Alrashed, S., Braunholz, C., Kaul, S., & Kassaye, L. (2015). Does Material Choice Drive Sustainability of 3D Printing. *World Academy of Science, Engineering and Technology, International Journal of Mechanical, Aerospace, Industrial, Mechatronic and Manufacturing Engineering*, *9*, 216-223.
- Faludi, J., Van Sice, C. M., Shi, Y., Bower, J., & Brooks, O. (2019). Novel materials can radically improve whole-system environmental impacts of additive manufacturing. *Journal of Cleaner Production*, *212*, 1580–1590. <https://doi.org/10.1016/j.jclepro.2018.12.017>
- Gauss, C., Pickering, K. L., & Muthe, L. P. (2021). The use of cellulose in bio-derived formulations for 3D/4D printing: A review. *Composites Part C: Open Access*, *4*, 100113. <https://doi.org/10.1016/j.jcomc.2021.100113>
- Ghomi, E. R., Khosravi, F., Ardahaei, A. S., Dai, Y., Khorasani, S. N., Foroughi, F., Wu, M., Das, O., & Ramakrishna, S. (2021). The Life Cycle Assessment for Polylactic Acid (PLA) to Make It a Low-Carbon Material. *Polymers*, *13*(11), 1854. <https://doi.org/10.3390/polym13111854>
- Gillispie, G. J., Prim, P. M., Copus, J., Fisher, J. P., Mikos, A. G., Yoo, J. J., Atala, A., & Lee, S. J. (2020). Assessment methodologies for extrusion-based bioink printability. *Biofabrication*, *12*(2), 022003. <https://doi.org/10.1088/1758-5090/ab6f0d>
- Gleuwitz, F. R., Sivasankarapillai, G., Siqueira, G., Friedrich, C., & Laborie, M. (2020).

Lignin in Bio-Based Liquid Crystalline Network Material with Potential for Direct Ink Writing. *ACS Applied Bio Materials*, 3(9), 6049–6058. <https://doi.org/10.1021/acsabm.0c00661>

Govindharaj, M., Roopavath, U. K., & Rath, S. N. (2019). Valorization of discarded Marine Eel fish skin for collagen extraction as a 3D printable blue biomaterial for tissue engineering. *Journal of Cleaner Production*, 230, 412–419. <https://doi.org/10.1016/j.jclepro.2019.05.082>

Gao, T., Gillispie, G. J., Copus, J., Pr, A. K., Seol, Y., Atala, A., Yoo, J. J., & Lee, S. J. (2018). Optimization of gelatin–alginate composite bioink printability using rheological parameters: a systematic approach. *Biofabrication*, 10(3), 034106. <https://doi.org/10.1088/1758-5090/aacdc7>

Gudipaty, T., Stamm, M. T., Cheung, L. S. L., Jiang, L., & Zohar, Y. (2010). Cluster formation and growth in microchannel flow of dilute particle suspensions. *Microfluidics and Nanofluidics*, 10(3), 661–669. <https://doi.org/10.1007/s10404-010-0700-6>

Guo, Z., Fei, F., Song, X., & Zhou, C. (2023). Analytical study and experimental verification of Shear-Thinning ink flow in direct ink writing process. *Journal of Manufacturing Science and Engineering-transactions of the Asme*, 145(7). <https://doi.org/10.1115/1.4056926>

Kim, M., & Choi, J. (2021). Rubber ink formulations with high solid content for direct-ink write process. *Additive Manufacturing*, 44, 102023. <https://doi.org/10.1016/j.addma.2021.102023>

Kostenko, A., Swioklo, S., & Connon, C. J. (2022). Effect of calcium sulphate pre-crosslinking on rheological parameters of alginate based Bio-Inks and on human corneal stromal fibroblast survival in 3D Bio-Printed constructs. *Frontiers in Mechanical Engineering*, 8. <https://doi.org/10.3389/fmech.2022.867685>

Lewis, J. A. (2006). Direct ink writing of 3D functional materials. *Advanced Functional Materials*, 16(17), 2193–2204. <https://doi.org/10.1002/adfm.200600434>

LignoStar Group BV. (2020, December 18). Lignin & Lignosulfonates - LignoStar Lignin Solutions. <https://www.lignostar.com/en/>

Li, L., Lin, Q., Tang, M., Duncan, A. J., & Ke, C. (2019). Advanced polymer designs for Direct Ink Write 3D printing. *Chemistry - a European Journal*, 25(46), 10768–10781. <https://doi.org/10.1002/chem.201900975>

Li, H., Tan, C., & Li, L. (2018). Review of 3D printable hydrogels and constructs. *Materials & Design*, 159, 20–38. doi:10.1016/J.MATDES.2018.08.023

Li, N., Qiao, D., Zhao, S., Lin, Q., Zhang, B., & Xie, F. (2021). 3D printing to innovate biopolymer materials for demanding applications: A review. *Materials Today Chemistry*, 20, 100459. <https://doi.org/10.1016/j.mtchem.2021.100459>

Littlefield, B. L., Fasina, O., Shaw, J. N., Adhikari, S., & Via, B. K. (2011). Physical and flow properties of pecan shells—Particle size and moisture effects. *Powder Technology*, 212(1), 173–180. <https://doi.org/10.1016/j.powtec.2011.05.011>

Liu, Y., Yu, Y., Chang-Shu, L., Regenstein, J. M., Liu, X., & Zhou, P. (2019). Rheological and mechanical behavior of milk protein composite gel for extrusion-based 3D food printing. *LWT*, 102, 338–346. <https://doi.org/10.1016/j.lwt.2018.12.053>

Maguire, A., Pottackal, N., Saadi, M. a. S. R., Rahman, M. M., & Ajayan, P. M. (2020). Additive manufacturing of polymer-based structures by extrusion technologies. *Oxford Open*

Mordor Intelligence. (2023). Pecan Market Size & Share Analysis - Growth Trends & Forecasts (2023 - 2028). In Mordor Intelligence. <https://www.mordorintelligence.com/industry-reports/pecan-market>

Mouser, V. H. M., Melchels, F. P. W., Visser, J., Dhert, W. J. A., Gawlitta, D., & Malda, J. (2016). Yield stress determines bioprintability of hydrogels based on gelatin-methacryloyl and gellan gum for cartilage bioprinting. *Biofabrication*, 8, 035003. doi:10.1088/1758-5090/8/3/035003

Naghieh, S., Sarker, M., Sharma, N. K., Barhoumi, Z., & Chen, D. (2019). Printability of 3D printed hydrogel scaffolds: influence of hydrogel composition and printing parameters. *Applied Sciences*, 10(1), 292. <https://doi.org/10.3390/app10010292>

National Agricultural Statistics Service (NASS), Agricultural Statistics Board, & United States Department of Agriculture (USDA). (2023). *Pecan Production (January 2023)*.

National Center for Biotechnology Information (2023). PubChem Compound LCSS for CID 23266, Sodium silicate. Retrieved from <https://pubchem.ncbi.nlm.nih.gov/compound/Sodium-silicate#datasheet=LCSS>.

Peng, T., Kellens, K., Tang, R., Chen, C., & Chen, G. (2018). Sustainability of additive manufacturing: An overview on its energy demand and environmental impact. *Additive Manufacturing*, 21, 694–704. <https://doi.org/10.1016/j.addma.2018.04.022>

Rocha, V. G., Saiz, E., Elizarova, I. S., & García-Tuñón, E. (2020). Direct ink writing advances in multi-material structures for a sustainable future. *Journal of Materials Chemistry A, Materials for Energy and Sustainability*, 8(31), 15646–15657. <https://doi.org/10.1039/d0ta04181e>

Romani, A., Suriano, R., & Levi, M. (2023). Biomass waste materials through extrusion-based additive manufacturing: A systematic literature review. *Journal of Cleaner Production*, 386, 135779. <https://doi.org/10.1016/j.jclepro.2022.135779>

Romberg, S. K., Islam, M. A., Hershey, C., DeVinney, M., Duty, C., Kunc, V., & Compton, B. G. (2021). Linking thermoset ink rheology to the stability of 3D-printed structures. *Additive Manufacturing*, 37, 101621. <https://doi.org/10.1016/j.addma.2020.101621>

Ruwoldt, J. (2020). A critical review of the physicochemical properties of lignosulfonates: chemical structure and behavior in aqueous solution, at surfaces and interfaces. *Surfaces*, 3(4), 622–648. <https://doi.org/10.3390/surfaces3040042>

Saadi, M. a. S. R., Maguire, A., Pottackal, N., Thakur, S. H., Ikram, M. M., Hart, A. J., Ajayan, P. M., & Rahman, M. M. (2022). Direct Ink Writing: a 3D printing technology for diverse materials. *Advanced Materials*, 34(28). <https://doi.org/10.1002/adma.202108855>

Sanandiya, N. D., Ottenheim, C., Phua, J. W., Caligiani, A., Dritsas, S., & Fernandez, J. G. (2020). Circular manufacturing of chitinous bio-composites via bioconversion of urban refuse. *Scientific Reports*, 10(1). <https://doi.org/10.1038/s41598-020-61664-1>

Sánchez-Acosta, D., Rodríguez-Uribe, A., Álvarez-Chávez, C. R., Mohanty, A. K., Misra, M., López-Cervantes, J., & Madera-Santana, T. J. (2019). Physicochemical Characterization and Evaluation of Pecan Nutshell as Biofiller in a Matrix of Poly(lactic acid). *Journal of Polymers and the Environment*, 27(3), 521–532. <https://doi.org/10.1007/s10924-019-01374-6>

- Sauerwein, M., Zlopaša, J., Doubrovski, Z., Bakker, C., & Balkenende, R. (2020). Reprintable Paste-Based materials for additive manufacturing in a circular economy. *Sustainability*, 12(19), 8032. <https://doi.org/10.3390/su12198032>
- Schwab, A., Levato, R., D'Este, M., Piluso, S., Eglin, D., & Malda, J. (2020). Printability and shape fidelity of bioINKs in 3D bioprinting. *Chemical Reviews*, 120(19), 11028–11055. <https://doi.org/10.1021/acs.chemrev.0c00084>
- Scott, C. (2023, April 5). *Wohlers Report 2023 Unveils Continued Double-Digit Growth - Wohlers Associates*. Wohlers Associates. <https://wohlersassociates.com/news/wohlers-report-2023-unveils-continued-double-digit-growth/>
- Shahbazi, M., & Jäger, H. (2020). Current status in the utilization of biobased polymers for 3D printing process: A Systematic review of the materials, processes, and challenges. *ACS Applied Bio Materials*, 4(1), 325–369. <https://doi.org/10.1021/acsabm.0c01379>
- Shaik, S. A., Schuster, J., Shaik, Y. P., & Kazmi, M. (2022). Manufacturing of biocomposites for domestic applications using Bio-Based filler materials. *Journal of Composites Science*, 6(3), 78. <https://doi.org/10.3390/jcs6030078>
- Suárez, L., & Somonte, M. D. (2019). Sustainability and environmental impact of fused deposition modelling (FDM) technologies. *The International Journal of Advanced Manufacturing Technology*, 106(3–4), 1267–1279. <https://doi.org/10.1007/s00170-019-04676-0>
- Su, C., Chen, Y., Tian, S., Lu, C., & Lv, Q. (2022). Natural materials for 3D printing and their applications. *Gels*, 8(11), 748. <https://doi.org/10.3390/gels8110748>
- Tagliaferri, S., Panagiotopoulos, A., & Mattevi, C. (2021). Direct ink writing of energy materials. *Materials Advances*, 2(2), 540–563. <https://doi.org/10.1039/d0ma00753f>
- TA Instruments. (n.d.). Rheological Techniques for Yield Stress Analysis (No. RH025). Retrieved August 8, 2023, from <https://www.tainstruments.com/pdf/literature/RH025.pdf>
- Van Sice, C., Shi, Y., Ghosh, S., Faludi, J. [2019, unpublished]. *Assessing environmental, mechanical, and printability performance of composites for sustainable Additive manufacturing*
- Vittadello, S. T., & Biggs, S. (1998). Shear history effects in associative thickener solutions. *Macromolecules*, 31(22), 7691–7697. <https://doi.org/10.1021/ma9714023>
- Xu, X., Yang, J., Jonhson, W., Wang, Y., Suwardi, A., Ding, J., Guan, C., & Zhang, D. (2022). Additive manufacturing solidification methodologies for ink formulation. *Additive Manufacturing*, 56, 102939. <https://doi.org/10.1016/j.addma.2022.102939>
- Yadav, C., Saini, A., Zhang, W., You, X., Chauhan, I., Mohanty, P., & Li, X. (2021). Plant-based nanocellulose: A review of routine and recent preparation methods with current progress in its applications as rheology modifier and 3D bioprinting. *International Journal of Biological Macromolecules*, 166, 1586–1616. <https://doi.org/10.1016/j.ijbiomac.2020.11.038>
- Zhan, S., Guo, A. X., Cao, S., & Liu, N. (2022). 3D Printing Soft Matters and Applications: A review. *International Journal of Molecular Sciences*, 23(7), 3790. <https://doi.org/10.3390/ijms23073790>

APPENDIX A

ALGINATE EXPLORATION FOR WATER INSOLUBILITY

As outlined in Chapter 3.1.2, Sodium Alginate was identified as a suitable binder for the ink formulation. This was primarily due to its capacity to generate a material that is both biodegradable and reprintable, while also offering the ability for it to be made water-insoluble through cross-linking. The fact that the reaction is reversible was deemed especially valuable.

However, prior research and tinkering revealed that alginate-based recipes had low print quality, with significant shrinkage, warpage, and cracking (Chapter 3.2). To address this, alginate was combined with other binders in the hope of still incorporating the reversible crosslinking feature of alginate, leading to the AB+SA recipe evaluated in Chapter 3.3. This Appendix delves into further experiments conducted to check this recipe's water-insolubility after crosslinking and discusses some alternative methods tried to improve the print quality of SA-based recipes.

1. POST CROSSLINKING OF ALL BINDER & SODIUM ALGINATE BASED RECIPE

The recipe developed in Chapter 3.2 with Sodium Alginate and All Binder, showed promising results in terms of print quality. However, achieving this level of quality required a substantial amount of non-crosslinkable all binder to be included. Sauerwein et al (2020) achieved water insolubility through post-crosslinking their material using a CaCl-solution.

However, their recipe only utilized alginate as a binder. As a result, it raises the question of whether the crosslinking of the alginate in the developed recipe would suffice to achieve water insolubility, despite the presence of

the additional water-soluble all binder in the formula. To answer the below described experiment was conducted.

1.1 METHOD

Using the AB+SA recipe from Table 6 Chapter 3.2.2.1, six calibration cubes were printed with 20x20x10 mm dimensions and a wall thickness of 2. A nozzle with an inner diameter of 0.81 mm was used for the printing. The cubes were printed at a speed of 8mm/s, with a layer height of 0.6mm and a line width of 0.8 mm. After printing the cubes were left to dry at ambient temperatures for 24 hours.

Dehydrated CaCl was gathered from sigma-Aldrich (Calciumchlorid Dihydrat > 99% Carl Roth) and fully dissolved in water to create 2 different concentrations of CaCl solution; one 2% CaCl solution (as used by Sauerwein) and one solution of 10% CaCl.

To crosslink the material, the printed calibration cubes were fully submerged in a CaCl solution. Different cubes were submerged for different durations: 10, 20 and 30 minutes. This was done for both the 2% solution as well as the 10% solution. Figure 101 shows the setup used for submerging the cubes. After the submerging, the cubes were again left to dry at ambient temperature for 24 hours.

Figure 101: Post-crosslinking setup of All Binder + Sodium Alginate prints



After the samples had dried, they then were submerged in water to check if they had become water-insoluble. Every 5 minutes the samples were stirred slightly to see if they were still intact. The observations were written down.

1.2 RESULTS

Table 27 shows the results of the water insolubility of the crosslinked samples. Though alginate crosslinking decreases the rate at which samples fall apart in water, the samples still lose a lot of their integrity.

With a low concentration of crosslinker (2%), and low submersion time (10 -20 min) samples fall apart and start to dissolve as soon as 5 min. Some improvements are visible when submerging times of 30 minutes are used, but we can not speak of water-insoluble samples.

Higher concentrations of crosslinker (10%), show some improvements in the rate at which the samples dissolve. Only at 10 minutes, the surface starts to dissolve and at 15 minutes the samples fall apart. No clear differences are seen in the different submerging times of these samples, indicating that all cross-linkable bonds could already be crosslinked before the 10-minute mark.

Figure 102 shows the 2% crosslinker samples after 10 min. Figure 103 shows the 10% crosslinker samples at 15 min.

Figure 102: 2% CaCL crosslinked AB+SA samples after 10 min

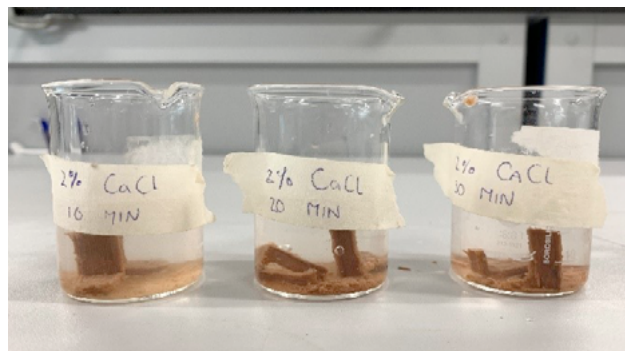


Figure 103: 10% CaCL crosslinked AB+SA samples after 10 min

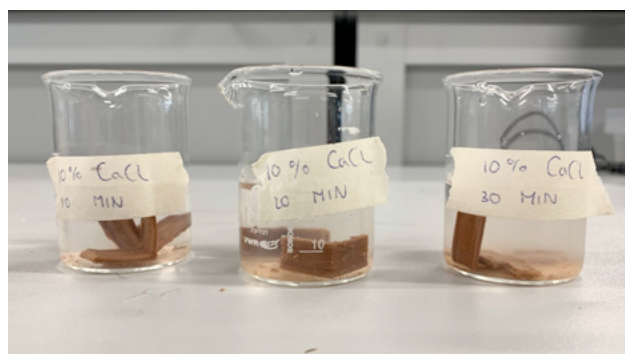


Table 27: Water insolubility test results after crosslinking with 2% and 10% CaCl solutions for 10, 20 and 30 min.

CaCl concentration in crosslink solution (%)	Crosslinked for 10 min	Crosslinked for 20 min	Crosslinked for 30 min
2%	5 min in water: Sample breaks and the surface is dissolving	5 min in water: Layers separate and the surface is dissolving	5 min in water: Layers separate a little bit, but the sample is mostly intact. The surface is starting to dissolve. 10 min: print falls apart.
10 %	10 min: Surface starts to dissolve 15 min: print falls apart	10 min: Surface starts to dissolve 15 min: print falls apart	10 min: Surface starts to dissolve 15 min: print falls apart

1.3 CONCLUSION

The crosslinking of alginate in a recipe with all binder does not seem to prevent the material from dissolving. It is not expected that higher crosslinker concentration or longer submerging times would significantly improve the water insolubility. Though the rate of dissolving can be slightly slowed down, the material almost immediately loses integrity.

These findings are in contrast to those of Sauerwein et al. (202), who achieved water insolubility with a crosslink concentration of 2% , a submerging time of 30, and a 3% concentration of alginate in their recipe. Based on this comparison, it is likely that the presence of the all binder, rather than insufficient Ca⁺ ions or submersion time, is the cause of the tested samples' water solubility.

To apply the reversible crosslinking for water insolubility, the recipes developed should not have other water-soluble binders except for the pre-crosslinked Alginate, or the concentration of the other binder should be significantly lower. The problem however is that recipes with predominantly sodium alginate as a binder show terrible results in print quality.

2. PRE-CROSSLINKING WITH CaSO₄

After discovering that adding a substantial amount of all binder to sodium alginate-based recipes to enhance print quality, had a detrimental effect on the material's potential for water insolubility, alternative methods for improving the print quality of such recipes were explored.

One approach to improve the print quality of alginate-based structures is to pre-crosslink a portion of the material using a CaSO₄ slurry. Previous attempts at printing with alginate-based recipes have resulted in structures collapsing under their own weight after a few layers. However, by increasing the Storage Modulus (*G'*) through pre-crosslinking, this issue may be mitigated, provided that the material still exhibits enough shear thinning

behaviour to avoid clogging when extruded through small nozzles.

Research from (Kostenko et al., 2022) has shown that this method can indeed enhance print quality, as well as promote greater uniformity in mechanical properties throughout the material.

2.1 METHOD

Three different recipes were mixed to test the effect of adding CaSO₄ slurry to the only alginate-based recipe developed during tinkering. Table 28 gives an overview of the recipes' compositions.

Table 28: Recipes used for pre-crosslinked AB+SA with CaSO₄

Recipe	Ingredients (g)
Control	15g PSF/ 2g SA/ 75g W
0.5CS	15g PSF/ 2g SA/ 75g W + 0.27 CaSO ₄
1Cs	15g PSF/ 2g SA/ 75 W + 0.5 CaSO ₄
1.5CS	15g PSF/ 2g SA/ 75 W + 1.0 CaSO ₄

The following steps were taken to prepare the recipes:

1. Initially, the alginate was dissolved in half of the water (37.5 g) with the aid of a laboratory mixer. The alginate was added gradually to the water and mixed until it was completely dissolved.
2. Subsequently, the dehydrated CaSO₄ procured from Sigma Aldrich (details to be filled in) was dissolved in the remaining water (37.5 g).
3. Finally, the PSF was sifted and half of it was added to both the alginate solution and the CaSO₄ solution. The two solutions were mixed together for 5 minutes.

Figure 104 shows the preparation of the mixtures. Each recipe was used to print two walled 20x20x15 mm calibration cubes to visualise the effect of the CaSO₄ slurry

addition. Cubes were printed using a nozzle with a 0.81 mm inner diameter, a print speed of 5 mm/s, a layer height of 0.6 mm and a line width of 0.7 mm

Figure 104: Preparation of CaSO₄ pre-crosslinked AB+SA



2.2. RESULTS

The slurry and alginate mixture proved to be problematic due to clumping that occurred even with small amounts of CaSO₄. Despite this issue, the materials were still used to attempt to print calibration cubes, but unfortunately, none were successful. Table 29 summarizes the result. Low concentrations of CaSO₄ did allow the material to be extruded through a 0.81 mm nozzle but with non-uniform extrusion and pressure. Higher concentrations of the slurry did not improve the mixture's homogeneity and only made the materials too viscous to print.

2.3. CONCLUSION

After experimenting with adding CaSO₄ to the alginate, it was observed that pre-crosslinking did occur. However, this process did not happen uniformly throughout the

material, resulting in a lumpy and unprintable mixture. Unfortunately, the results obtained by [SOURCE] were not reproducible with this recipe. [additional information on this] One possible explanation for this discrepancy is the use of different sources of alginate. It is likely that the alginate used in their research was of higher quality than the cooking store-bought alginate utilized in this study. Ultimately, it was found that pre-crosslinking for improved printability was unsuccessful in this research.

3. IN SITU CROSSLINKING WITH CaCL MIST

As a last attempt to improve the print quality of alginate-based recipes, a technique used by MacCallum et al (2020) was applied. This technique included the in situ crosslinking of Sodium Alginate by using a CaCL mist. MacCallum et al. designed a specialized nozzle add-on to diffuse a CaCL mist over the print after each layer. This allow the alginate to crosslink in between layers and improves the shape retention of the structure.

A standard cleaning fluid diffuser with a CaCL solution of 2% was first used to test this technique by hand spraying the printed sample in-between layers. This immediately displayed crosslinking and resulted in layers not adhering to each other Based on this, the decision was made not to move further with this technique, since it clearly required precise deposition of a fine mist, with good drainage of excess mist to prevent extreme crosslinking causing layers not to adhere. Developing such a system would require time that was not in the scope of this research. However, could be interesting for future research in this field.

Table 29: CaSO₄ pre-crosslinked AB+SA results

Recipe	Extrusion Pressure (Mpa)	Results
0.5CS	0.2	Ununiform extrusion. The material can not be printed in a continuous line with continuous pressure.
1Cs	>0.6	The material does not extrude at all through the 0.81 mm nozzle. Without the nozzle, the material extrudes ununiformly.
1.5CS	> 0.6	The material does not extrude at all through the 0.81 mm nozzle. Without the nozzle, the material extrudes ununiformly.